

A STUDY OF THIN FILM
VACUUM DEPOSITED JUNCTIONS

N 65-33282

(ACCESSION NUMBER)	(THRU)
<u>39</u>	<u>1</u>
(PAGES)	(CODE)
<u>CR 64812</u>	<u>26</u>
(NASA CR OR TMX OR AD NUMBER)	(CATEGORY)

Semiannual Status Report
on
NASA Grant NsG-340

GPO PRICE \$ _____

CSFTI PRICE(S) \$ _____

Hard copy (HC) 2.00

Microfiche (MF) .50

Submitted by:
Dr. Robert L. Ramey
Professor of Electrical Engineering

ff 653 July 65

Research Laboratories for the Engineering Sciences

University of Virginia

Charlottesville



Report No. EE-4012-104-65U

July 1965

A STUDY OF THIN FILM
VACUUM DEPOSITED JUNCTIONS

Semiannual Status Report

on

NASA Grant NsG-340

Submitted by:

Dr. Robert L. Ramey

Professor of Electrical Engineering

DIVISION OF ELECTRICAL ENGINEERING
RESEARCH LABORATORIES FOR THE ENGINEERING SCIENCES
SCHOOL OF ENGINEERING AND APPLIED SCIENCE
UNIVERSITY OF VIRGINIA
CHARLOTTESVILLE, VIRGINIA

Report No. EE-4012-104-65U

July 1965

Copy No. 3

TABLE OF CONTENTS

<u>Section</u>		<u>Page</u>
	LIST OF ILLUSTRATIONS	iv
I.	REPORT COVERAGE	1
II.	OBJECTIVES AND STATUS OF RESEARCH	2
III.	A THEORETICAL EXPRESSION FOR CURRENT DENSITY IN POLYCRYSTALLINE FILMS	4
IV.	SPACE CHARGE EFFECTS IN THIN FILMS	18
V.	A NEW SiO SUBLIMATION SOURCE	22
VI.	DEVICE DESIGN AND FABRICATION	24
VII.	ELECTRON TUNNELING CALCULATIONS	26

LIST OF ILLUSTRATIONS

<u>Figure</u>		<u>Page</u>
1	A polycrystalline film which consists of crystallites (II) and intercrystallite transition regions (I). Electron traps within Region I produce potential wells for holes in the valence band. The effect of an applied field is shown in (C).	5
2	Mobility Ratio as a Function of Film Thickness	9
3	Trial Solutions for Effective Barrier Width as a Function of ΔV	14
4	Comparison of Experimental Data Points and the Theoretical Equation	16
5	Typical Energy Bands for an Extrinsic Semiconductor Film - Note that the effect of any substrate has been neglected.	19
6	Film with Field Plate and Pulse Technique Bridge	20
7	Silicon Monoxide Sublimation Source	23

SECTION I
REPORT COVERAGE

This semi-annual report covers the period from December 5, 1964 to June 5, 1965. This research program is currently in its third year of operation.

SECTION II
OBJECTIVES AND STATUS OF RESEARCH

This research program is proceeding in a threefold manner as outlined in the last Semi-annual Status Report (Report No. EE-4012-103-65U for the period 6-5-64 to 12-5-64). Specifically:

- (1) Theoretical and analytical research on the effects of surface states and grain boundaries upon the free carrier concentration, mobility, and mean-free-path of the charge carriers in thin films. As mentioned in the preceding status report, two papers are in preparation:
 - (a) The development of a suitable theoretical expression for current density in thin, polycrystalline, semiconducting films. The tentative results of this study are presented in Section III and will be submitted for publication in several weeks.
 - (b) The extension of the theories of Schrieffer, Kingston, Greene, and others on the role of surface states in controlling the surface conductivity of semiconductors. We are applying these theories to thin films where the boundary conditions of bulk semiconductors do not exist. This work will probably be completed within the next two months. A brief outline of this phase of the research appears in Section IV.
- (2) Research in laboratory methods has proceeded to the point where we have excellent control over the physical and electronic properties of the films which we deposit. On April 2, 1965 we were granted a Notification of Determination and License (NASA Case No. 4614) by the

U. S. Government on a method for depositing germanium films of controlled hole mobility¹. A new concept in the design of a boat for the evaporation of insulating films, such as SiO, has been perfected in our laboratory and is described in Section V.

- (3) Experimental research in the design and fabrication of thin film electronic devices. We are now in a position to capitalize on our ability to produce thin films of controlled characteristics for use in the fabrication of devices. An intensive effort has been launched in this field. The first phase of this program is outlined in Section VI. This includes the fabrication of field effect transistors and electron tunneling devices.

REFERENCE

1. See the Semiannual Status Report (Report No. EE-4012-103-65U, 6-5-64 to 12-5-64) for a discussion of this method.

SECTION III
A THEORETICAL EXPRESSION FOR
CURRENT DENSITY IN POLYCRYSTALLINE FILMS

The introduction of the concept of an effective mean-free path to the model of a polycrystalline semiconductor provides an interesting foundation for the derivation of an expression for the current density in a semiconducting film as a function of the applied potential, film temperature, and the physical parameters which characterize the film. The model employed has been used to represent bulk polycrystalline material and bicrystals by Mueller^{1, 2}, Waxman et al.³, Petritz⁴, Berger⁵, Volger⁶ and others. With reference to Figure 1, the two dimensional model of the polycrystalline film is assumed to consist of a series of crystallites separated by potential barriers. Within these barriers lie conducting channels. Because of the p-type nature of many thin films, the following discussion is limited to films wherein essentially all conduction is by holes. Thus, in the energy diagram shown in Figure 1b the intercrystallite boundaries are assumed to contain a large number of traps for electrons. The resultant band bending at these boundaries gives rise to potential wells for holes at the top of the valence band.

In the actual film the potential barrier which surrounds each boundary establishes a channel wherein charge carriers (both holes and electrons) may move and give rise to a component of film current which has been observed to be essentially independent of temperature.⁷ The bulk of the film current at room temperature consists of holes which possess sufficient energy to escape from the wells and traverse both wells and crystallites. An effective mean-free-path may be defined for these holes in the following manner. Consider a group of holes which start in the potential well of a channel at point $x = 0$. It is assumed that any hole which possesses sufficient energy to surmount the barrier presented by the first well will also possess sufficient energy to cross all succeeding barriers. The effective m. f. p. is found by computing the weighted mean path for all holes

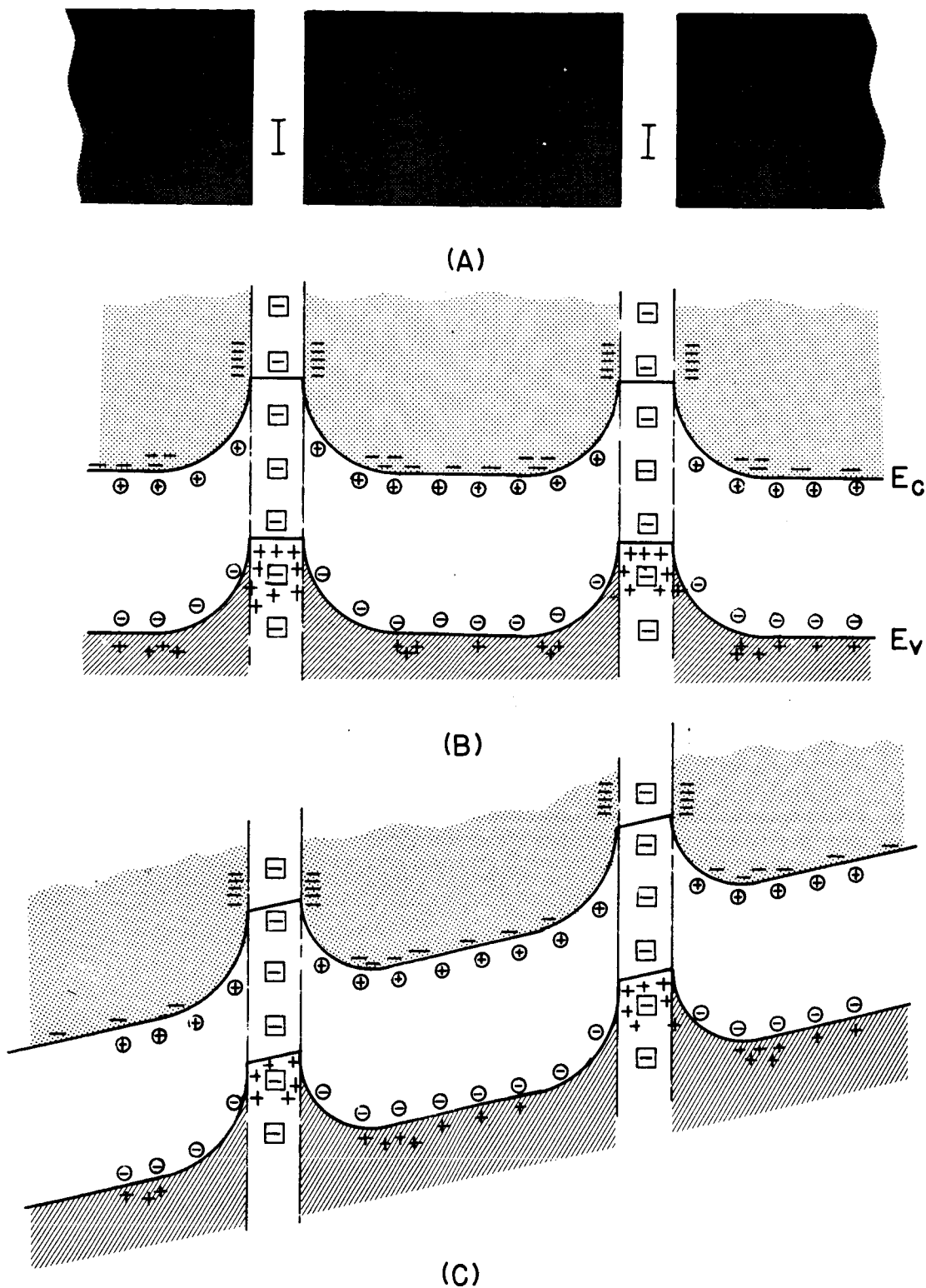


FIGURE 1

A polycrystalline film which consists of crystallites (II) and intercrystallite transition regions (I). Electron traps within Region I produce potential wells for holes in the valence band. The effect of an applied field is shown in (C).

which can clear the barrier and whose free paths terminate in lattice collisions either in or beyond the channel (the first two terms of Equation (1)) plus the weighted mean path of those holes which collide with the barrier and thereby travel only a channel width, ξ

$$\lambda_{\text{eff}} = \frac{\int_0^{\xi} x \epsilon^{-x/\lambda_0} dx + \int_{\xi}^{\infty} x \epsilon^{-x/\lambda_0} \epsilon^{-q(\phi - V_B)/kT} dx}{\int_0^{\infty} \epsilon^{-x/\lambda_0} dx} + \left(1 - \epsilon^{-q(\phi - V_B)/kT}\right) \xi \epsilon^{-\xi/\lambda_0} \quad (1)$$

where λ_0 is the m. f. p. in bulk, single crystal material, ϕ is the barrier height in volts, and V_B is the applied barrier bias in volts. The probability for a hole to clear the barrier is $\exp[-q(\phi - V_B)/kT]$ and of course the probability of colliding with the barrier is $1 - \exp[-q(\phi - V_B)/kT]$. Upon completing the indicated integration we obtain for the effective m. f. p.

$$\lambda_{\text{eff}} = \lambda_0 \left[1 + \epsilon^{-\xi/\lambda_0} (\epsilon^{-q(\phi - V_B)/kT} - 1)\right] \quad (2)$$

Note that the bulk m. f. p. is a function of temperature.

The expression for the current density or the current in a sample of semiconductor material may be approached by starting with the general expression for mobility:

$$\mu = \frac{q\tau}{m} \quad (3)$$

where μ is the hole mobility, q is the electronic charge, τ is the relaxation time, and m is the effective mass of the charge carrier. At this point the discussion will be narrowed to apply to thin films. The single crystal bulk m.f.p., λ_0 , is replaced by λ_1 which represents the m.f.p. in thin single crystal films. Surface scattering reduces the m.f.p. in thin films. Further, the derivation of λ_{eff} in Equation (2) was limited to one degree of freedom; therefore

$$\lambda_{\text{eff}} = \langle v_1 \rangle \tau_1 \quad (4)$$

where $\langle v_1 \rangle$ is the average velocity of the charge carrier when restricted to one degree of freedom. Equation (4) may be combined with Equation (3) to yield an expression for the effective mobility in the thin film

$$\mu_{\text{eff}} = \frac{q}{m \langle v_1 \rangle} \lambda_{\text{eff}} \quad (5)$$

The current density in the film is given by

$$J = \sigma E \quad (6)$$

or

$$\frac{I}{wa} = pq\mu_{\text{eff}} E \quad (7)$$

where w is the film width, a is the film thickness, and p is the hole density.

An expression for the film current in terms of the effective m.f.p. may be obtained from Equations (5) and (7):

$$I = \frac{waq^2 E}{m \langle v_1 \rangle} p(T) \lambda_{\text{eff}}(T) \quad (8)$$

Substitute Equation (2) in (8).

$$I = \frac{w a q^2 E}{m \langle v_1 \rangle} p(T) \lambda_1(T) \left[1 + \epsilon^{-\xi/\lambda_1(T)} (\epsilon^{-q(\phi - V_B)/kT} - 1) \right] \quad (9)$$

Observe that if $\xi \ll \lambda_1$ Equation (10) reduces to the diode equation under conditions of forward bias (which is the only possible bias for the case under consideration) as used by Waxman, et al.³ in their treatment of the current in vacuum deposited CdS films.

The temperature dependence of λ_1 may be ascertained by first expressing λ_1 in terms of the single crystal thin film mobility.

$$\mu_1 = \frac{q \lambda_1}{m \langle v_3 \rangle} \quad (10)$$

where $\langle v_3 \rangle$ is the average velocity in the case of three dimensional space and hence bulk material. The relationship between μ_1 and the single crystal bulk mobility, μ_0 , is known from the work of Ham and Mathis⁸ and is plotted in Figure 2. Let

$$\mu_1 = K_1 \mu_0 \quad (11)$$

Equations (10) and (11) yield

$$\lambda_1(T) = K_1 \frac{m \langle v_3 \rangle}{q} \mu_0(T) \quad (12)$$

The average velocity⁹

$$\langle v_3 \rangle = \left(\frac{8kT}{\pi m} \right)^{1/2} = 4 \langle v_1 \rangle \quad (13)$$

Also an explicit expression for the temperature dependence of hole mobility

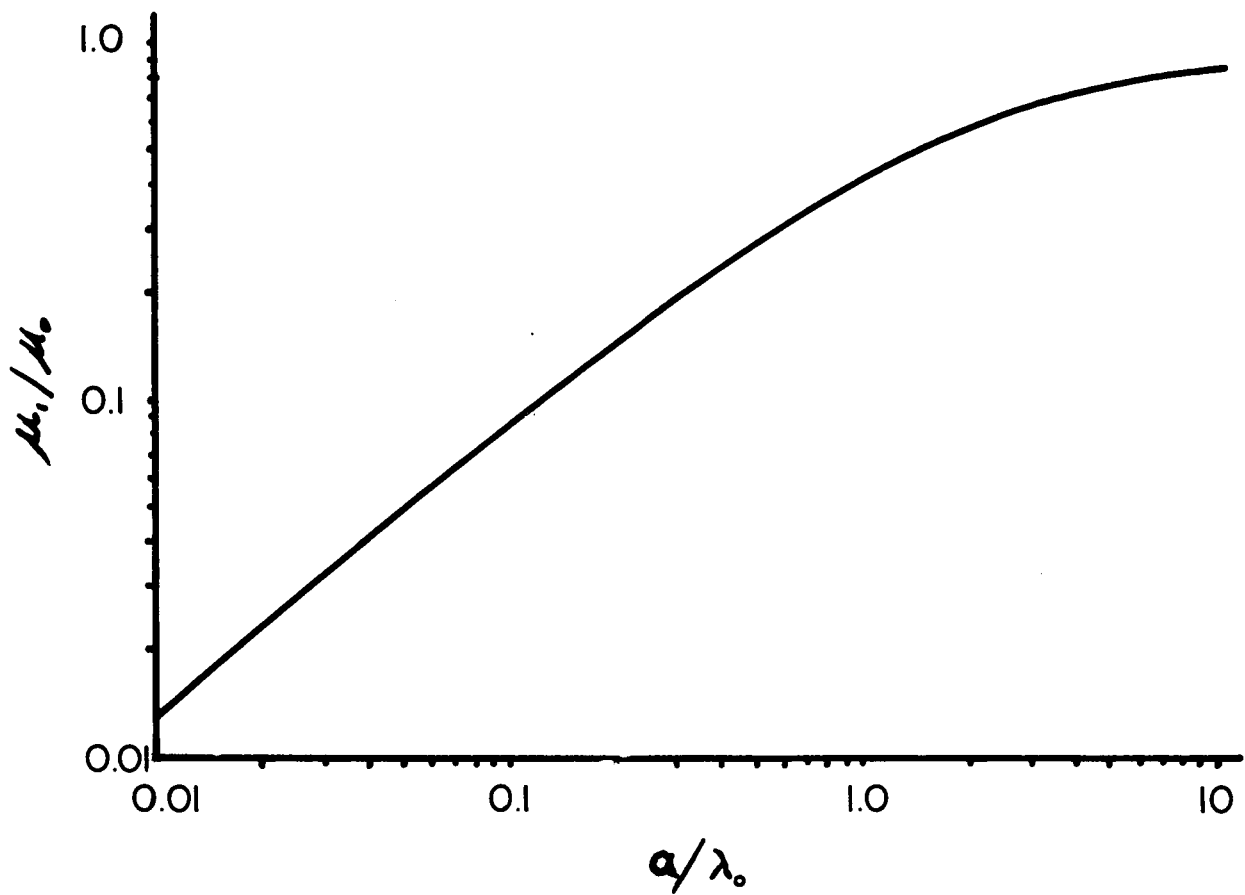


FIGURE 2

Mobility Ratio as a Function of Film Thickness

in germanium is available^{10,11,12}

$$\mu_o = 1.05 \times 10^5 T^{-2.33} \quad (14)$$

meters squared per volt second. Therefore, by use of Equations (12) and (14) an explicit temperature dependence for λ_1 is available.

$$\begin{aligned} \lambda_1 &= 2 \frac{K_1}{q} \left(\frac{2mk}{\pi} \right)^{1/2} (1.05 \times 10^5) T^{-1.83} \\ &= 3.72 \times 10^{-3} K_1 \left(\frac{m}{m_o} \right)^{1/2} T^{-1.83} \end{aligned} \quad (15)$$

where $m_o = 9.11 \times 10^{-31}$ kg. If a ratio of effective hole mass to electron mass of 1/4 is used then the thin film m. f. p. at 300°K would be 540 K_1 angstrom units. For a film thickness of 2400 angstroms the coefficient $K_1 = 0.675$ from Figure 2 and the calculated m. f. p. for the holes is 363 angstroms.

The final expression for the film current takes the form

$$I = 6.71 \times 10^{-14} wa EK_1 p(T) T^{-2.33} \left[1 + \epsilon \frac{\xi/\lambda_1(T)}{(\epsilon^{q(\phi - V_B)/kT} - 1)} \right] \quad (16)$$

As the temperature of the film approaches zero the holes are trapped in the channels defined by the potential wells between crystallites. The current through the film is then carried only by holes and electrons whose movement is confined to the channels. This channel current has been observed to be essentially independent of temperature.⁷ In Equation (16), let T approach zero:

$$I \Big|_{T \rightarrow 0} = I_c = 1.81 \times 10^{-11} wa E \xi \left(\frac{m_o}{m} \right)^{1/2} p(T) T^{-1/2} \quad (17)$$

which is the channel current.

If the channel current is to be essentially temperature independent then the product

$$p(T) T^{-1/2} = \text{constant}$$

or, the hole density

$$p(T) = bT^{1/2} \quad (18)$$

This is a weak temperature dependence which does not differ significantly from experimental observations¹⁰.

Application of Theory to Experimental Data

In view of Equations (17) and (18), the expression for film current (Equation (16)) may be written

$$I = KT^{-1.83} \left[1 + \epsilon \frac{-\xi/\lambda_1(T) - q(\phi - V_B)/kT}{(\epsilon - 1)} \right] \quad (19)$$

where

$$K = 6.71 \times 10^{-14} \text{ wa EK}_1 p(T) T^{-1/2} \quad (20)$$

and may be shown to be independent of temperature by the substitution of Equation (18).

Measured film current as a function of temperature is listed in Table I. Consider two temperatures, T_1 and T_2 . Equation (16) or (18) may be placed in the form:

$$\frac{I(T_1)}{I(T_2)} = \left(\frac{T_1}{T_2} \right)^{-1.83} \frac{\left[1 + \epsilon \frac{-\xi/\lambda_1(T_1) - q(\phi - V_B)/kT_1}{(\epsilon - 1)} \right]}{\left[1 + \epsilon \frac{-\xi/\lambda_1(T_2) - q(\phi - V_B)/kT_1}{(\epsilon - 1)} \right]} \quad (21)$$

This is a transcendental equation. By use of the first two data entries in Table I it is possible to establish the following bounds on the parameters

TABLE I

OBSERVATION NO.	TEMPERATURE °K	CURRENT MA
1	97	0.480
2	145	0.586
3	171	0.643
4	182	0.694
5	195	0.727
6	207	0.763
7	217	0.795
8	222	0.815
9	225	0.815
10	229	0.840
11	233	0.850
12	247	0.897
13	250	0.900
14	251	0.915
15	260	0.940
16	269	0.970
17	272	0.980
18	275	0.990
19	281.5	1.03
20	288	1.05
21	295.9	1.07
22	300.5	1.08
23	302	1.10
24	308.5	1.12
25	316	1.145
26	328	1.17
27	339	1.21
28	347	1.21

FILM THICKNESS = 2400 Å
 APPLIED POTENTIAL = 2 VOLTS

in Equation (21)

$$\xi < 2.24 \times 10^{-6} \text{ meters}$$

$$\Delta V = (\phi - V_B) > 9.5 \times 10^{-3} \text{ volts}$$

At this point it was necessary to employ a Burroughs B5500 digital computer. With data from the first two entries of Table I a plot of ξ as a function of assumed values of ΔV was made. This process was repeated for temperature T_3 , T_4 , and T_5 , T_6 and so forth until all the data entries in Table I had been used. Fourteen curves of $\xi(\Delta V)$ were plotted (Figure 3). Nine of these curves have intersections in the region

$$8 < \xi < 11 \text{ angstroms}$$

$$0.08 < \Delta V < 0.10 \text{ volts}$$

In this manner the possible ranges for both channel width, ξ , and net barrier potential, ΔV , have been established.

Again resorting to the computer and using the experimental values from Table I, Equation (19) was solved for K as a function of selected values for ξ and ΔV . For each selected pair ξ and ΔV , twenty-eight values of K were computed at different temperatures. Now K should be temperature independent; therefore an inspection of each computed set of values for K indicated that only for

$$\xi = 10 \text{ angstroms}$$

$$\Delta V = 0.085 \text{ volts}$$

was it possible to achieve a value for K which was essentially independent of temperature. The mean value for K was 591. A comparison between

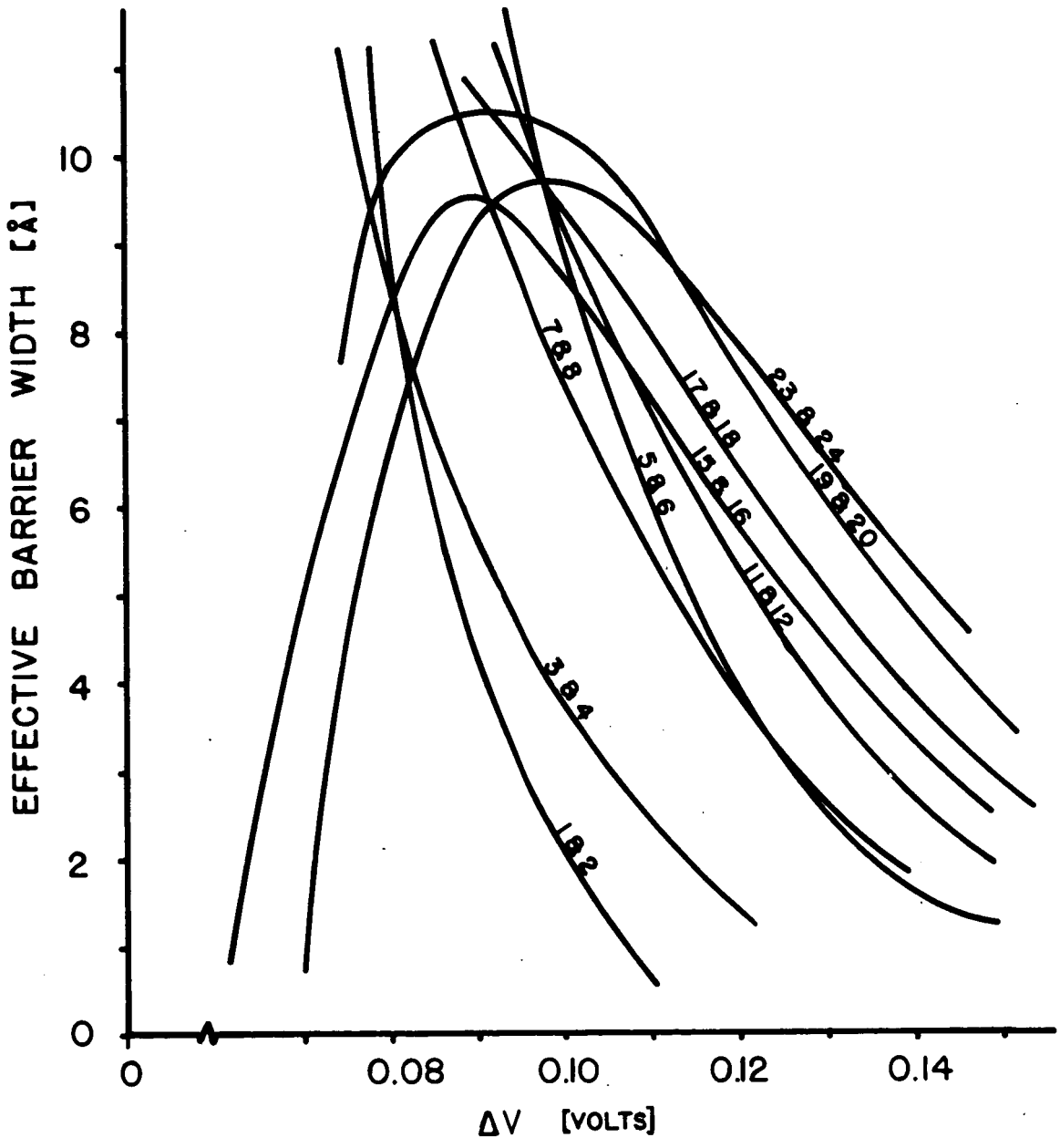


FIGURE 3

Trial Solutions for Effective Barrier Width as a Function of ΔT

the observed film current and Equation (16) or (19) appears in Figure 4.

Results

If it is assumed that most of the voltage drop, in the film, occurs across the barriers as bias voltage, V_B , then

$$V_B = \left(\frac{\delta}{L} \right) V \quad (22)$$

where δ is the mean grain size and V is the potential drop across a length, L , of the film. Electron microscope observations indicated a grain size of approximately 1000 angstroms. From the data of Table I the barrier bias voltage would be

$$V_B = 0.000125$$

volts which means that the barrier potential

$$\phi = 0.0851$$

volts. This is in agreement with the value 0.095 observed by Waxman³ for CdS films. The weak dependence of the exponential term on V_B is consistent with the ohmic characteristic of the film.

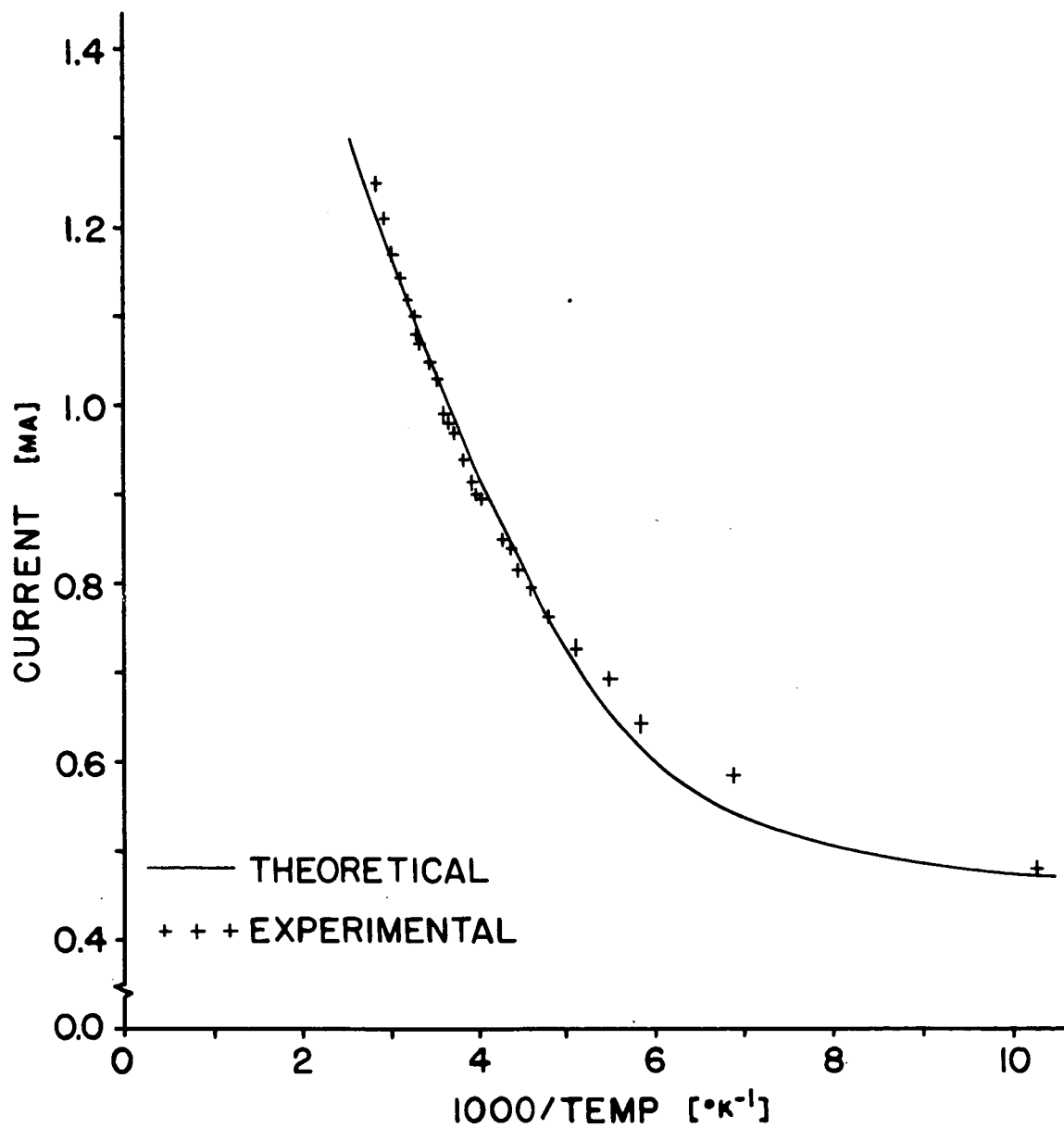


FIGURE 4

Comparison of Experimental Data Points and the Theoretical Equation

REFERENCES

1. R. K. Mueller, J. Appl. Phys. 30, 546 (1959).
2. R. K. Mueller, J. Appl. Phys. 32, 635 (1961).
3. A. Waxman, J. E. Henrich, F. V. Shallcross, H. Borkan and P. K. Weimer, J. Appl. Phys. 36, 168 (1965).
4. R. L. Petritz, Phys. Rev. 104, 1508 (1956).
5. H. Berger, Phys. Status Solidi 1, 739 (1961).
6. J. Volger, Phys. Rev. 79, 1023 (1950).
7. H. F. Mataré, J. Appl. Phys. 30, 581 (1959).
8. E. S. Ham and D. C. Mattis, IBM Jour., April (1960).
9. R. L. Ramey, Physical Electronics, p. 26.
10. F. J. Morin, Phys. Rev. 93, 62 (1954).
11. E. M. Conwell, Proc. IRE, 40, 1327 (1952).
12. E. M. Conwell, Proc. IRE, 46, 1281 (1958).

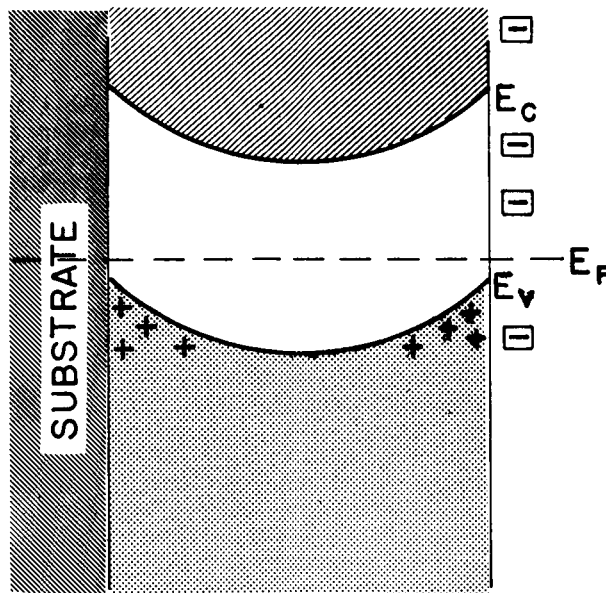
SECTION IV

SPACE CHARGE EFFECTS IN THIN FILMS

Space charge effects in germanium may extend as far as 10^{-4} cm. into the sample from the surface.¹ Thus, conduction in very thin films (less than 5000\AA) depends strongly on the space charge in the sample. The surface states modify the potential distribution inside the film to such an extent that the excess carriers generated by the band-bending are much more numerous than the normal bulk material carrier concentration. See Figure 5.

Calculations are in progress to find the number of excess carriers generated by band-bending and the potential distribution inside the film for typical values of surface charge densities. These calculations follow, in general, the work of Kingston and Neustadter² as modified by Goldberg.³ Because of the relation of the expressions for potential and carrier density to the other variables in this problem the calculations will be carried out with the aid of a Burroughs B5500 digital computer. When the theoretical carrier density is known, it will be compared with carrier densities obtained experimentally. Once agreement has been attained between the experimental and theoretical data, the theoretical work will continue along the line followed by Greene⁴, in the calculation of charge carrier mobility by solution of the one dimensional Boltzmann equation.

Field plate measurements based upon pulse techniques are being used to measure the extent of the band-bending at the surfaces of the thin semi-conducting films.^{5, 6, 7, 8} A sketch of the pulse technique bridge with the film and deposited field plate are shown in Figure 6. The effective germanium film is approximately $3/16$ inch square with gold electrodes at each end. A silicon monoxide film 3000 angstroms thick insulates the Ge film from a gold field plate which has the same effective area as the Ge film.



+ HOLES
 ⊖ TRAPPED ELECTRONS

FIGURE 5

Typical Energy Bands for an Extrinsic Semiconductor Film -
 Note that the effect of any substrate has been neglected.

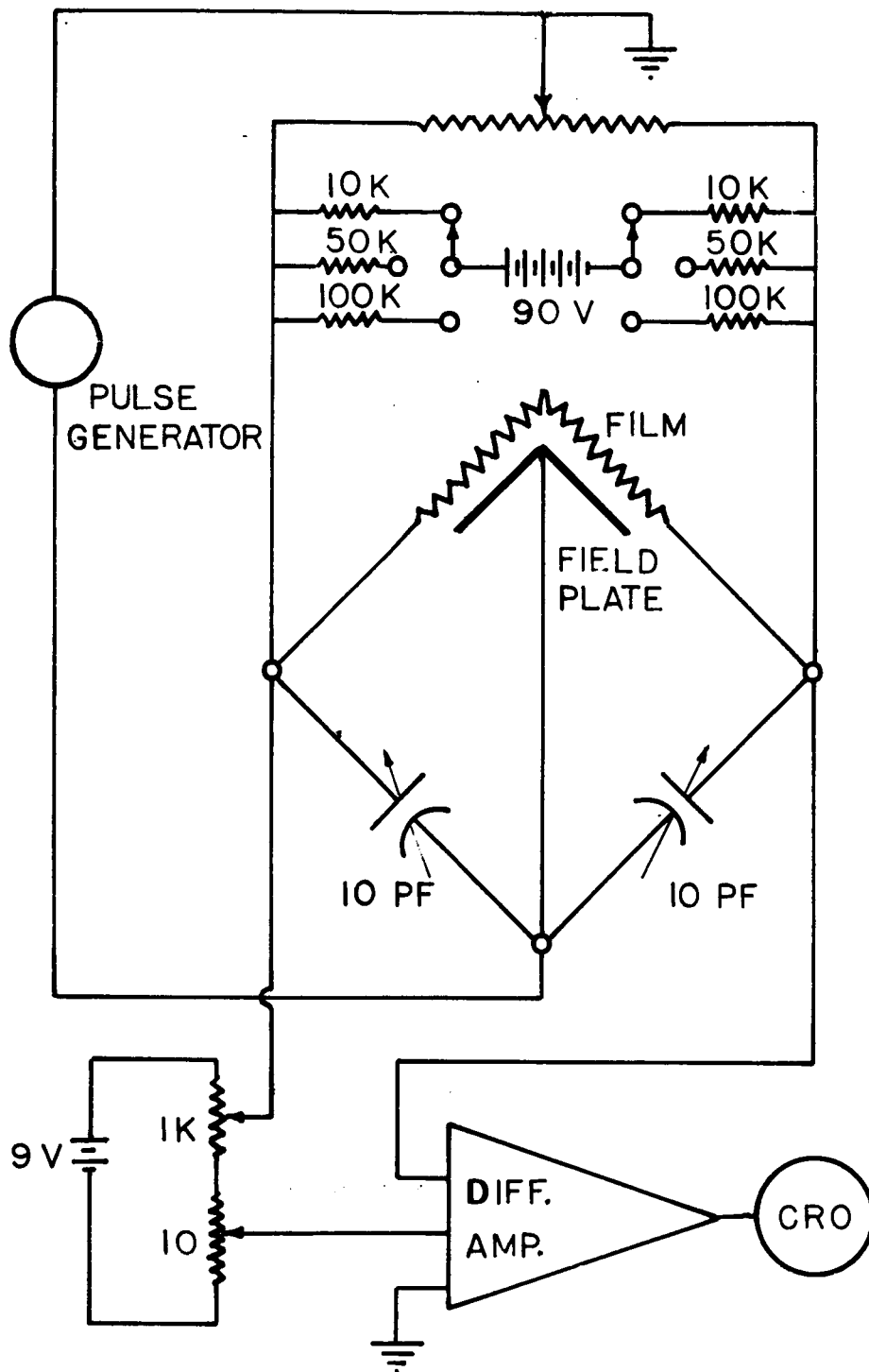


FIGURE 6

Film with Field Plate and Pulse Technique Bridge

REFERENCES

1. C. G. B. Garrett, W. H. Brattain, "Physical Theory of Semiconductor Surfaces," Phys. Rev. 99, 376 (1955).
2. Robert H. Kingston, and Siegfried F. Neustadter, "Calculation of the Space Charge, Electric Field, and Free Carrier Concentration at the Surface of a Semiconductor," Jour. App. Phys. 26, 718 (1955).
3. Colman Goldberg, "Space Charge Regions in Semiconductors," Solid-State Electronics 7, 593 (1964).
4. R. F. Greene, D. R. Frankl, and Jay Zemel, "Surface Transport in Semiconductors," Phys. Rev. 118, 967 (1960).
5. G. Rupprecht, "Measurement of Germanium Surface States by Pulsed Channel Effect," Phys. Rev. 111, 75 (1958).
6. G. Rupprecht, J. Gilbert and T. H. Bergeman, "Study of Surface States in Semiconductors," Technical Documentary Report #RADC-TDR-64-17 March 1964, Tyco Laboratories, Inc.
7. Paul Handler and William M. Portnay, "Electronic Surface States and the Cleaned Germanium Surface," Phys. Rev. 116, 516 (1959).
8. G. A. DeMars, H. Satz and L. Davis, Jr., "Measurement and Interpretation of Conductance of P-Type Inversion Layers on Germanium," Phys. Rev. 98, 539 (1955).

SECTION V

A NEW SiO SUBLIMATION SOURCE

A new silicon monoxide sublimation source suitable for electron bombardment heating has been developed. A sketch of the crucible or boat is shown in Figure 7. The three filaments for electron bombardment heating and the heat shield are also shown. The crucible is machined from reactor grade carbon. The cover of the crucible contains a chimney whose exact length and bore are selected to provide the desired molecular oven beam of SiO molecules. As may be seen from the sketch, the gas must make two 180 degree turns before reaching the chimney. In this way, emission of SiO particles is prevented.

The placement of the three filaments is extremely important if SiO vapor is to be prevented from condensing on the cover and the bottom of the center well of the crucible. One filament is placed directly under the crucible and a filament is placed on each side as shown. The filaments consist of 10 turns of 7 mil tungsten wire wound in a self-supporting helix 0.050 inches in diameter and 0.25 inches long. The filaments are operated at approximately 4.3 amperes each at 12 volts. The accelerating voltage (approximately 700 volts) is applied to the two molybdenum wires which support the crucible. The crucible electron bombardment current is 300 ma.

Silicon monoxide deposition rates up to 14 angstroms per second have been obtained with a total input power (filaments plus accelerating) of about 365 watts. Multiple beam interferometer measurements of deposited film thickness indicate that the deposition is uniform to within 2 percent over a square area measuring 0.65 cm on a side.

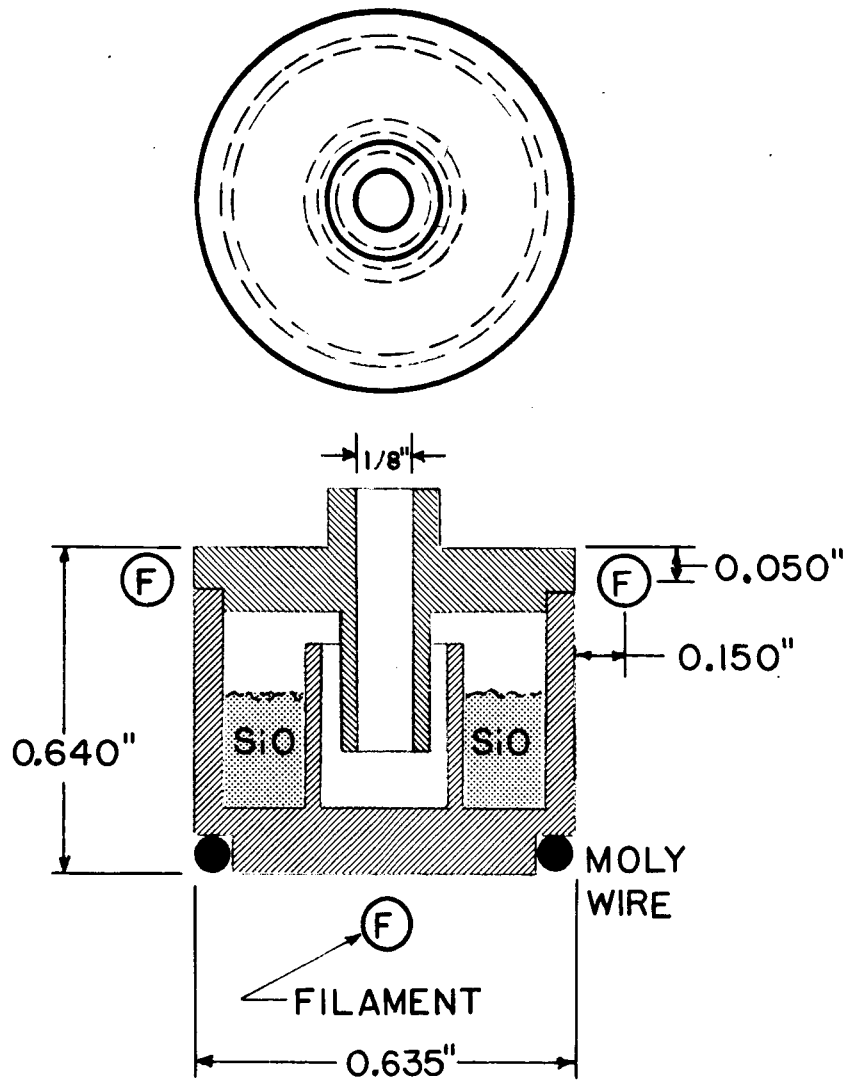


FIGURE 7

Silicon Monoxide Sublimation Source

SECTION VI

DEVICE DESIGN AND FABRICATION

Now that all the necessary deposition and instrumentation is ready for the fabrication of thin film devices, an extensive design, test, and evaluation program has been initiated. Currently, five devices are under study. They are:

1. Microwave Bolometer ,
2. Field Effect Transistor ,
3. Metallic Whisker Tunneling Device,
4. Electron Multiplier,
5. Magnetometer.

The microwave bolometer research is currently based upon flat, thin films of selected metals and semiconductors. As more experience is gained the design will be optimized. Based upon the results of this thin film bolometer study, other applications of thin films to the microwave measurement and transmission art may be investigated.

Field effect transistors are being produced and a study aimed at the selection of efficient semiconducting films for use in these devices has been initiated. At present the possible doping of Ge films by codeposition of Fe and other metals is in progress.

Problems associated with the insulation of the gate control electrode from the source and sink electrodes had delayed this work. The silicon monoxide sublimation source developed in our lab and described in Section V has completely removed this problem.

Considerable effort at many laboratories has been devoted to the study of electron tunneling through thin insulating films. The possibility of using this phenomenon in the design of transducers and active devices as well as the fabrication of diodes has received limited attention. The possibility of combining the geometry of grown metallic whiskers with electron tunneling to form metallic whisker tunneling devices looks promising. Our basic idea

is to construct the usual electrode-insulating film-electrode structure for electron tunneling experiments with the additional feature of growing metallic whiskers on the electrode that is to be the cathode prior to depositing the insulating film. The enhanced emission from the whiskers should result in a diode characteristic with a high forward to reverse current ratio. Certain theoretical aspects of electron tunneling have been reviewed and a computed solution to the general problem has been made. The results of this work are contained in Section VII.

We have had some experience in the design, fabrication, and study of thin film magnetic electron multipliers. These units were similar to those marketed by the Bendix Corporation. The original units were built in 1962 and employed semiconducting secondary electron emission surfaces which were chemically prepared. Quality control in the formation of these surfaces was very difficult to maintain and as a result the research was terminated. It now appears that we are in a position to prepare vacuum deposited films for this purpose. Hence, preparations are being made to fabricate several thin film electron multipliers.

Several designs of thin film magnetometers are under investigation. Two basic designs will be evaluated; one based upon the isothermal Hall effect and the other designed along the general lines of the flux gate concept.

SECTION VII
ELECTRON TUNNELING CALCULATIONS

The phenomenon of electron tunneling has received considerable attention in recent years¹ because of the possibility of designing electronic devices for amplification and as transducers which rely upon this method of electron transport in their operation. Sommerfeld and Bethe² were able to establish mathematical expressions for the electron tunneling current density which were applicable to very low and very high voltage cases. Holm³ extended the theory to include the intermediate voltage range; however, certain anomalies which appeared in his work were later corrected by Simmons.⁴

From these works it is possible to obtain data to plot theoretical current-voltage relationships for a tunnel junction. If a rectangular potential barrier is assumed and the image force is neglected then current density as a function of the thickness, s , of the insulating film and the metal-insulator barrier height (work function), ϕ , may be computed. This has been done using an effective electron mass of $1/4$ of the free electron mass. It has been suggested that this will produce a better correlation between theoretical and experimental results^{5,6}.

Following the work of Simmons⁴, the following equations were employed. The current density-voltage characteristics are divided into three regions according to the value of the applied voltage, V . To agree with the notation used in the literature, the units are expressed in J [amperes/cm²], ϕ [volts], and s [angstrom units].

(a) For $V \approx 0$

$$J = \left[\frac{(2me\phi)^{1/2}}{s} \left(\frac{e}{h} \right)^2 V \right] \exp \left[-(4\pi s/h)(2me\phi)^{1/2} \right]$$

$$= 1.57 \times 10^{10} \phi^{1/2} \left(\frac{V}{s} \right) \exp [-0.5125 s \phi^{1/2}] \quad (1)$$

This is the Sommerfeld-Bethe² result for low voltages.

(b) For $0 < V < \phi$

$$\begin{aligned}
 J &= \left(\frac{e}{2\pi h s^2} \right) \left\{ \left(e\phi - \frac{eV}{2} \right) \exp \left[- \frac{4\pi s}{h} (2m)^{1/2} \left(e\phi - \frac{eV}{2} \right)^{1/2} \right] \right. \\
 &\quad \left. - \left(e\phi + \frac{eV}{2} \right) \exp \left[- \frac{4\pi s}{h} (2m)^{1/2} \left(e\phi + \frac{eV}{2} \right)^{1/2} \right] \right\} \\
 &= \left(\frac{6.2 \times 10^{10}}{s^2} \right) \left\{ \left(\phi - \frac{V}{2} \right) \exp \left[- 0.5125s \left(\phi - \frac{V}{2} \right)^{1/2} \right] \right. \\
 &\quad \left. - \left(\phi + \frac{V}{2} \right) \exp \left[- 0.5125s \left(\phi + \frac{V}{2} \right)^{1/2} \right] \right\} \quad (2)
 \end{aligned}$$

which is due to Holm with the exception of an omitted term which Simmons⁴ showed was an error.

(c) For $V > \phi$

$$\begin{aligned}
 J &= \frac{2.2e^2E^2}{8\pi h\phi} \left\{ \exp \left[- \frac{8\pi}{2.96 h e E} (2m)^{1/2} (e\phi)^{3/2} \right] \right. \\
 &\quad \left. - \left(1 + \frac{2V}{\phi} \right) \exp \left[\frac{8\pi}{2.96 h e E} (2m)^{1/2} (e\phi)^{3/2} \left(1 + \frac{2V}{\phi} \right)^{1/2} \right] \right\} \\
 &= 3.38 \times 10^{10} \frac{E^2}{\phi} \left\{ \exp \left[-0.345 \frac{\phi^{3/2}}{E} \right] \right. \\
 &\quad \left. - \left(1 + \frac{2V}{\phi} \right) \exp \left[-0.345 \frac{\phi^{3/2}}{E} \left(1 + \frac{2V}{\phi} \right)^{1/2} \right] \right\} \quad (3)
 \end{aligned}$$

where $E = V/s$ is the electric field strength in the insulator. The first term of Equation (3) is the well-known Fowler-Nordheim equation⁷ with the exception of a slight modification introduced by Simmons. In the region of interest the second term in this equation is negligible.

The accompanying set of curves are plots of the tunnel current density as a function of the applied potential for various barrier heights, ϕ , and insulator film thickness, s . The transition from one equation to another is marked on each curve by a small circle. It is proposed that these curves may be used to compare experimental to theoretical data and in this manner the effective barrier height may be estimated. The insulator thickness may be accurately determined by use of a multiple beam interferometer.

REFERENCES

1. J. C. Fisher and I. Giaver, J. Appl. Phys. 32, 172 (1961).
2. A. Sommerfeld and H. Bethe, Handbuch der Physik (Edited by Geiger and Schul) Vol. 24/2, p. 450 (1933).
3. R. Holm, J. Appl. Phys. 22, 569 (1951).
4. J. G. Simmons, J. Appl. Phys. 34, 1793 (1963).
5. R. Stratton, J. Phys. Chem. Solids23, 1177 (1962).
6. D. Meyerhofer and S. A. Ochs, J. Appl. Phys. 34, 2537 (1963).
7. R. H. Fowler and L. Nordheim, Proc. Roy. Soc. (London) 119, 173 (1928).

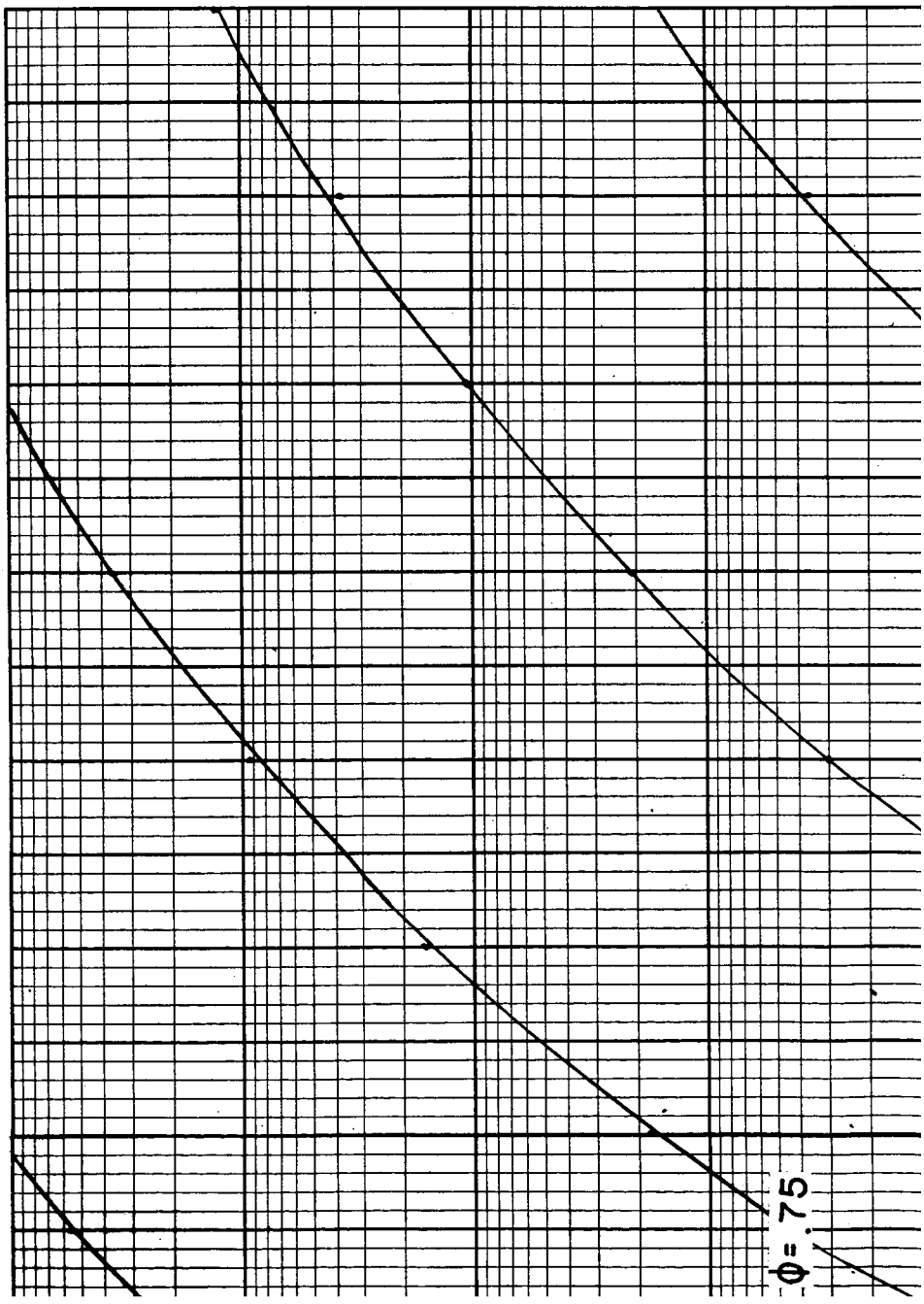
DISTRIBUTION LIST

Copy No.

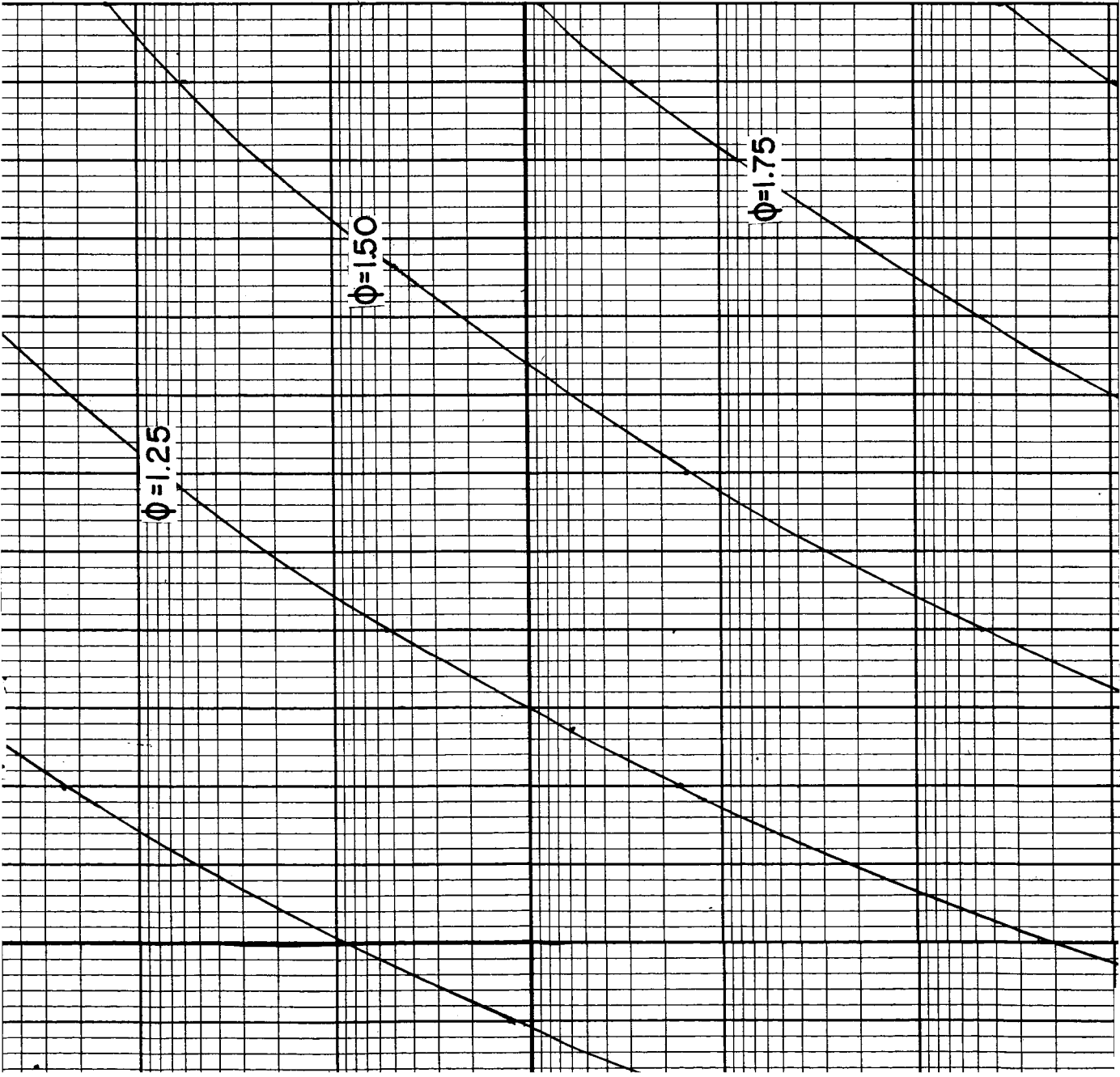
1 - 25	Office of Grants and Research Contracts Code CD National Aeronautics and Space Administration Washington, D. C. 20545
26	A. R. Kuhlthau
27 - 41	R. L. Ramey
42 - 46	RLES Files

①

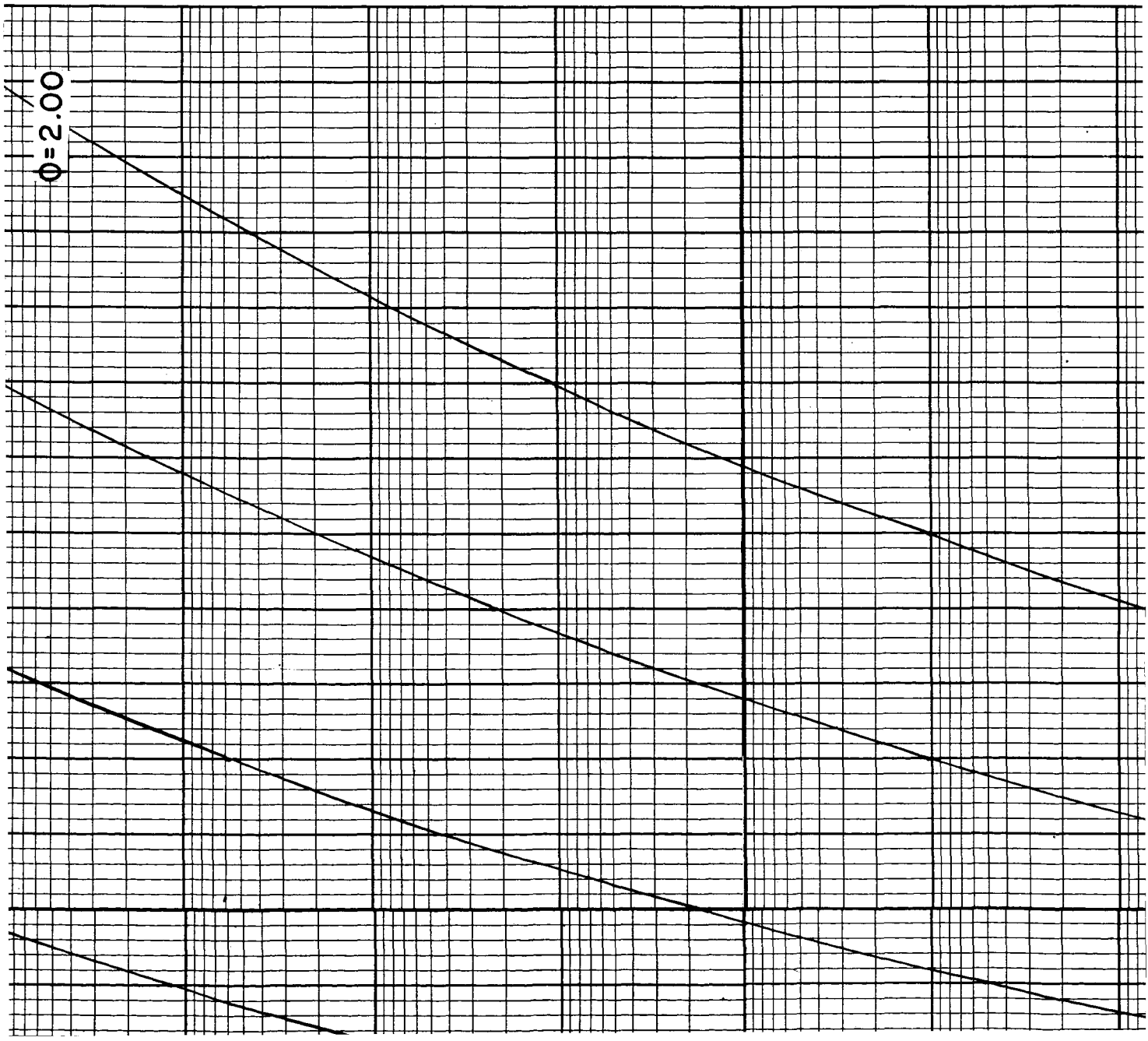
THICKNESS = 180 Å



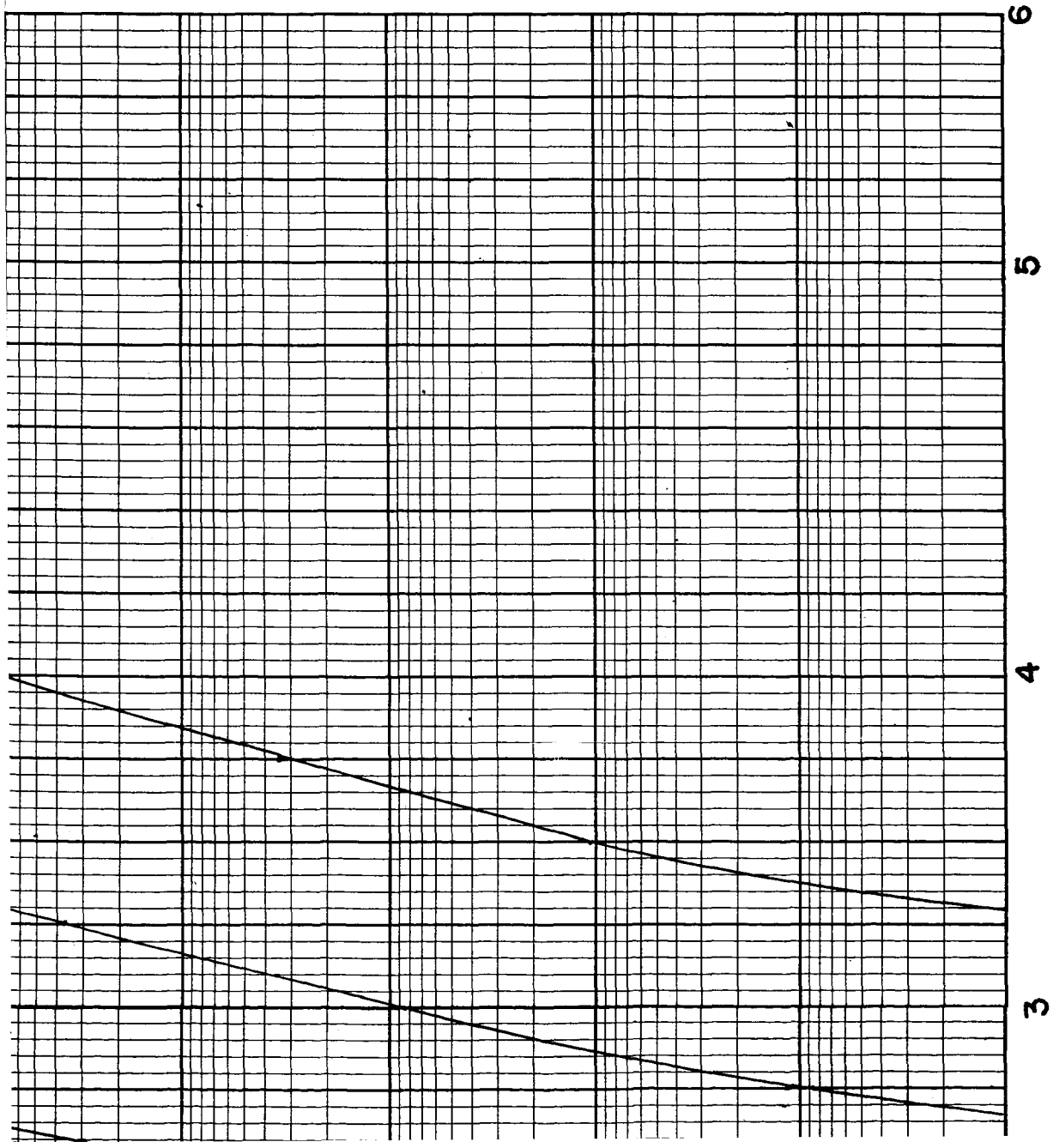
2



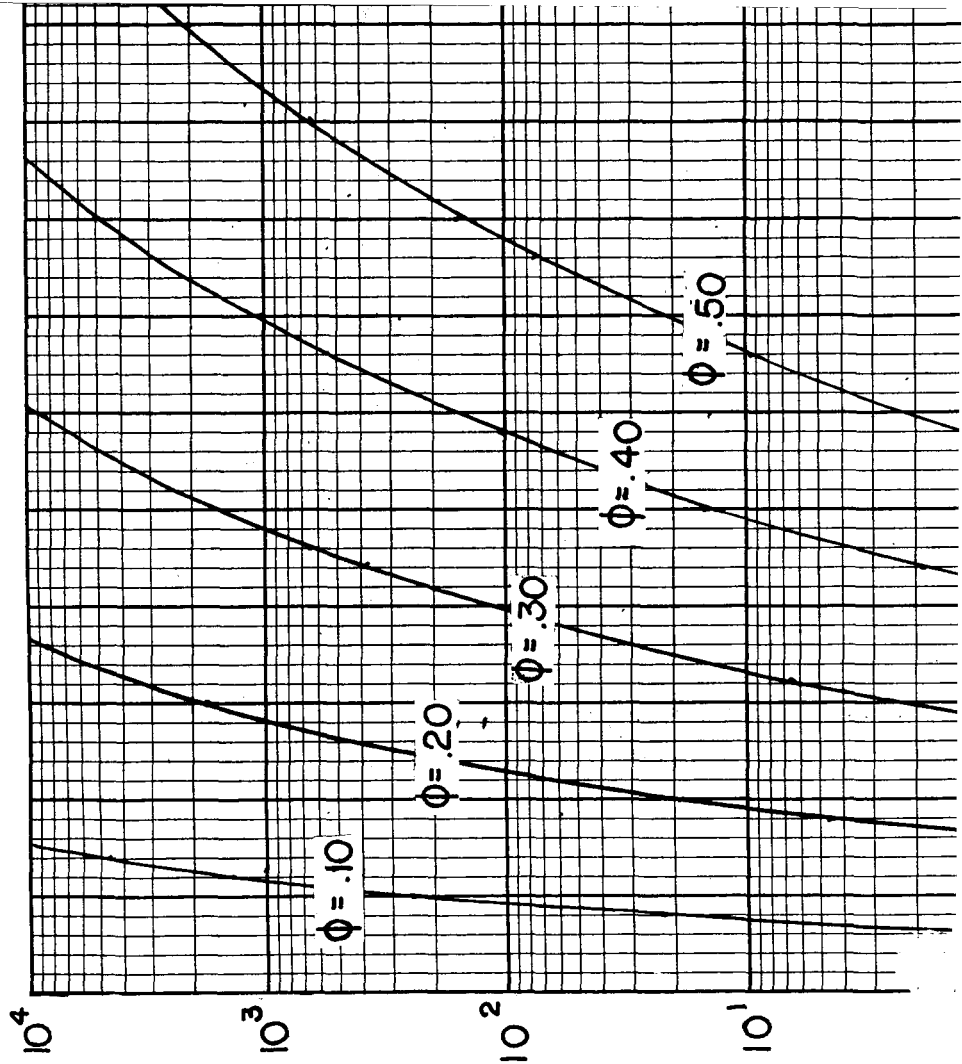
3



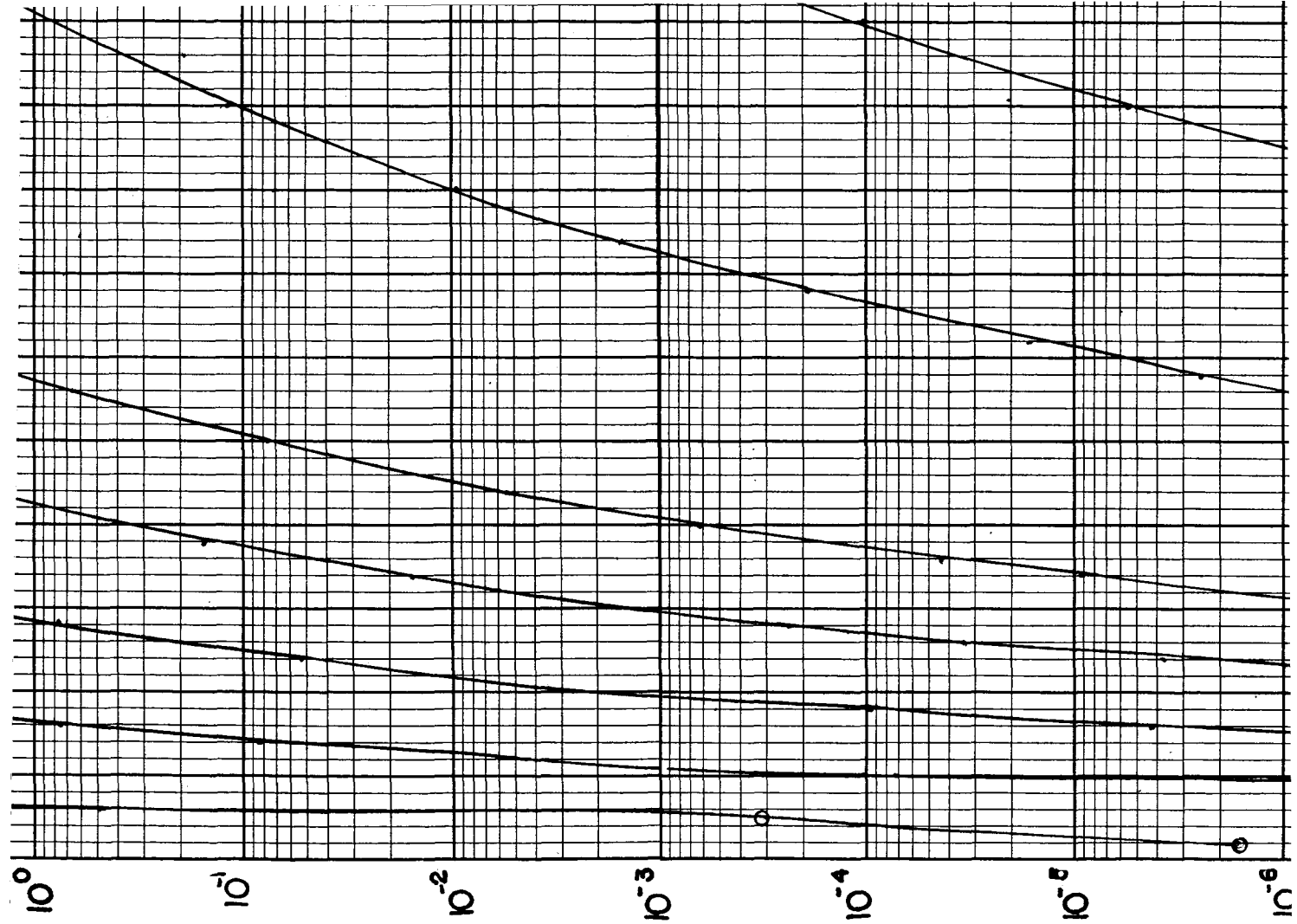
4



VOLTAGE [VOLTS]



57

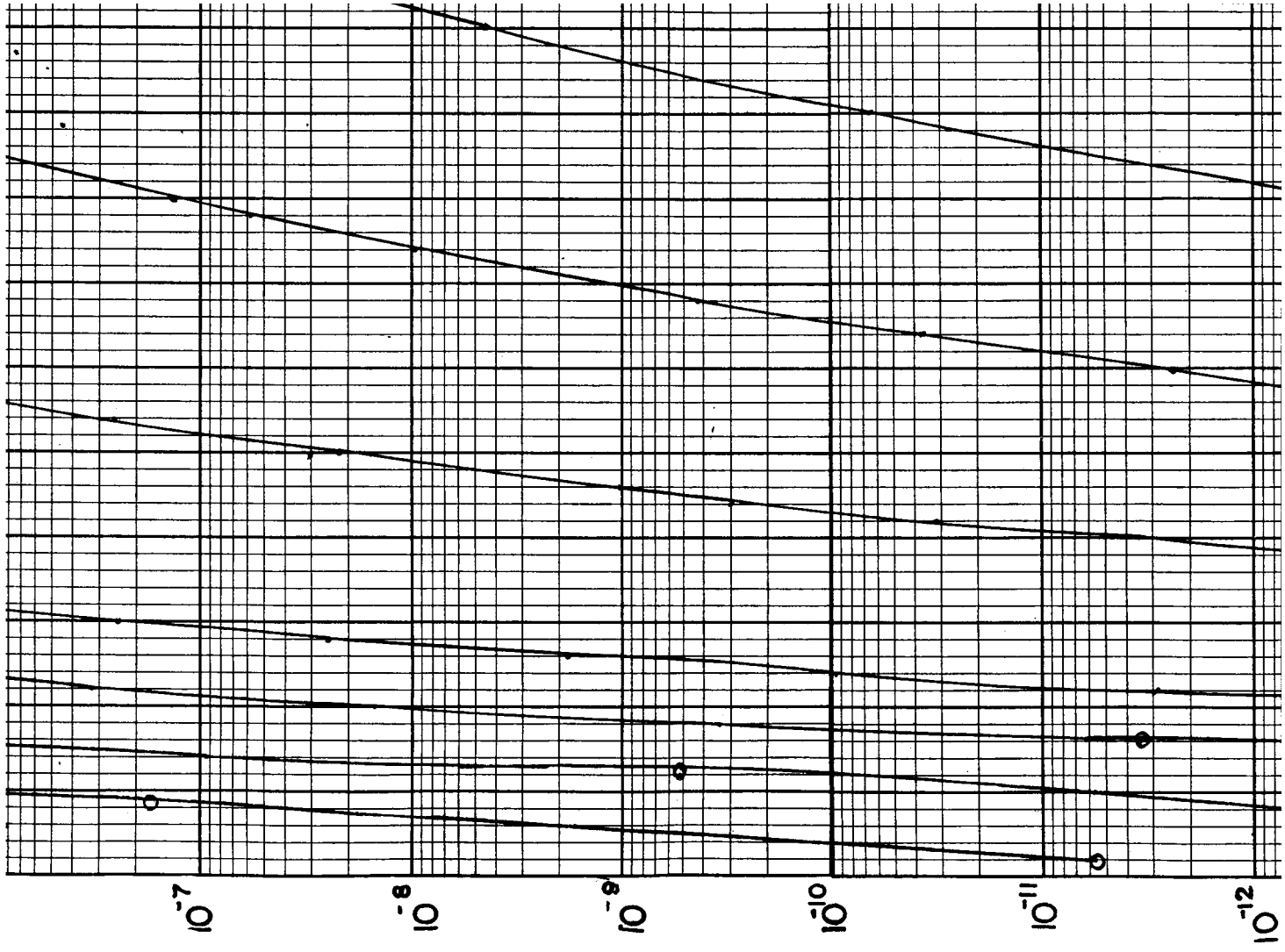


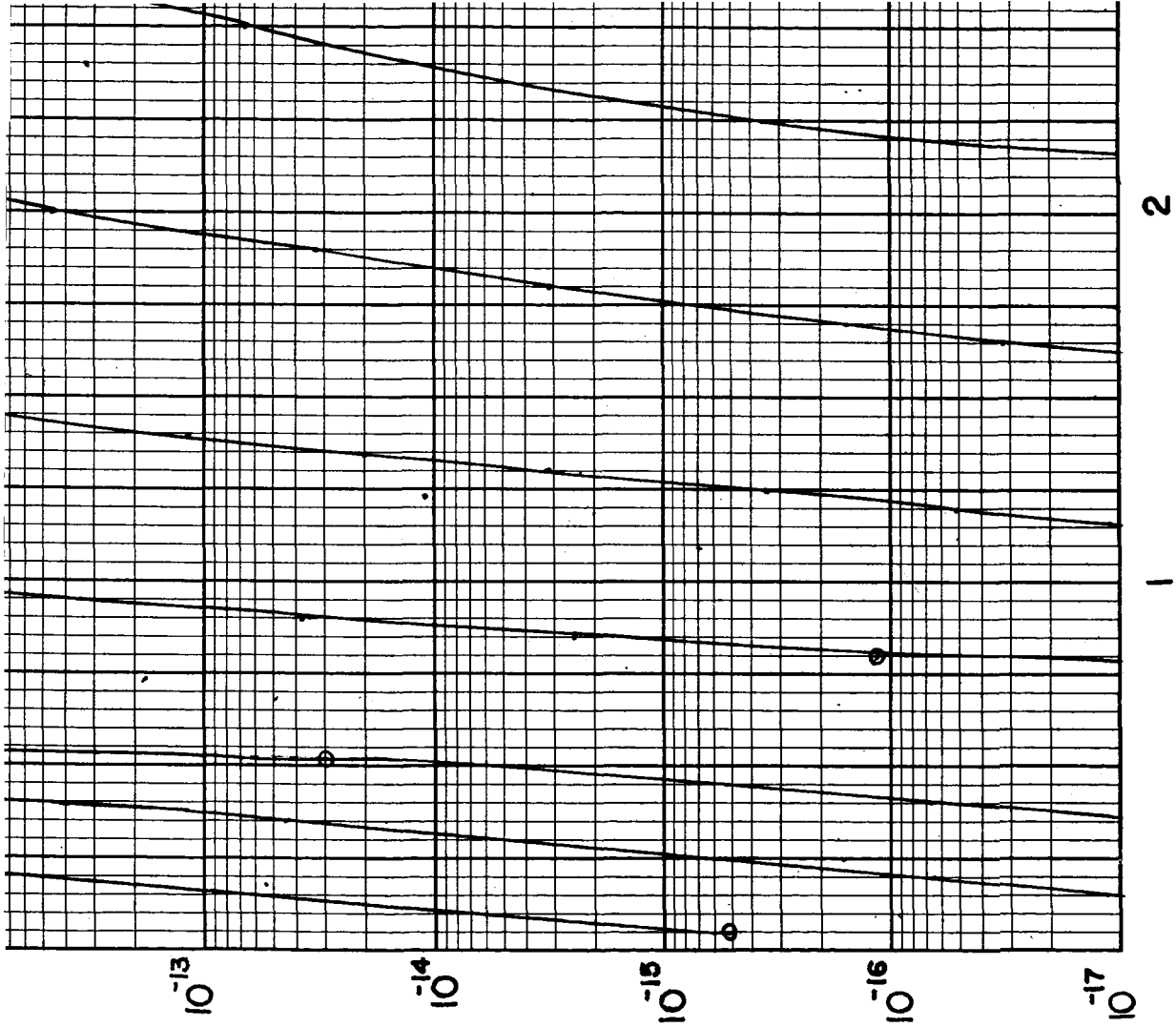
[AMP / CM²]

6

7

CURRENT DENSITY





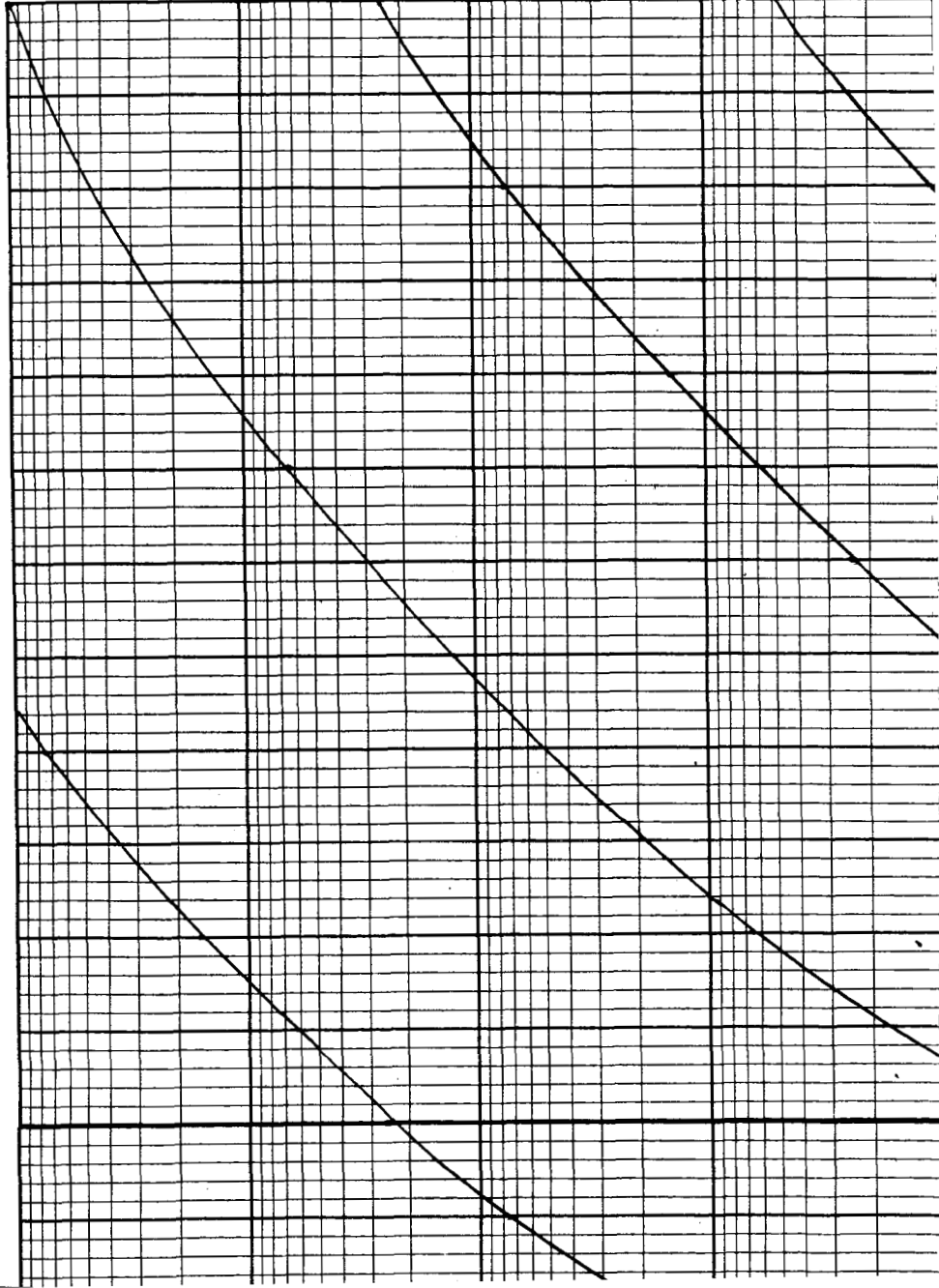
8

2

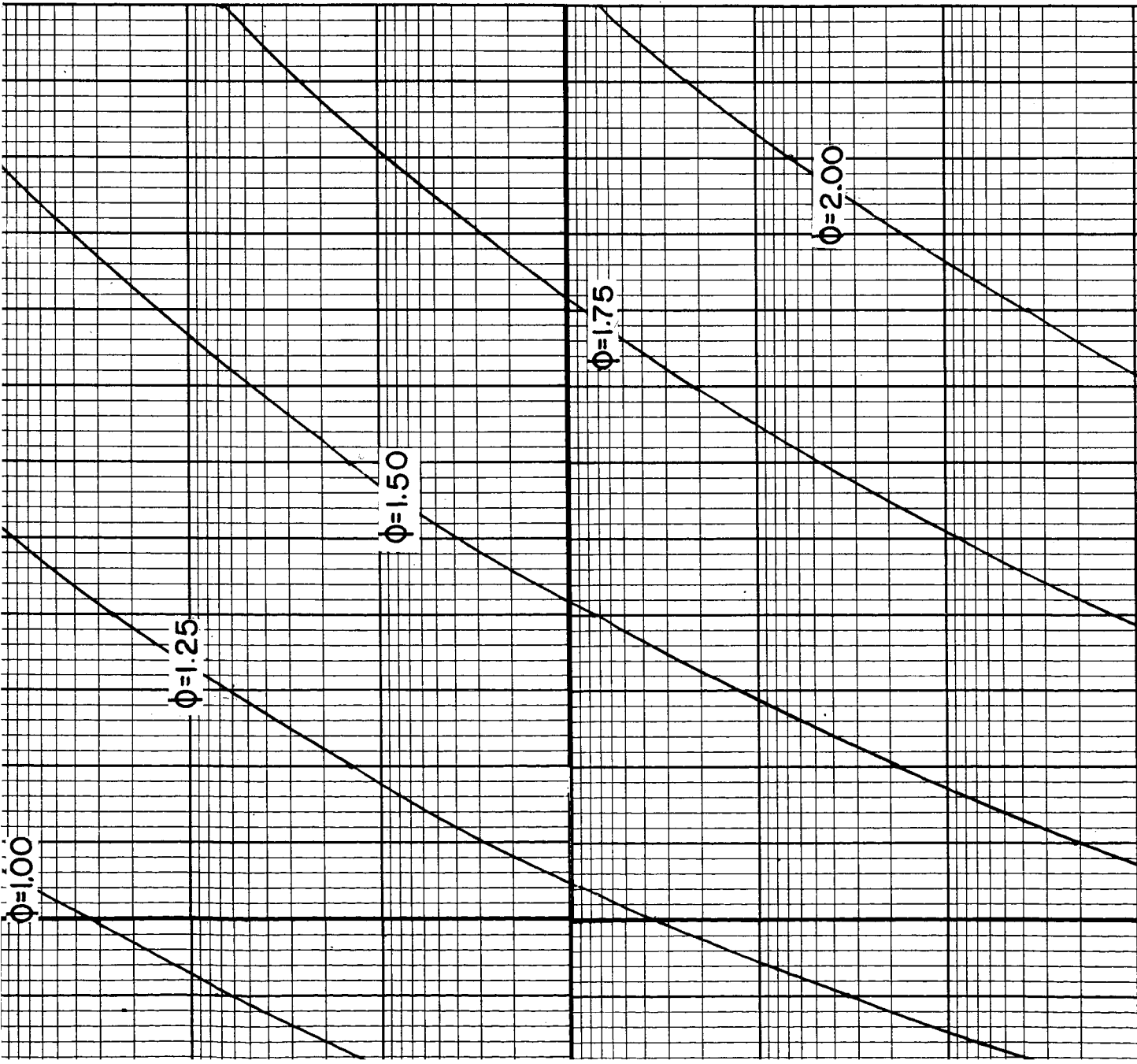
1

(2)

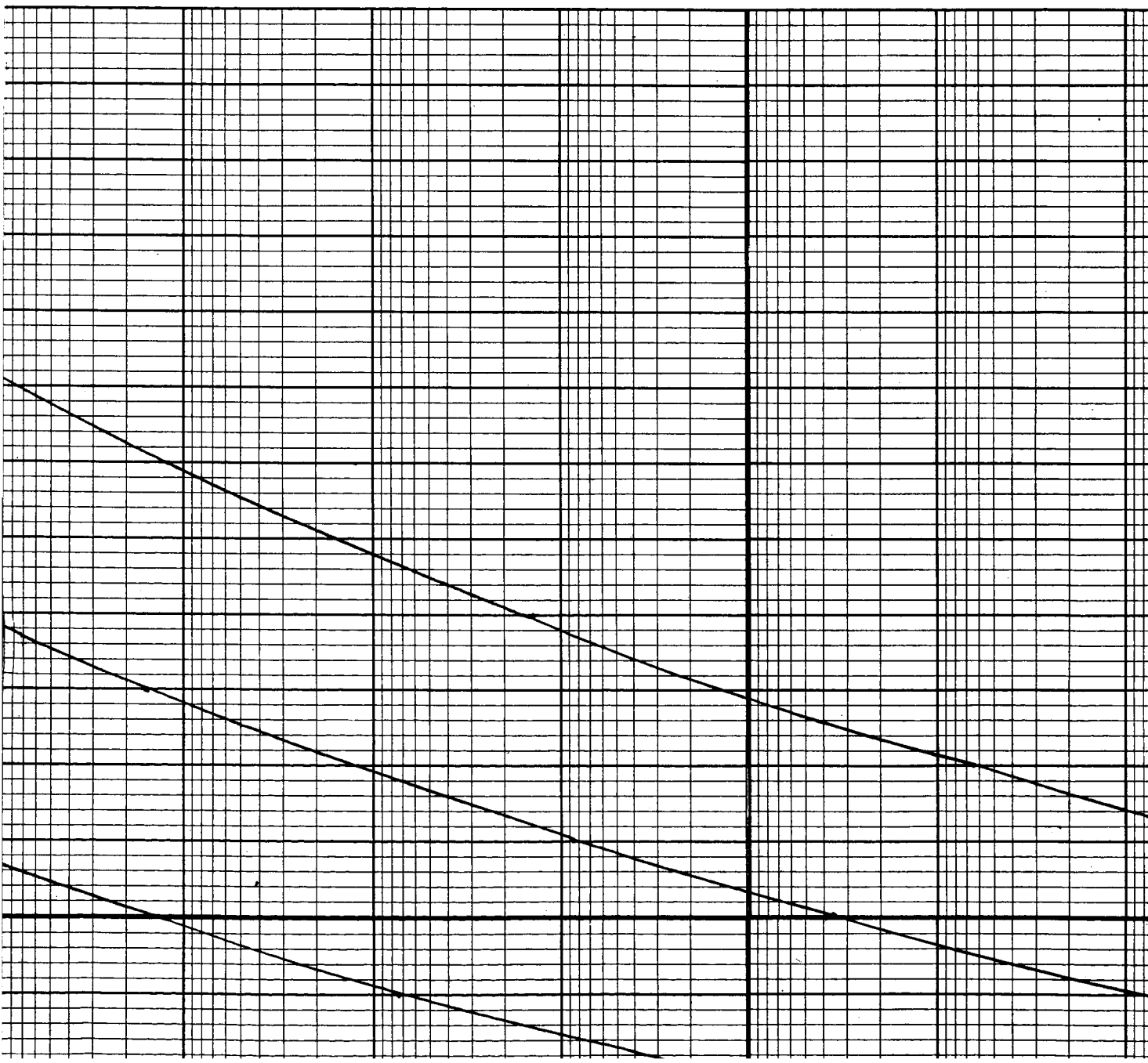
THICKNESS = 150 Å



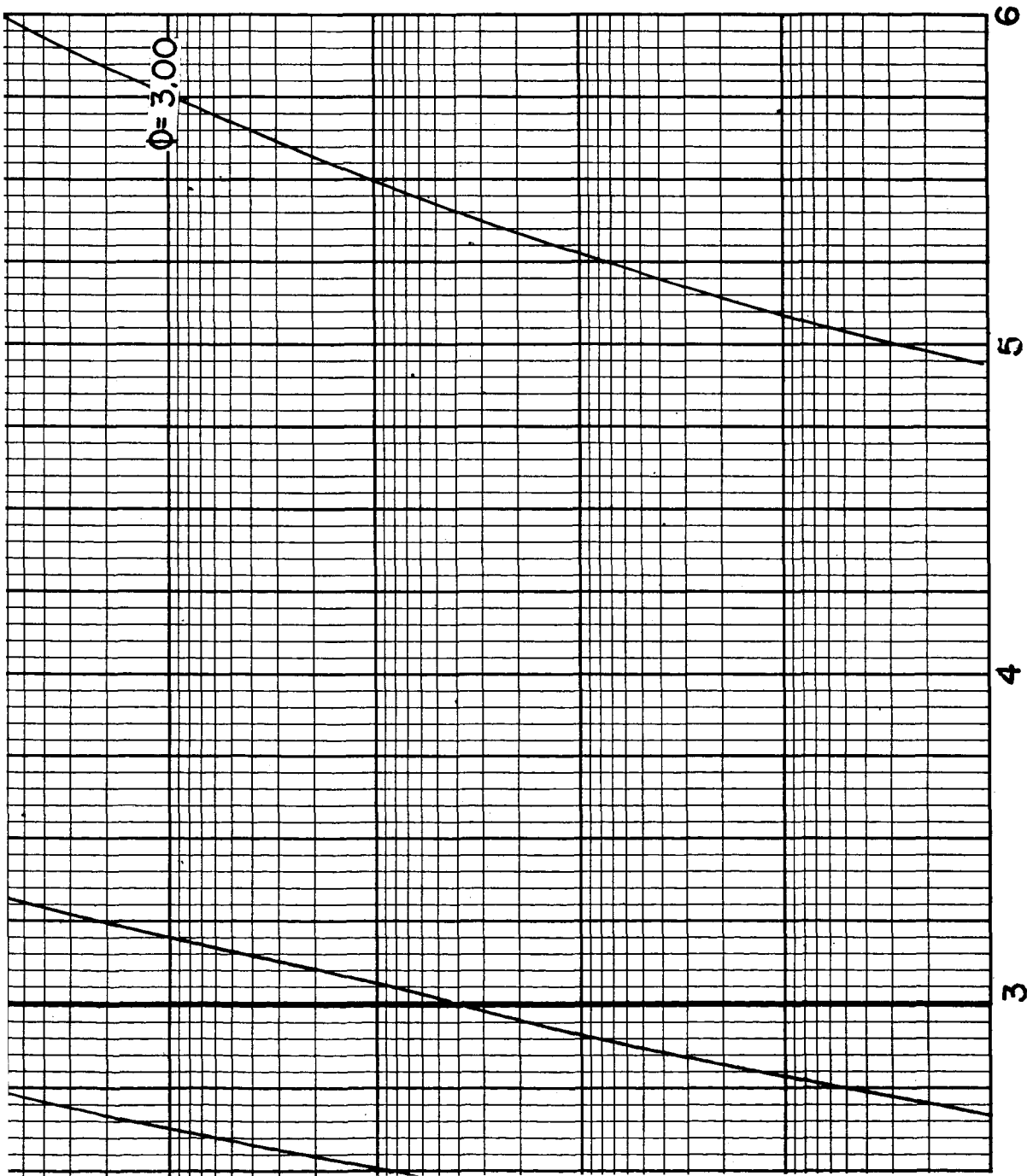
2



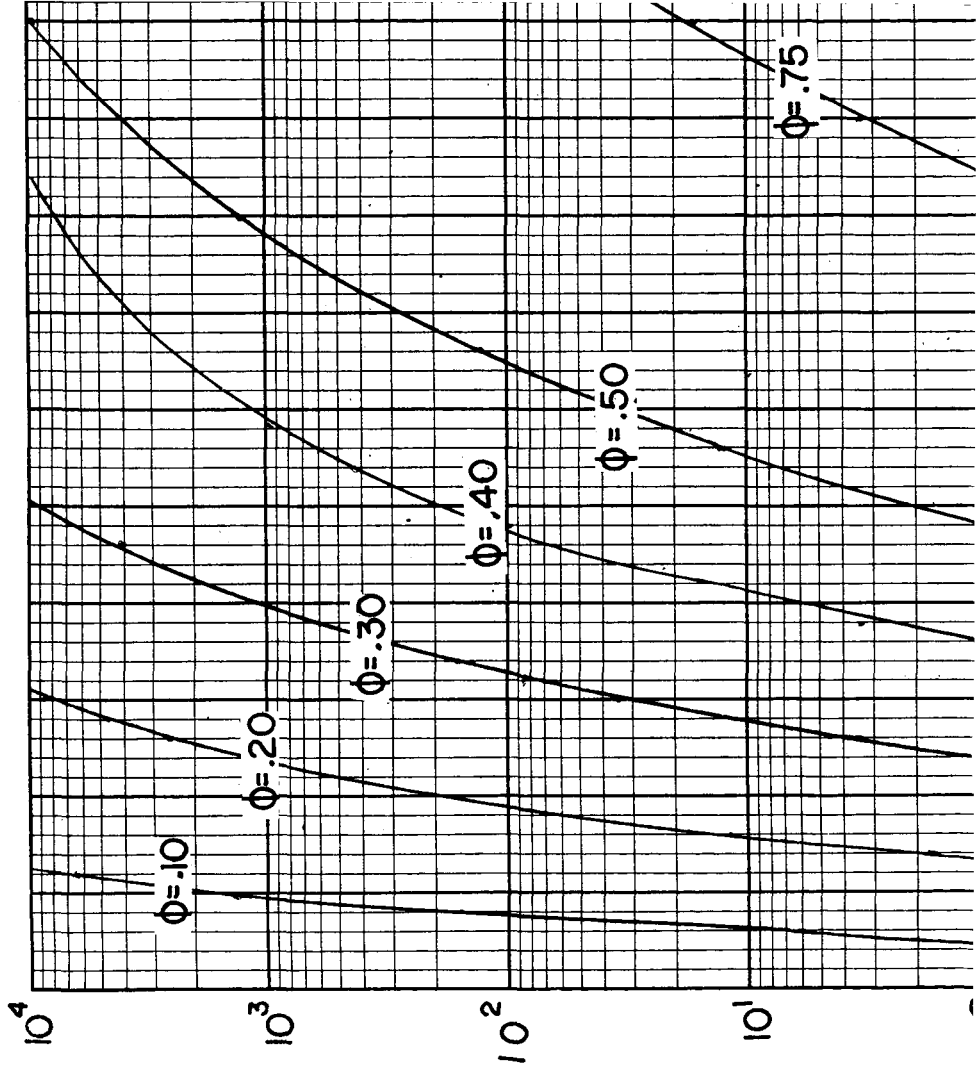
3



4

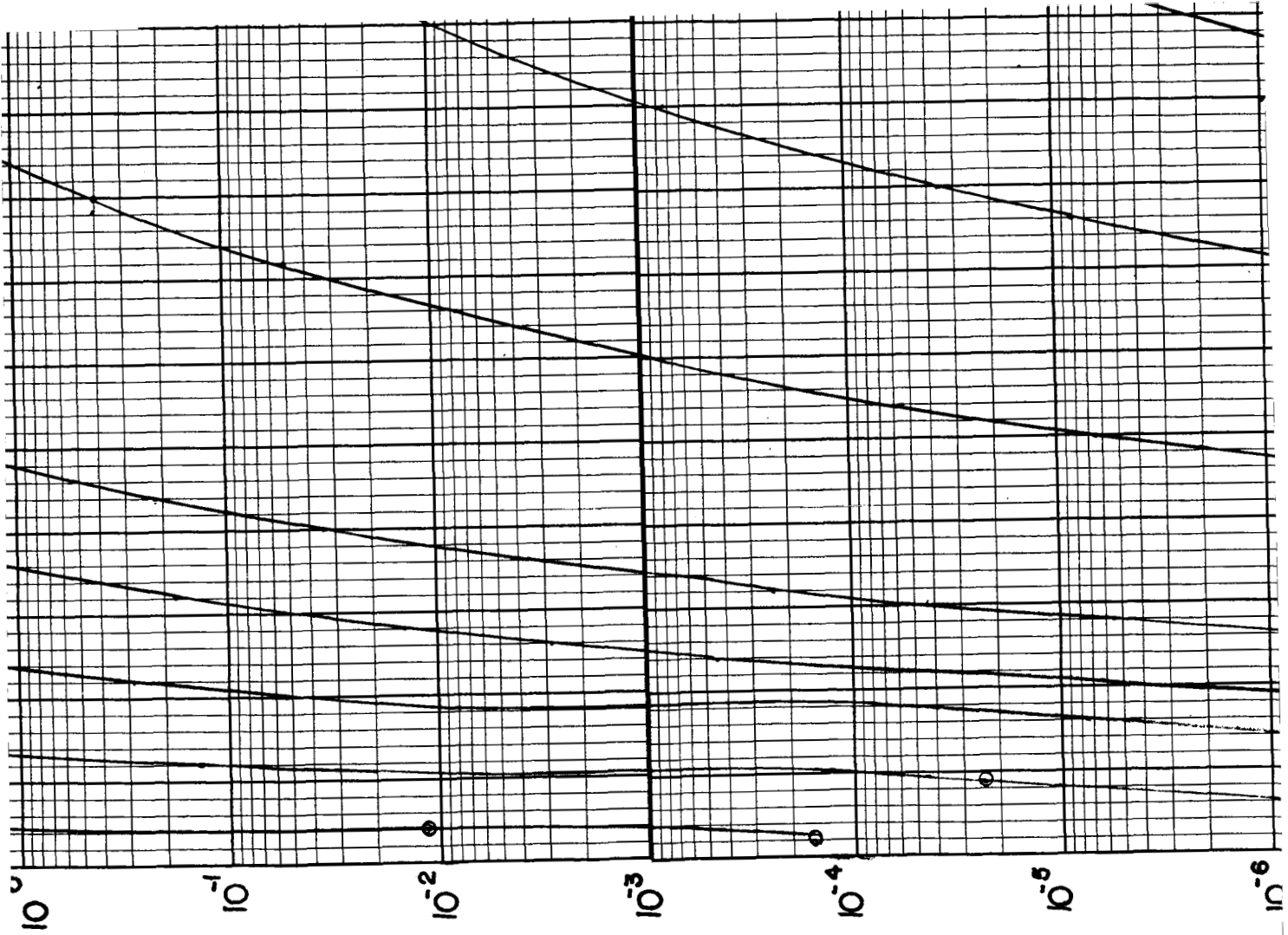


VOLTAGE [VOLTS]



~~scribble~~

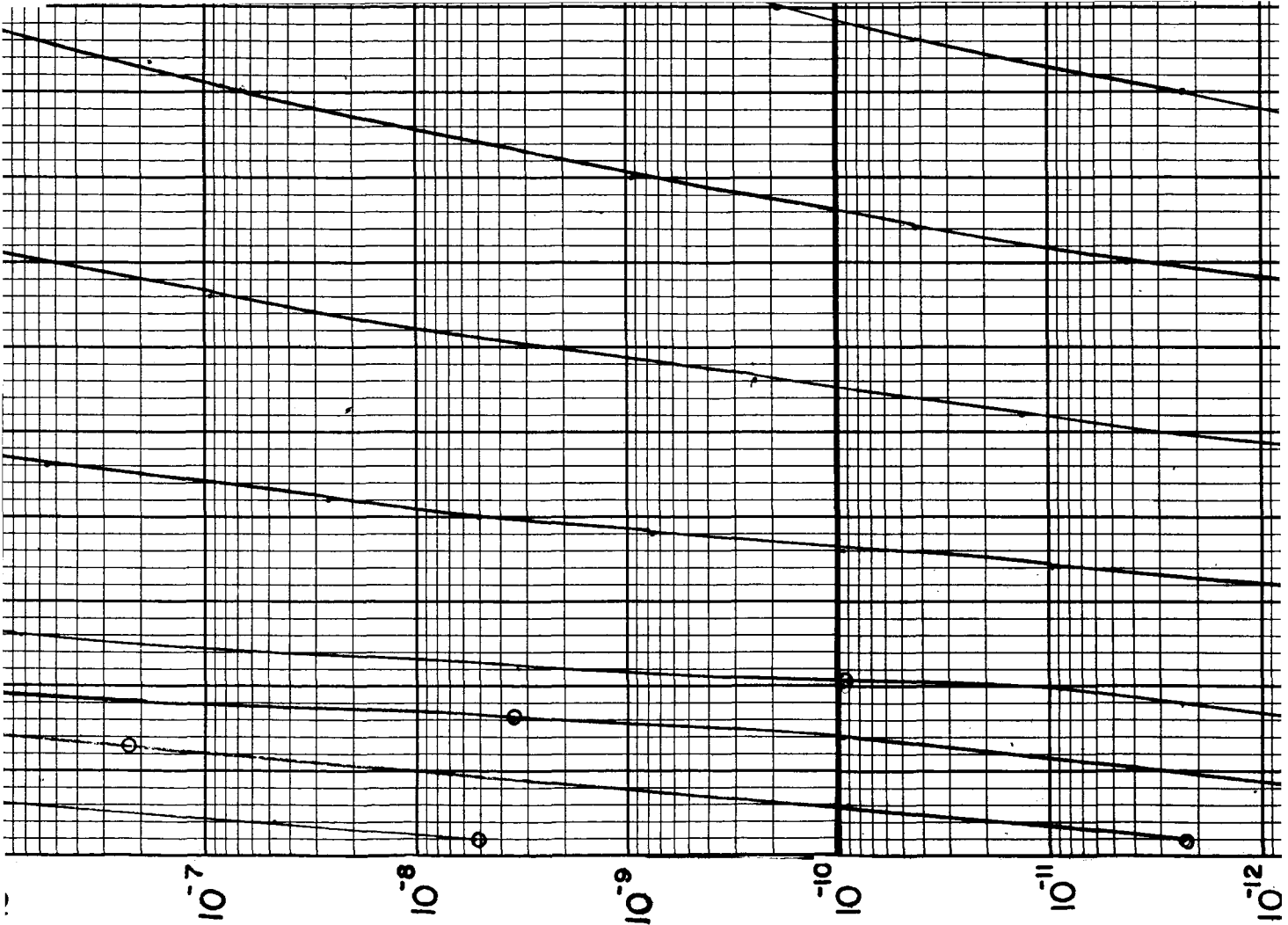
5



[AMP / CM²]

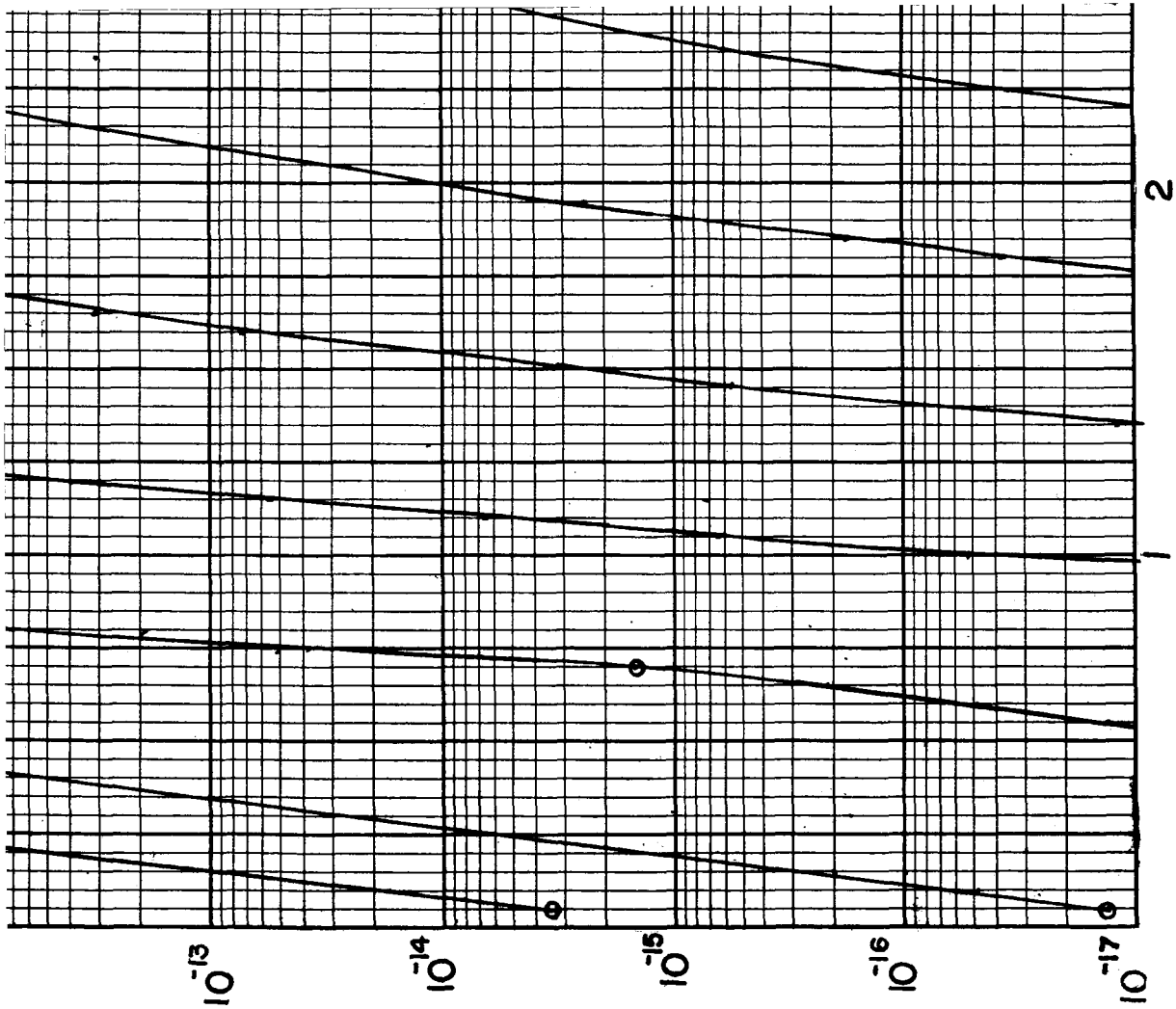
NSITY

2



CURRENT DE

7

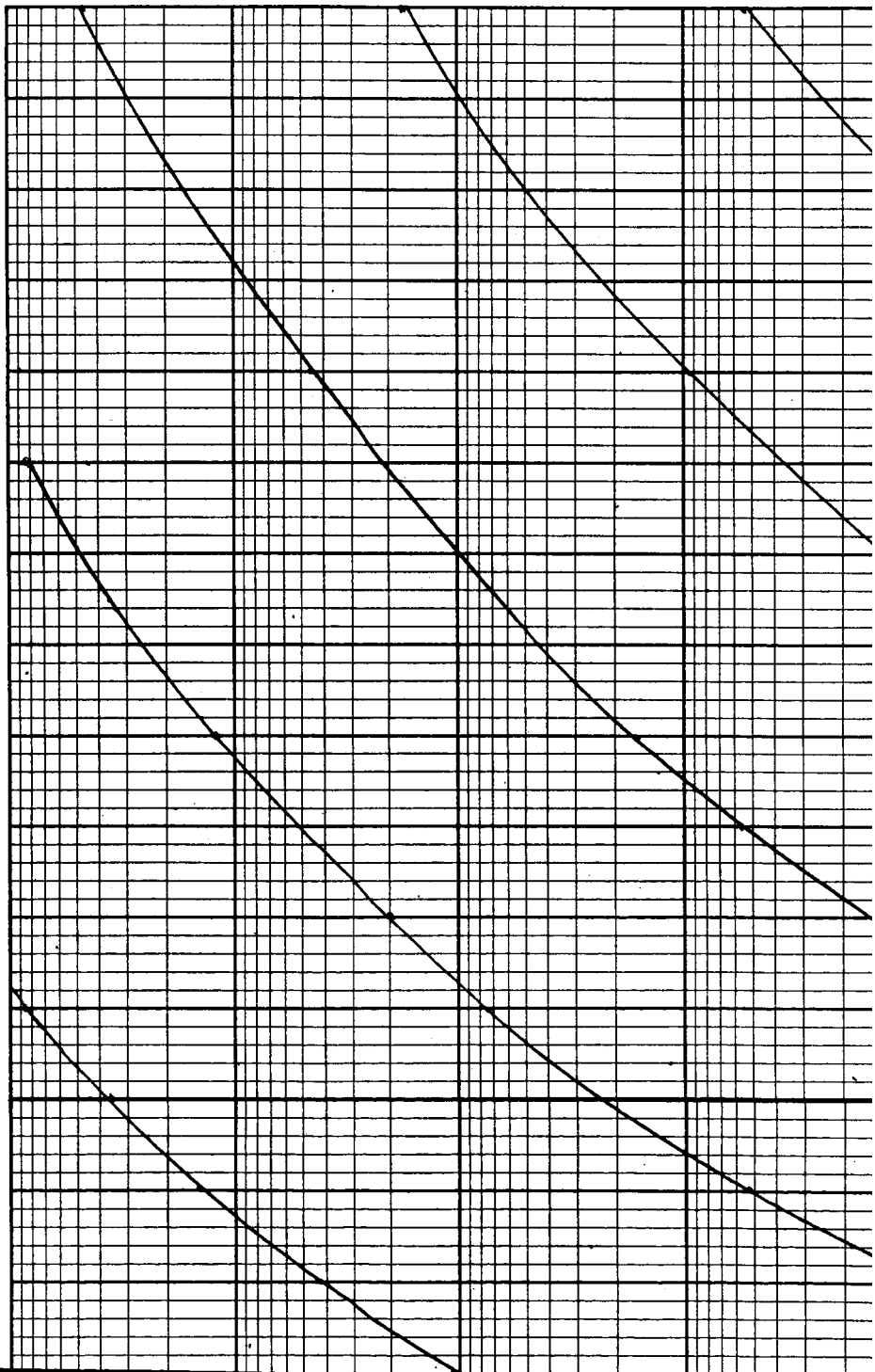


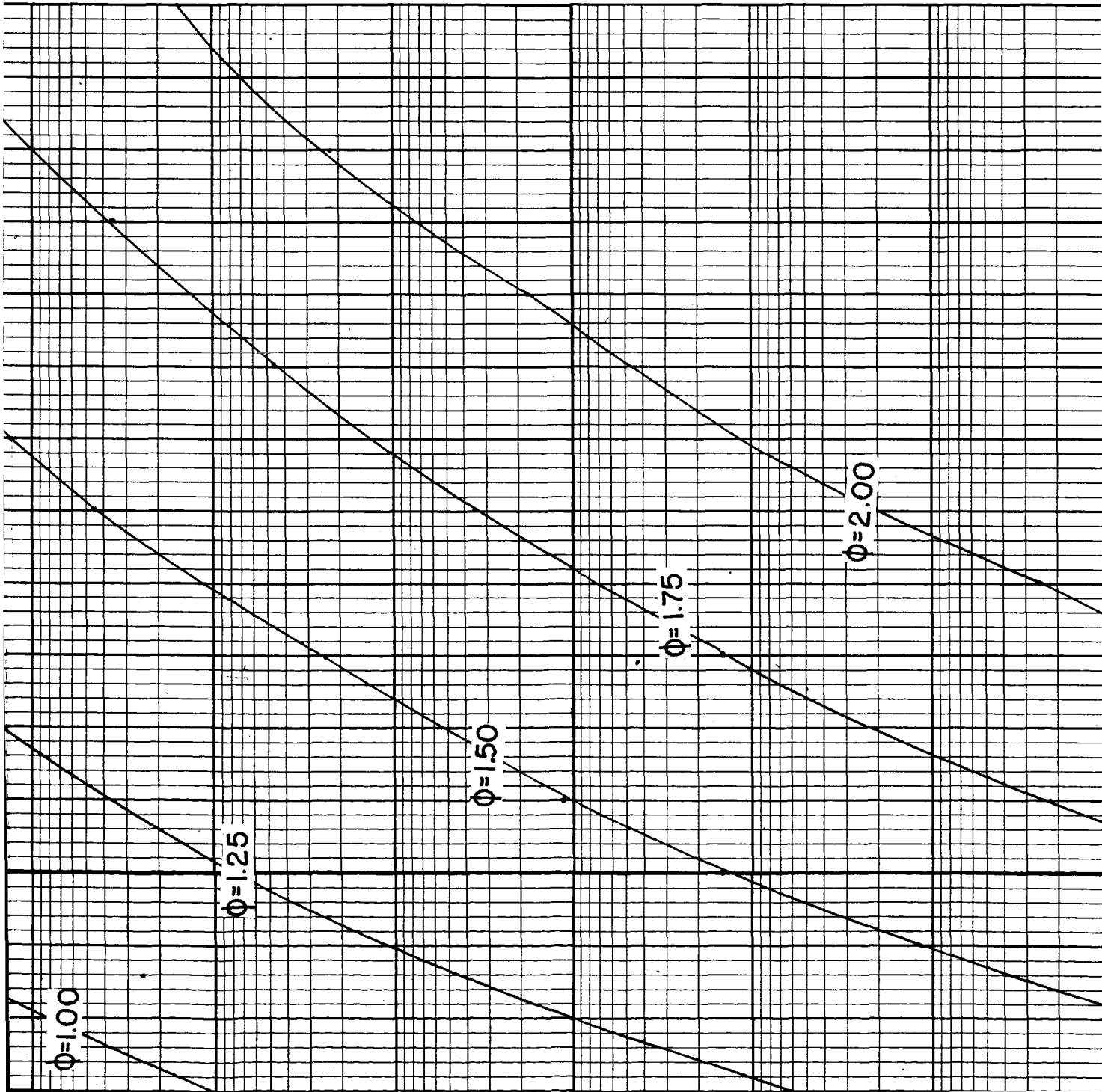
8

V

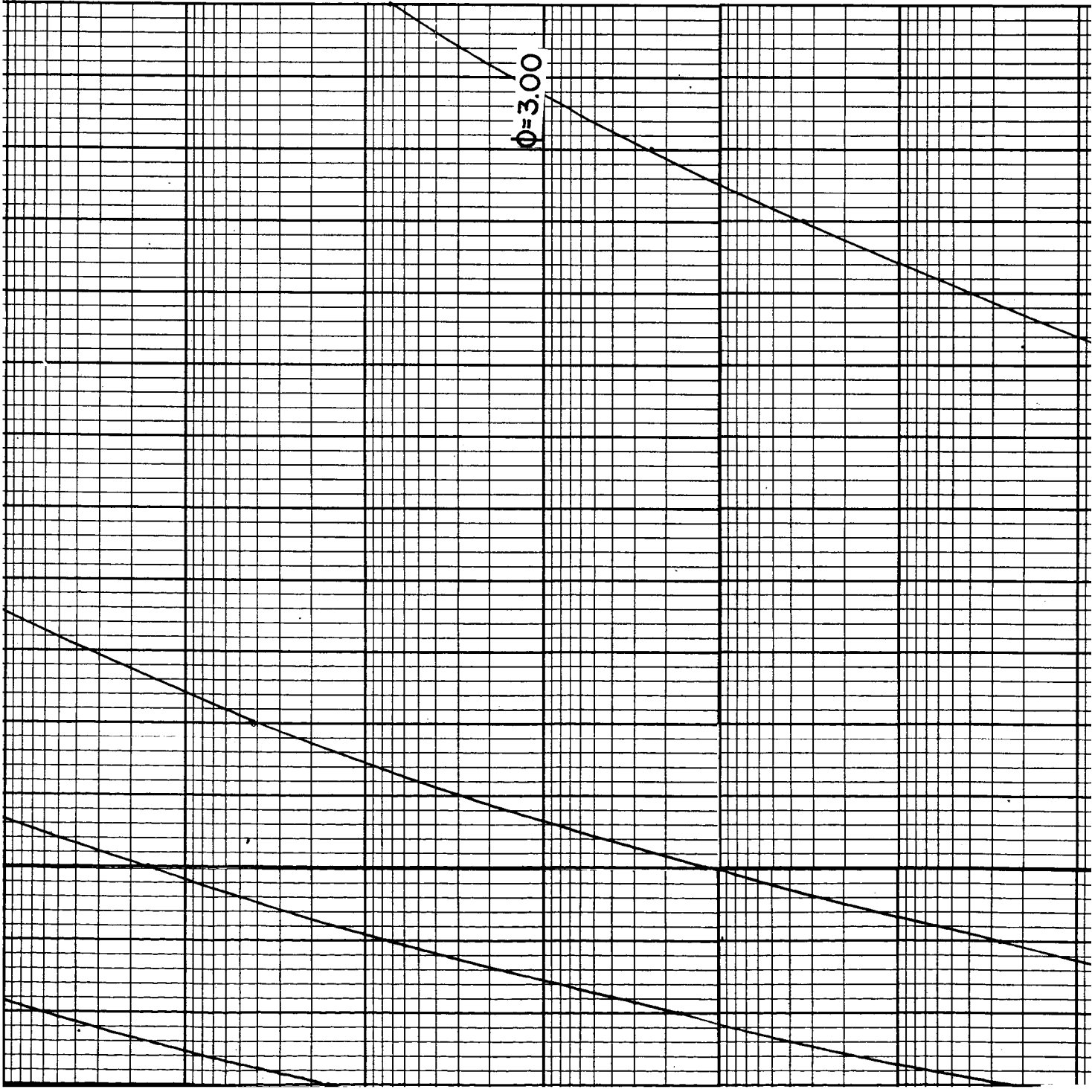
3

THICKNESS = 120 Å

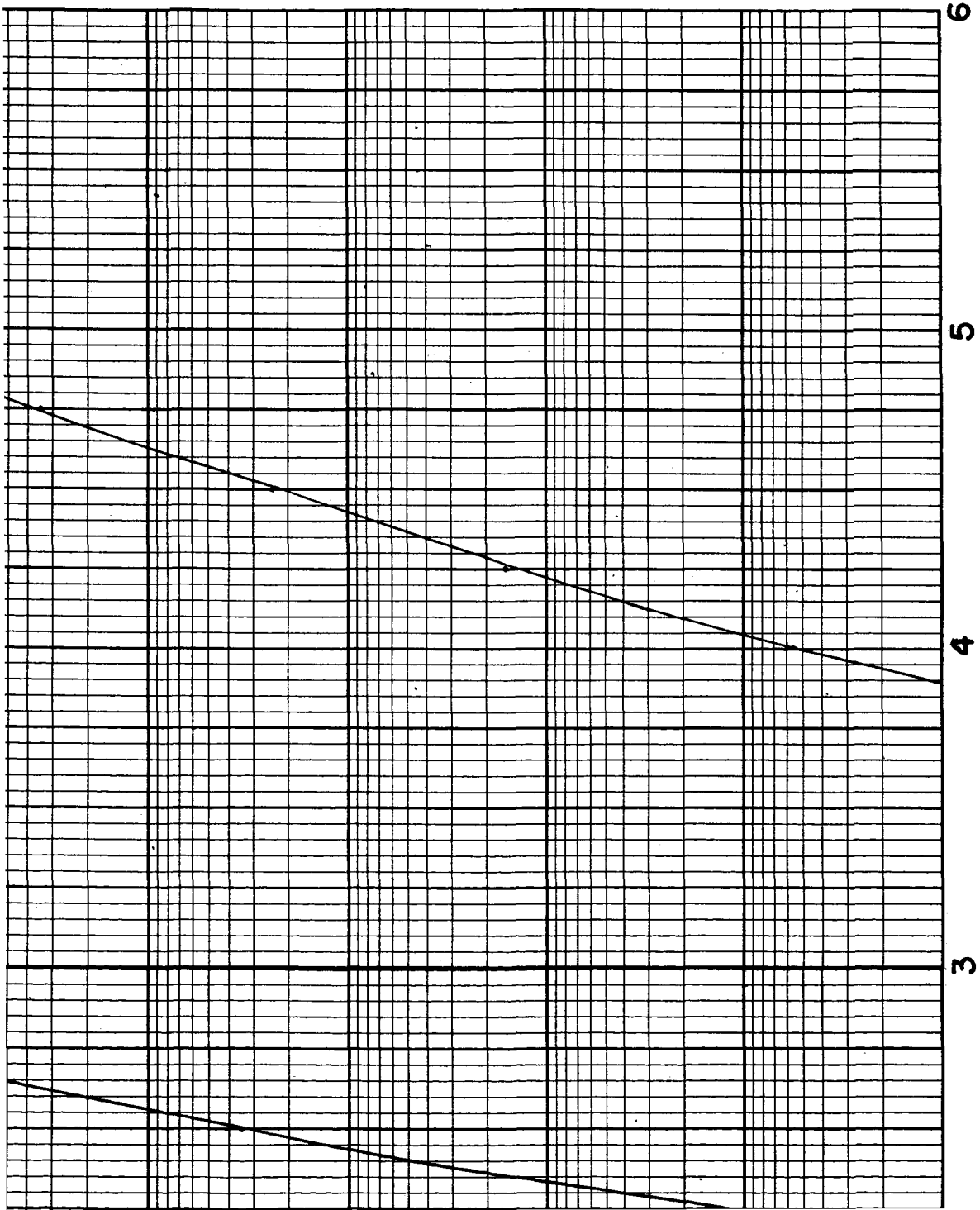




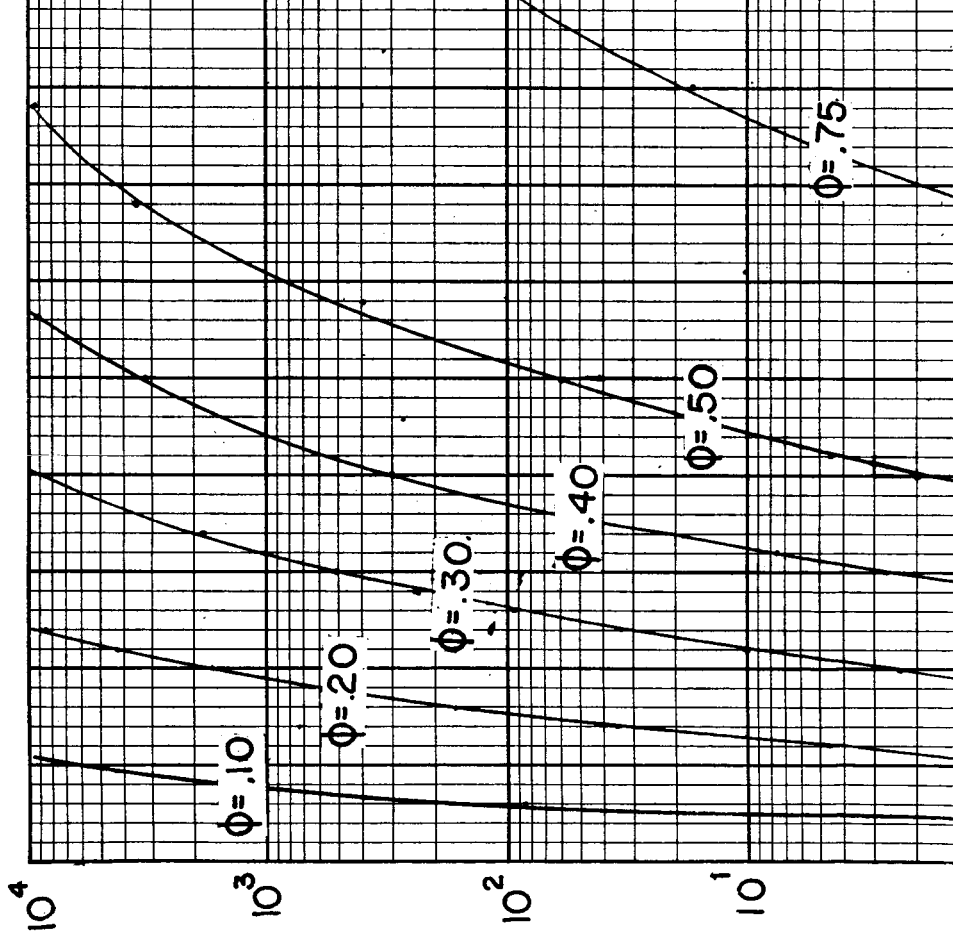
3



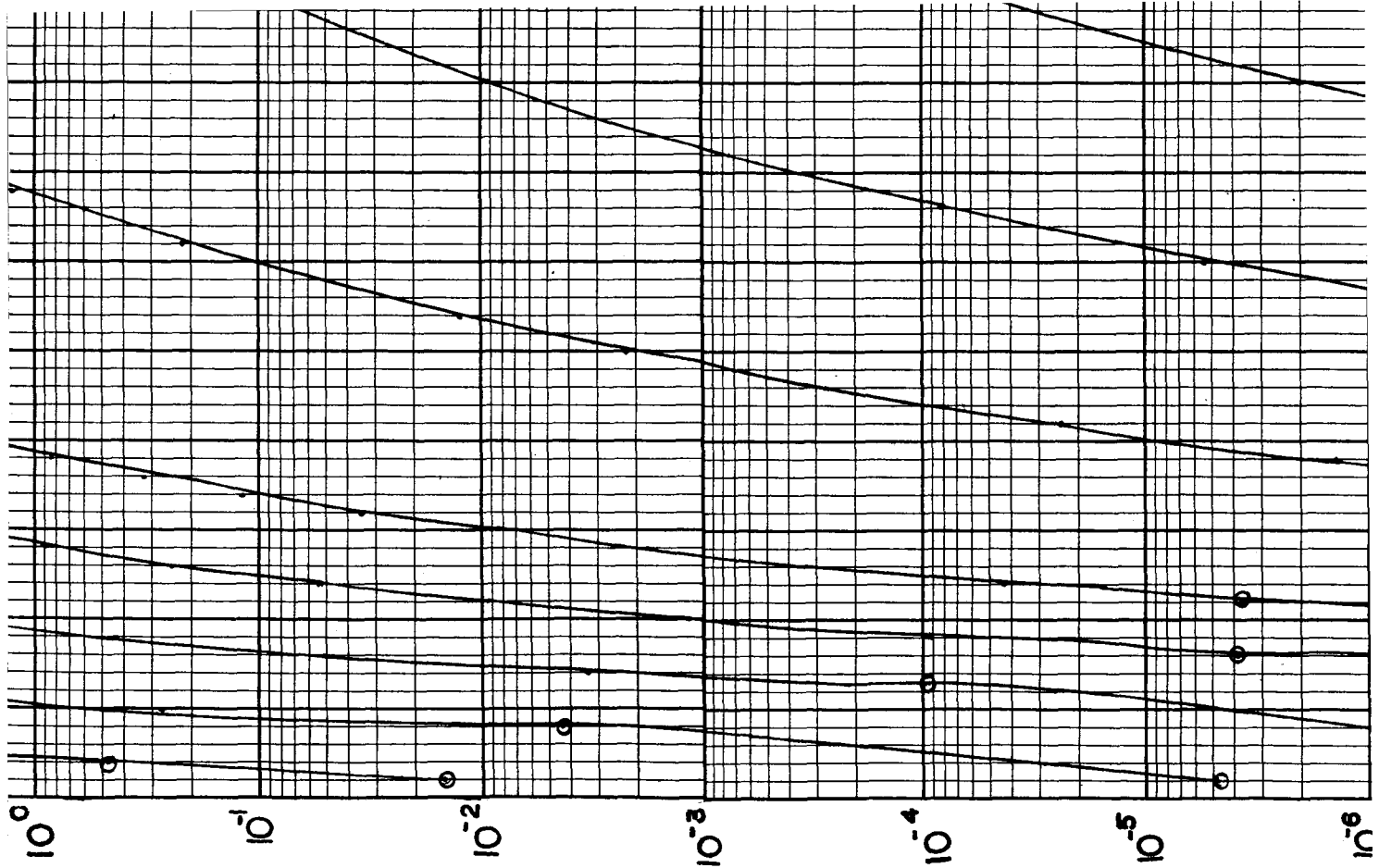
4



VOLTAGE [VOLTS]



W

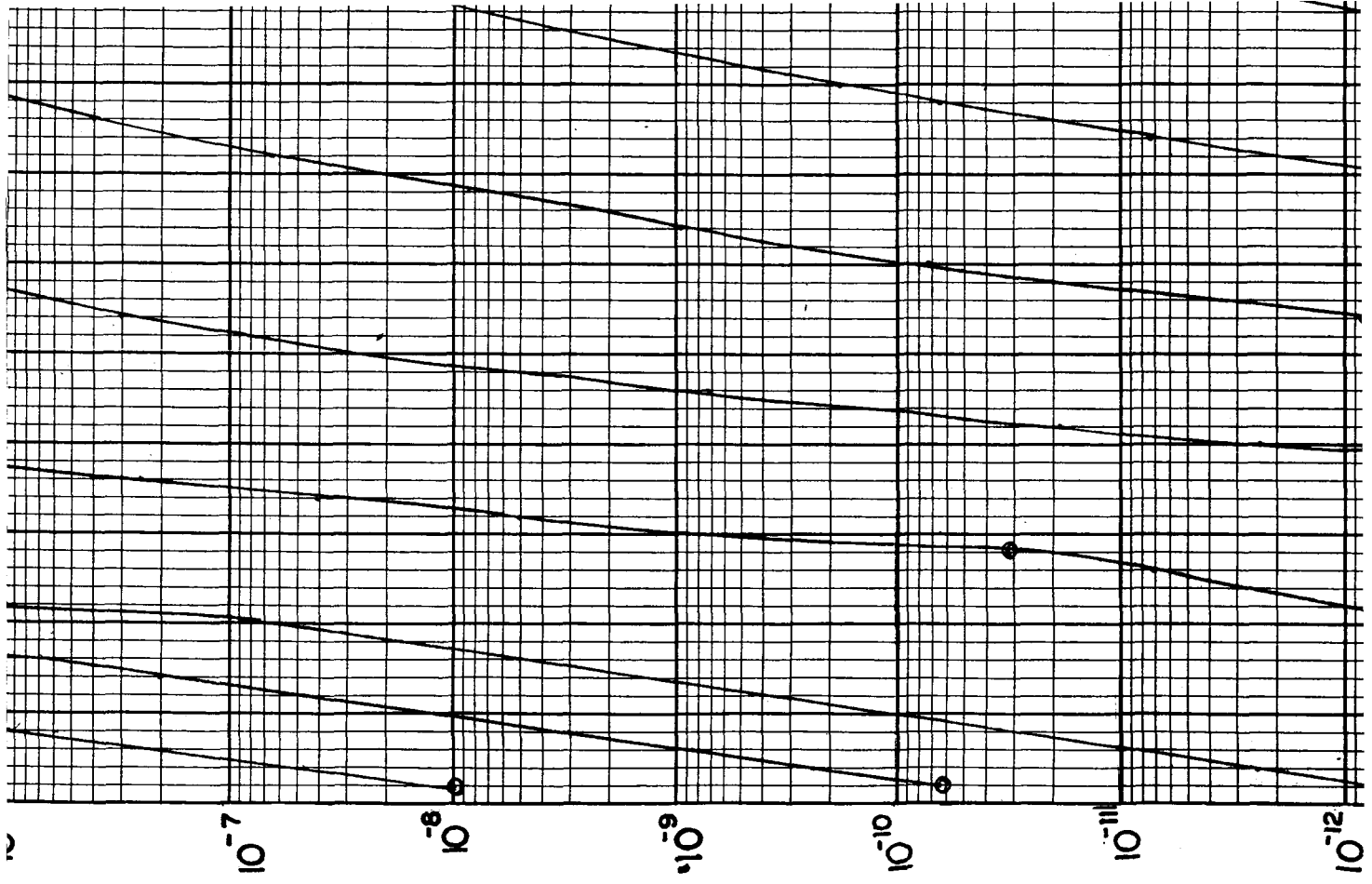


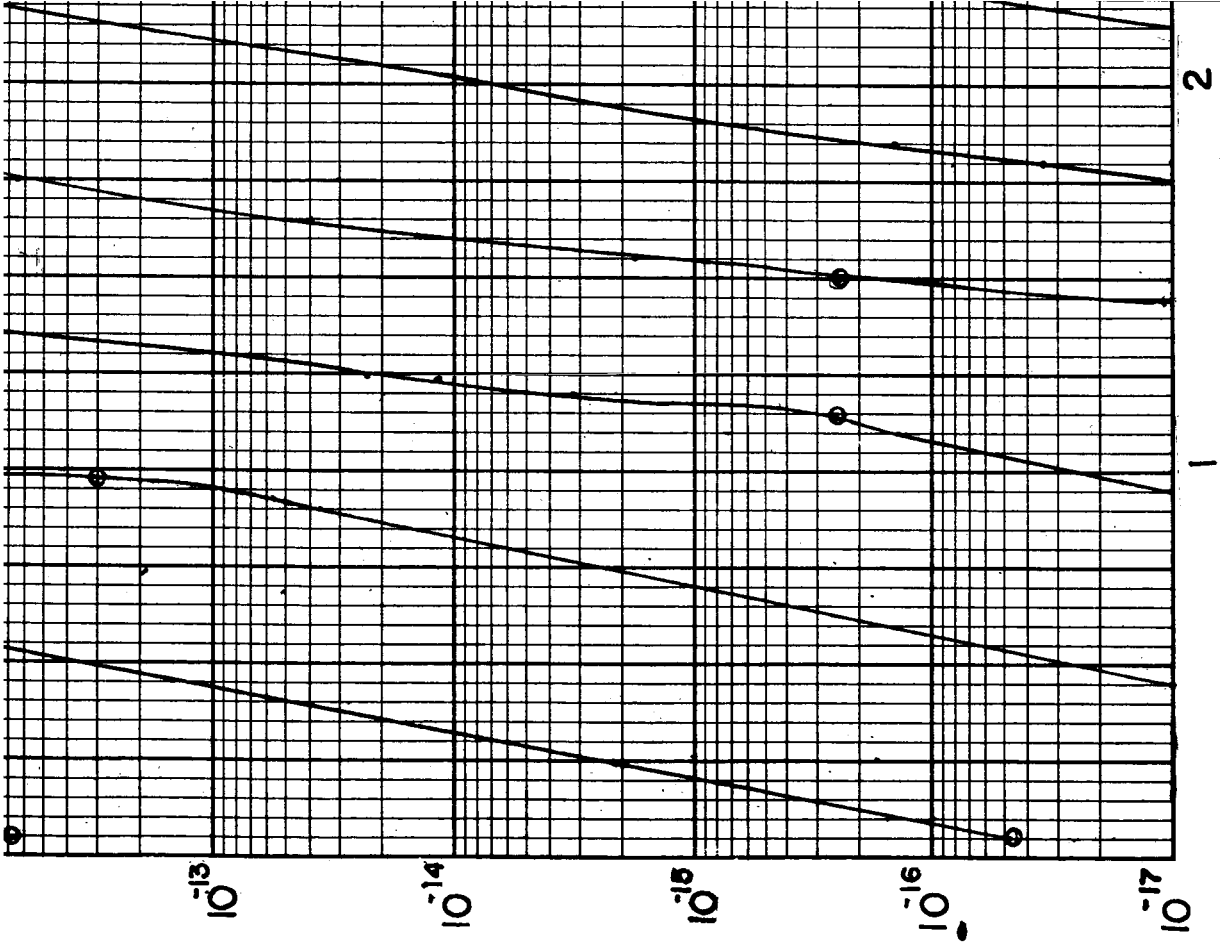
2

[AMP / CM²]

Y

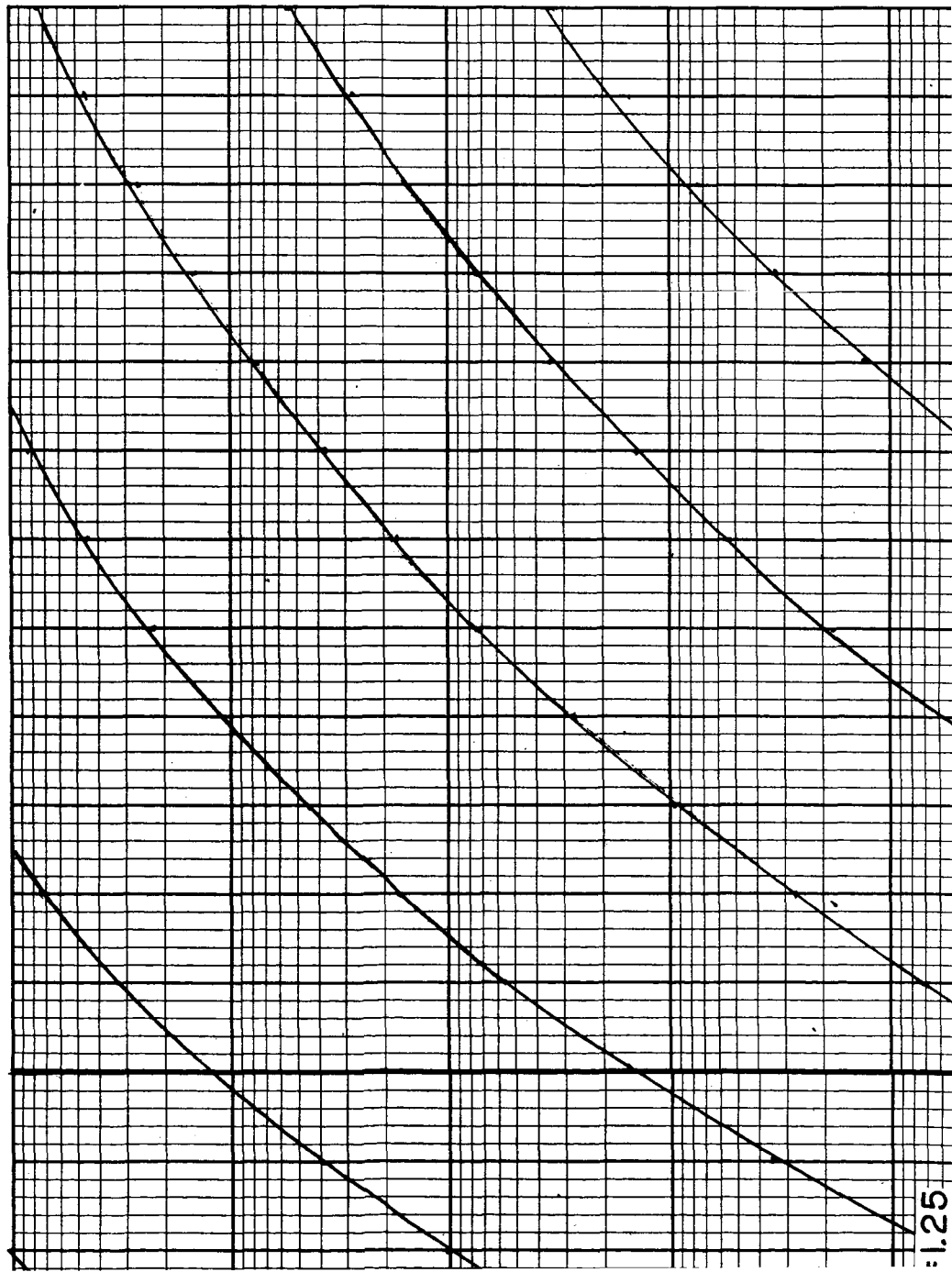
7
CURRENT DENSITY





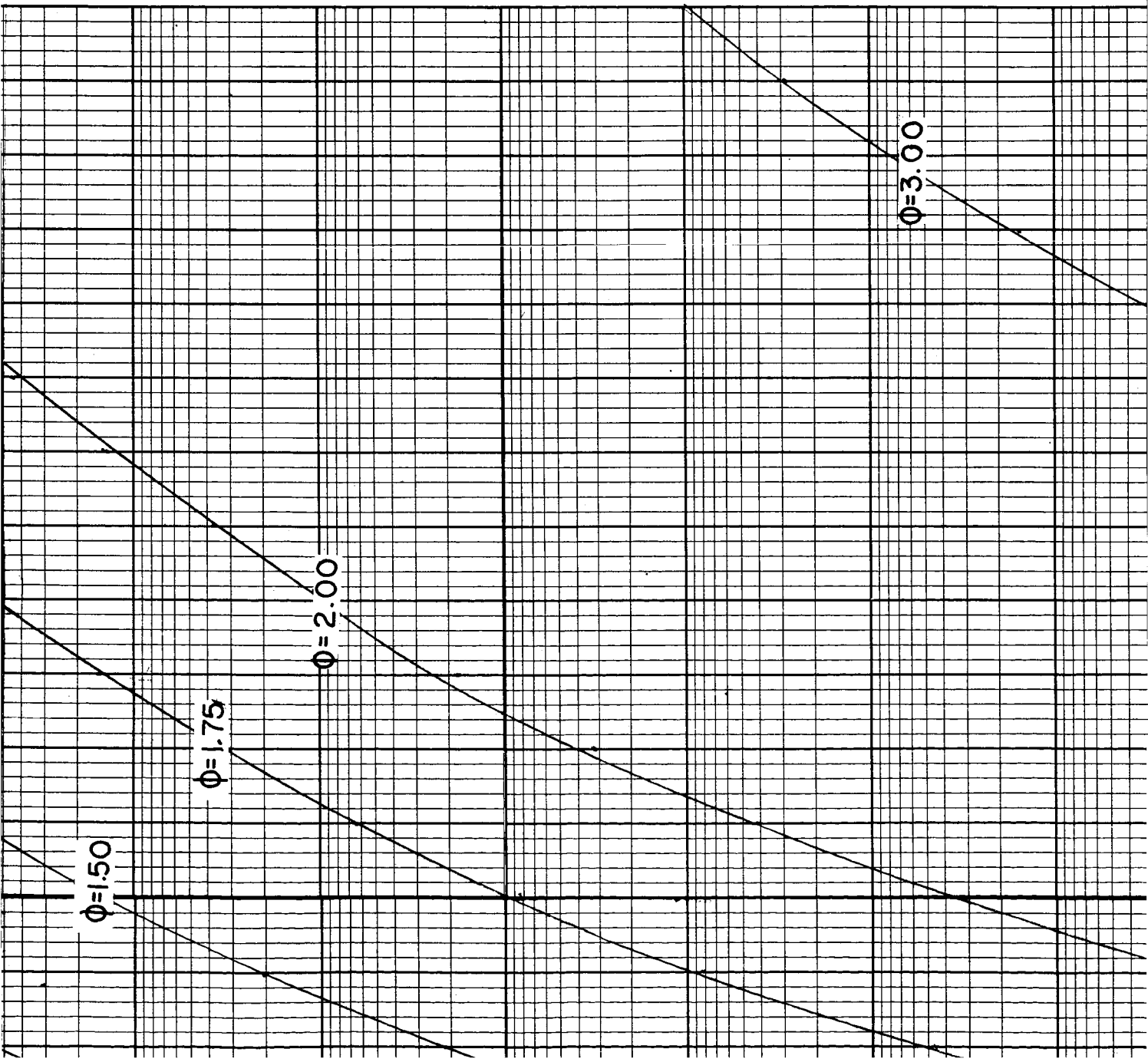
8

THICKNESS = 90 Å

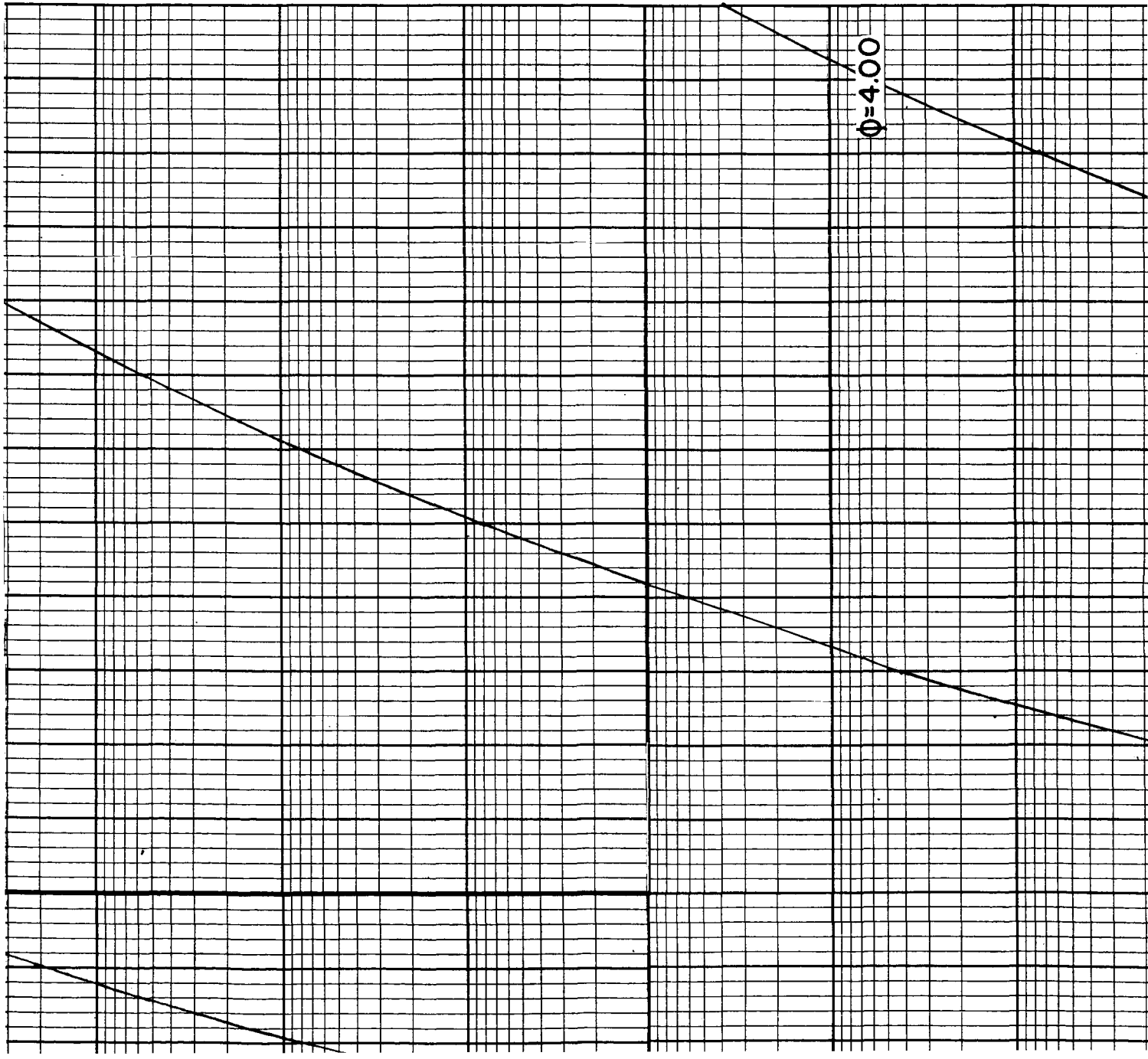


1.25

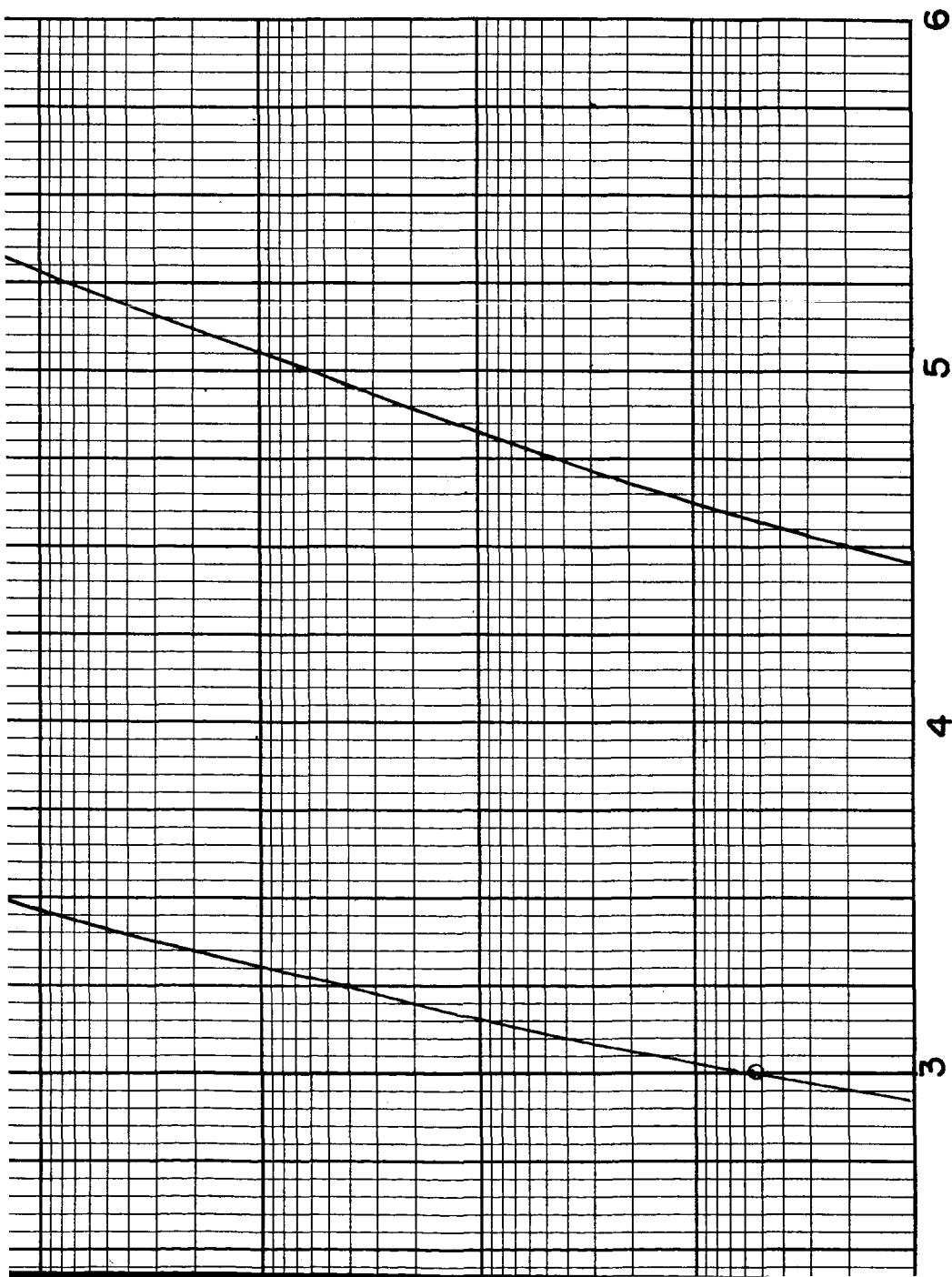
2



3

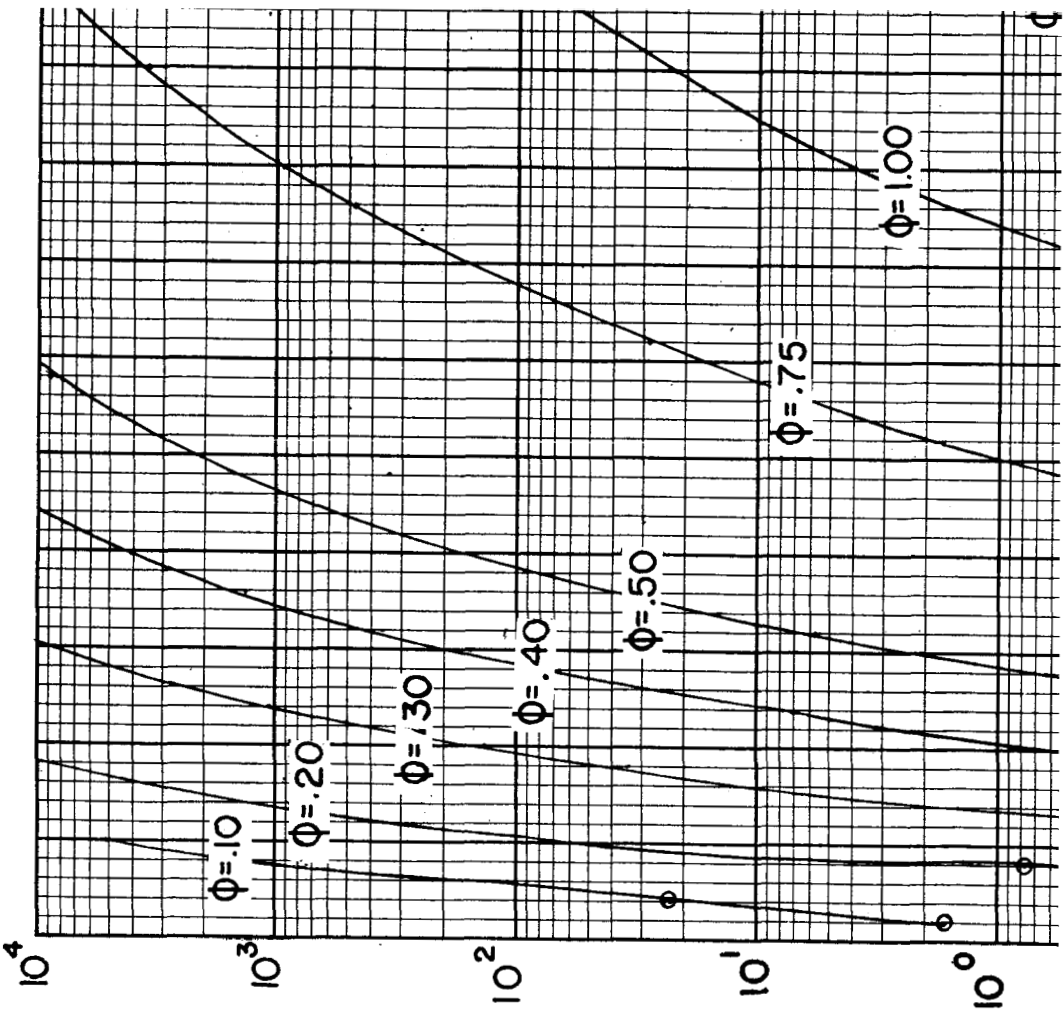


4

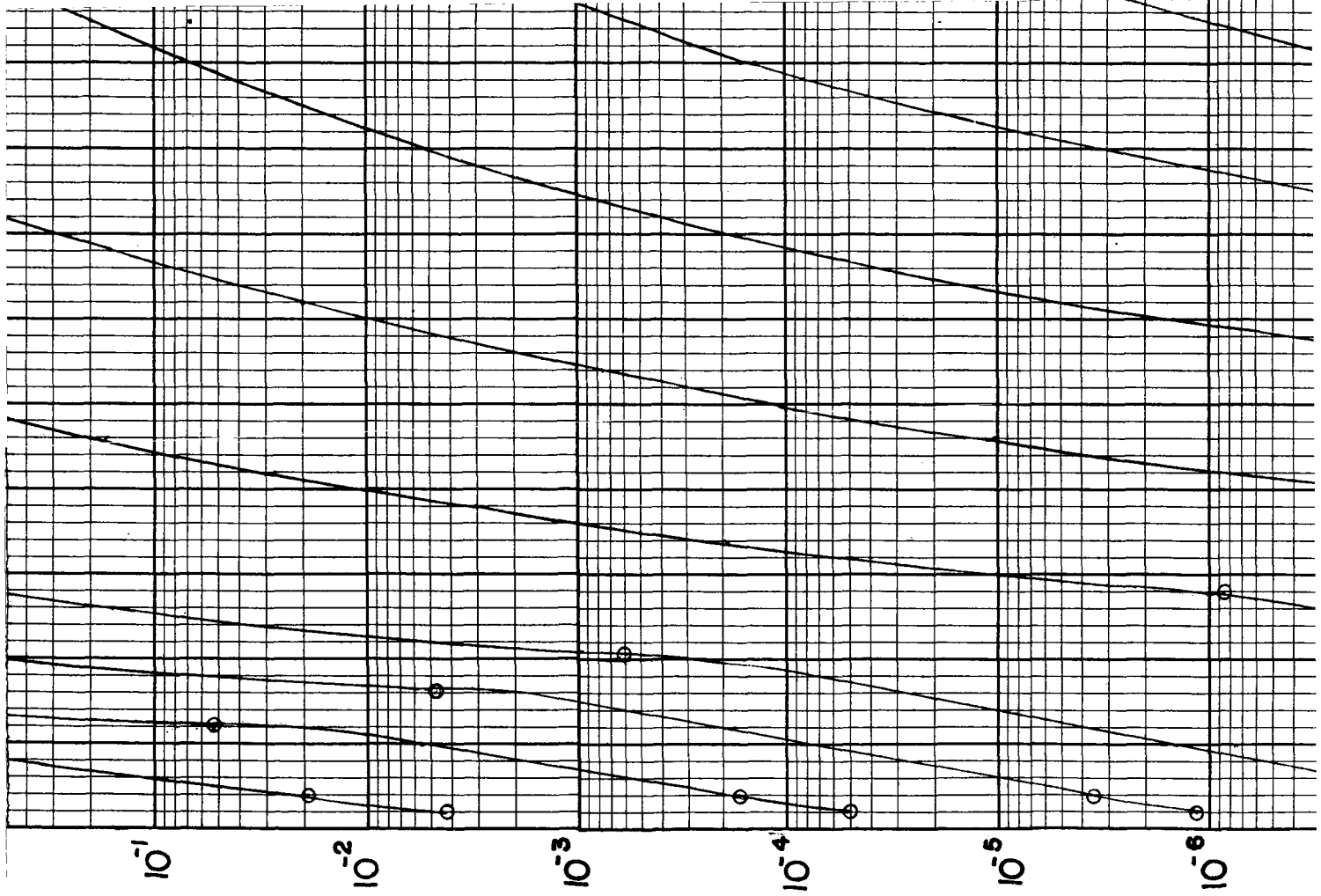


VOLTAGE [volts]

(4)



5



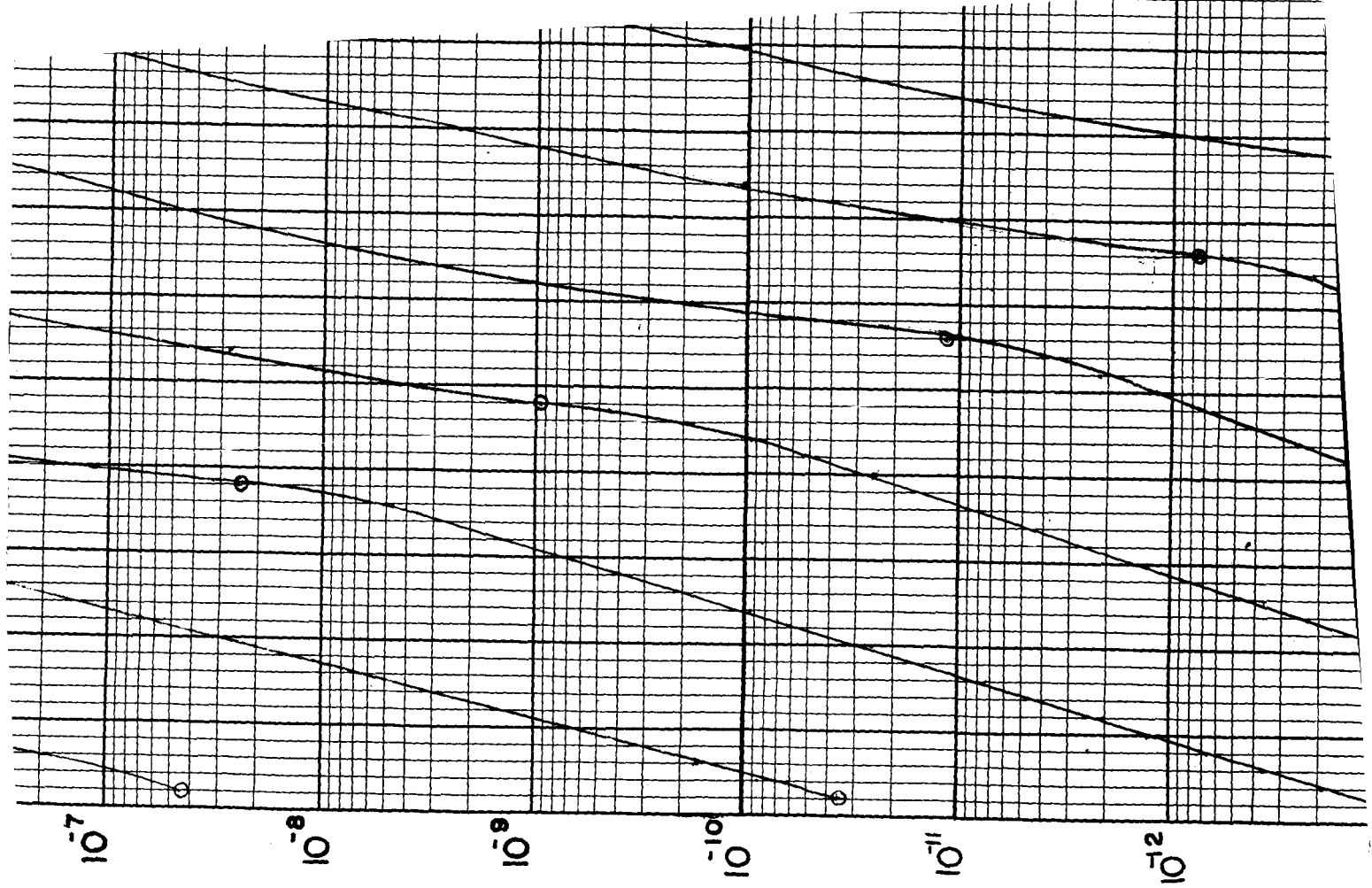
g

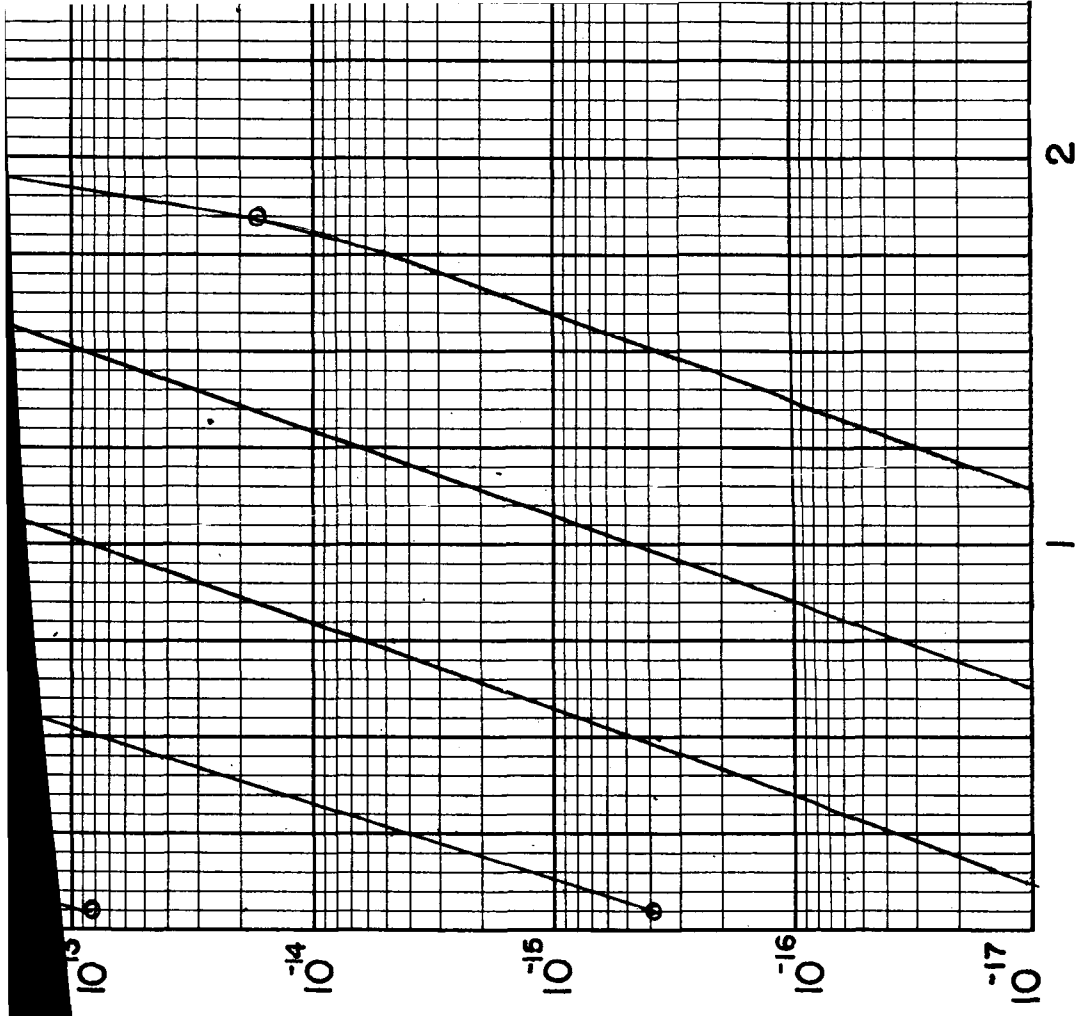
[AMP/CM²]

SITY

CURRENT DEL

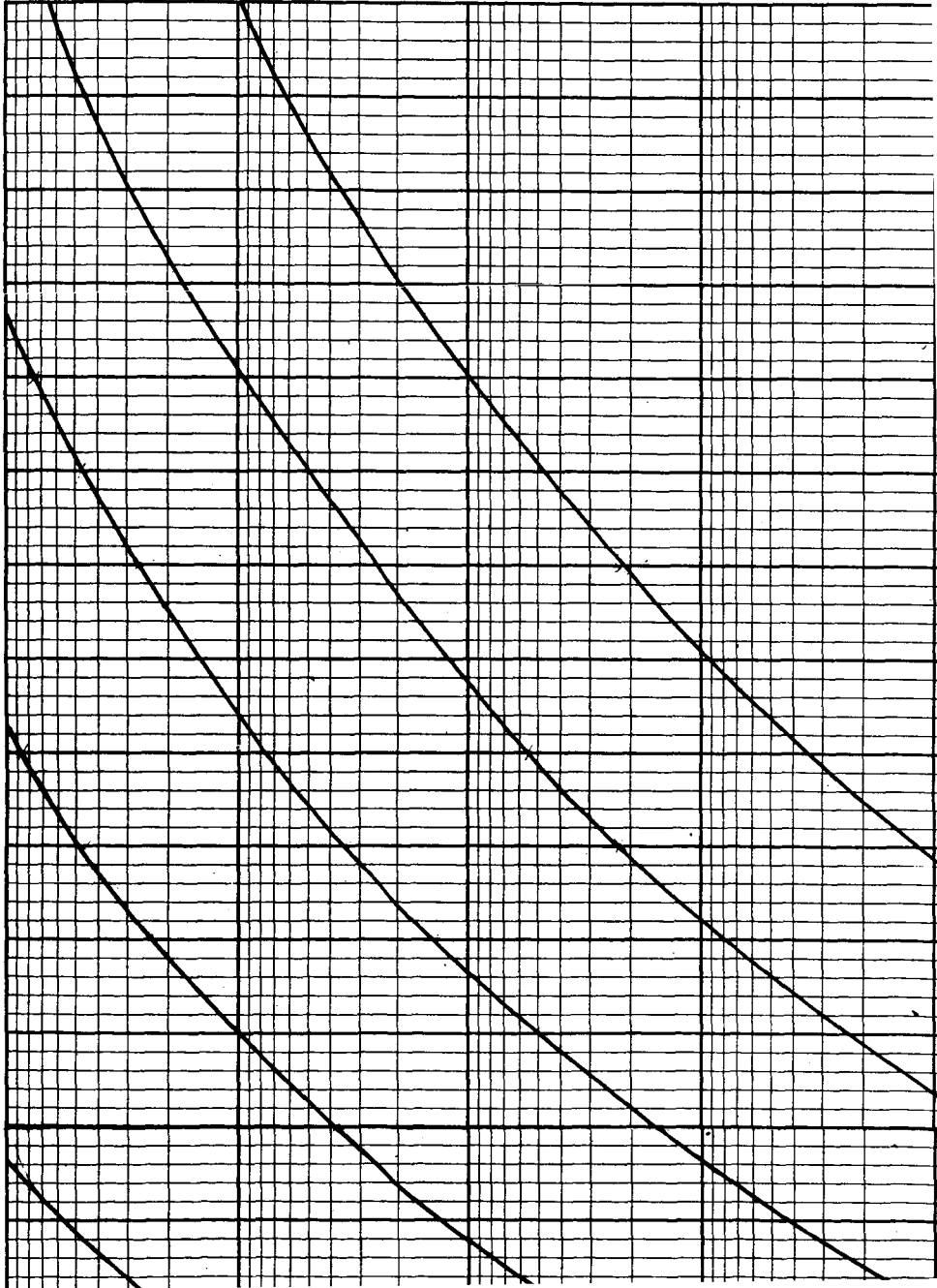
7





8

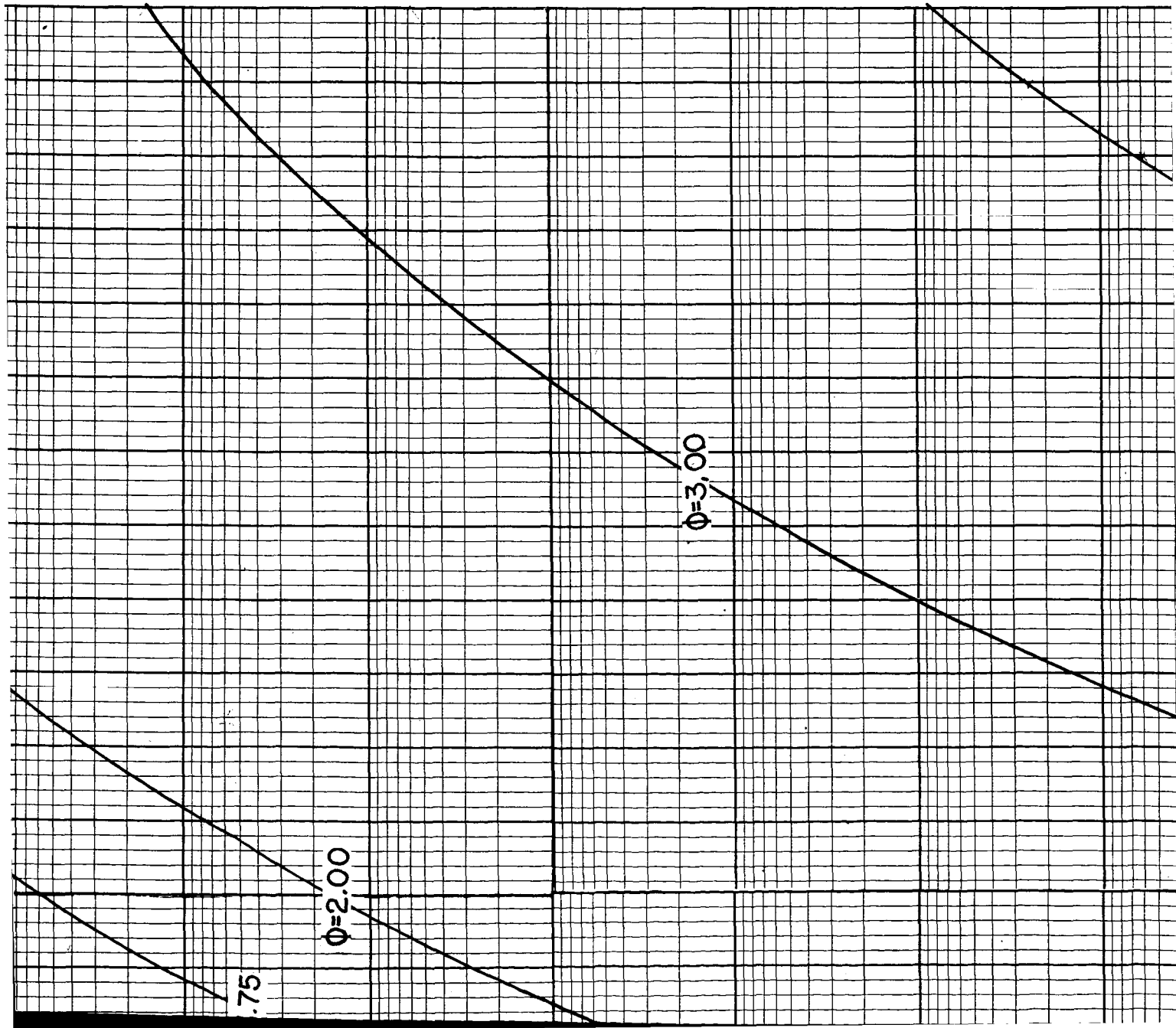
1



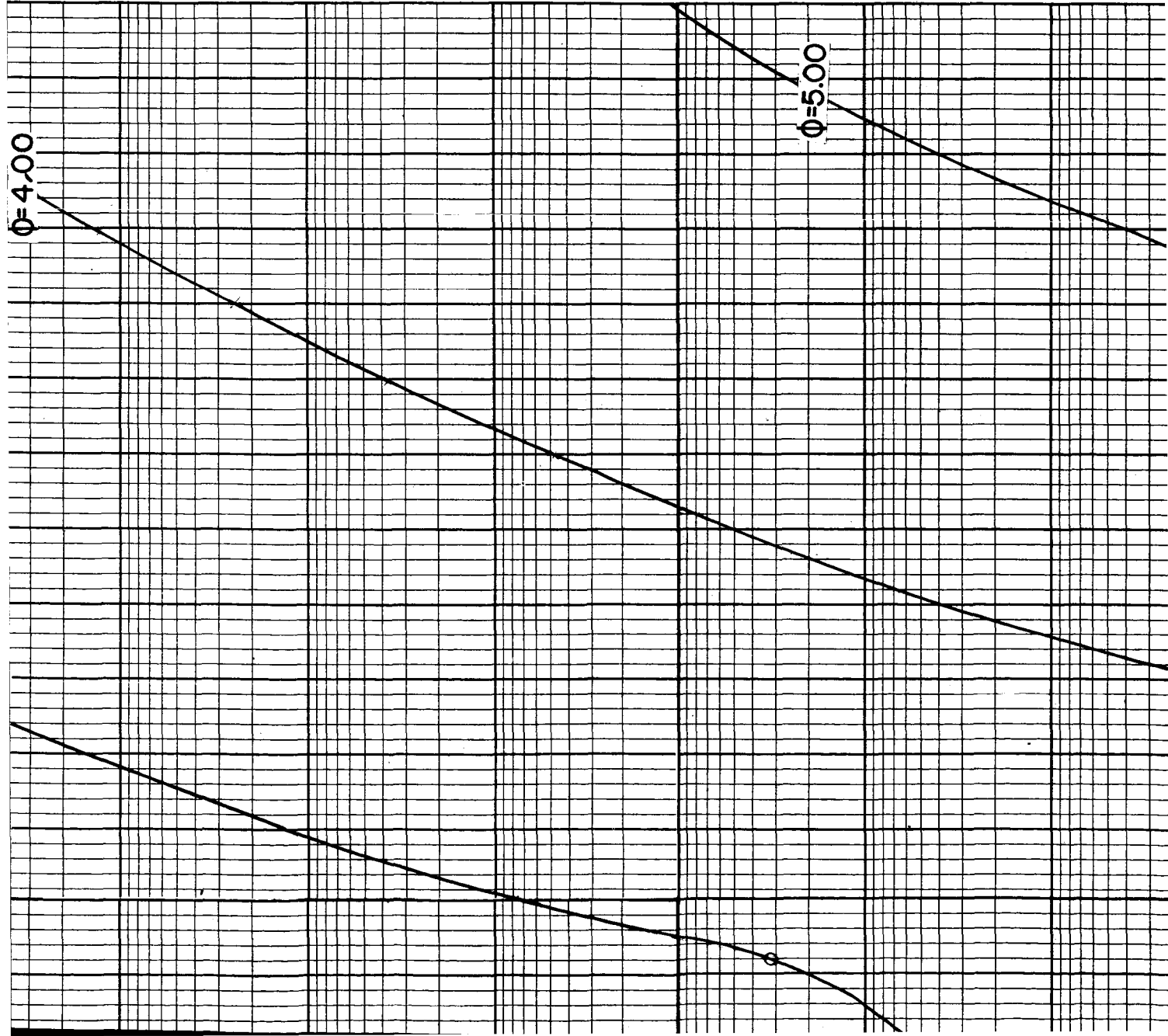
5

THICKNESS = 60 Å

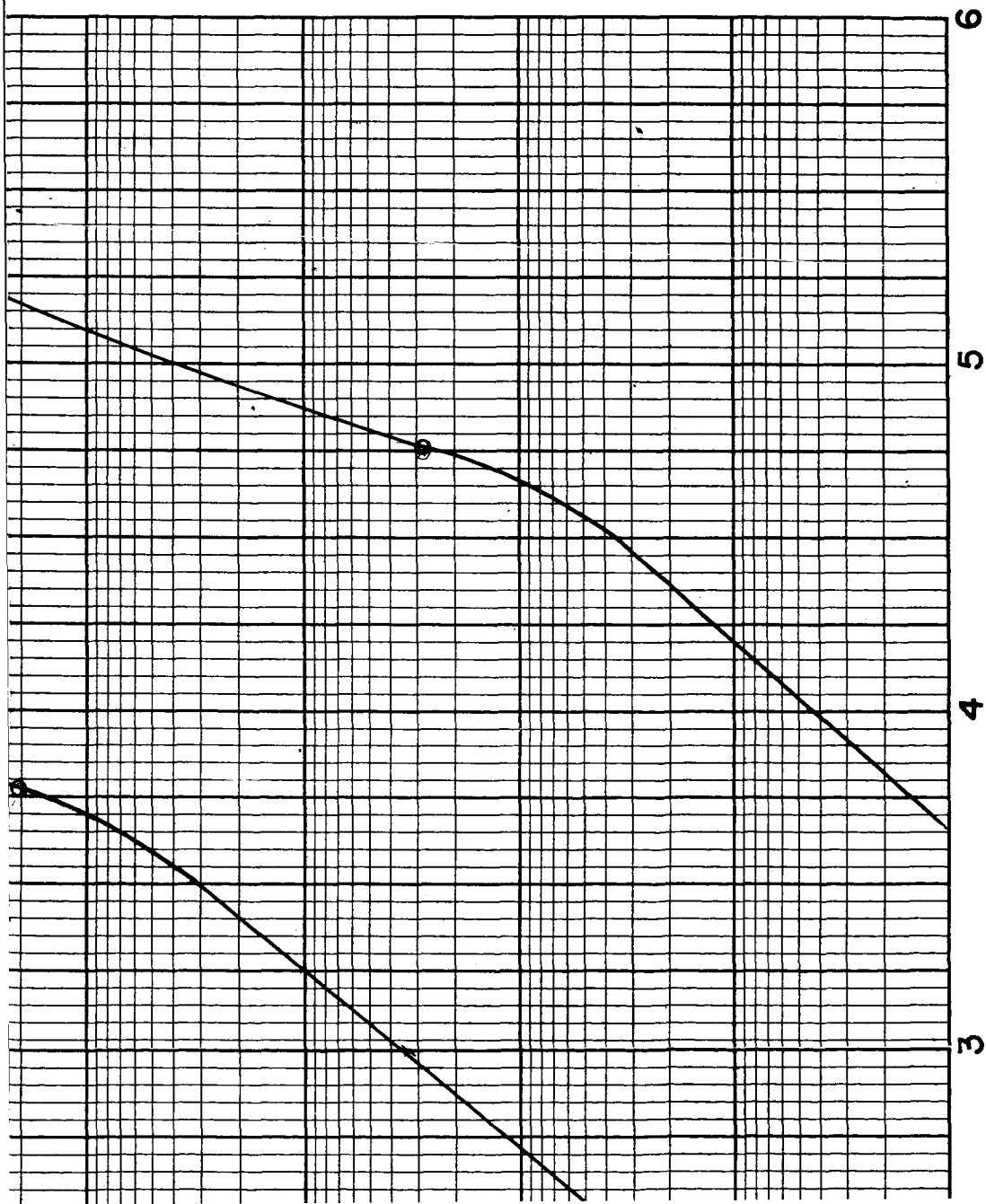
2



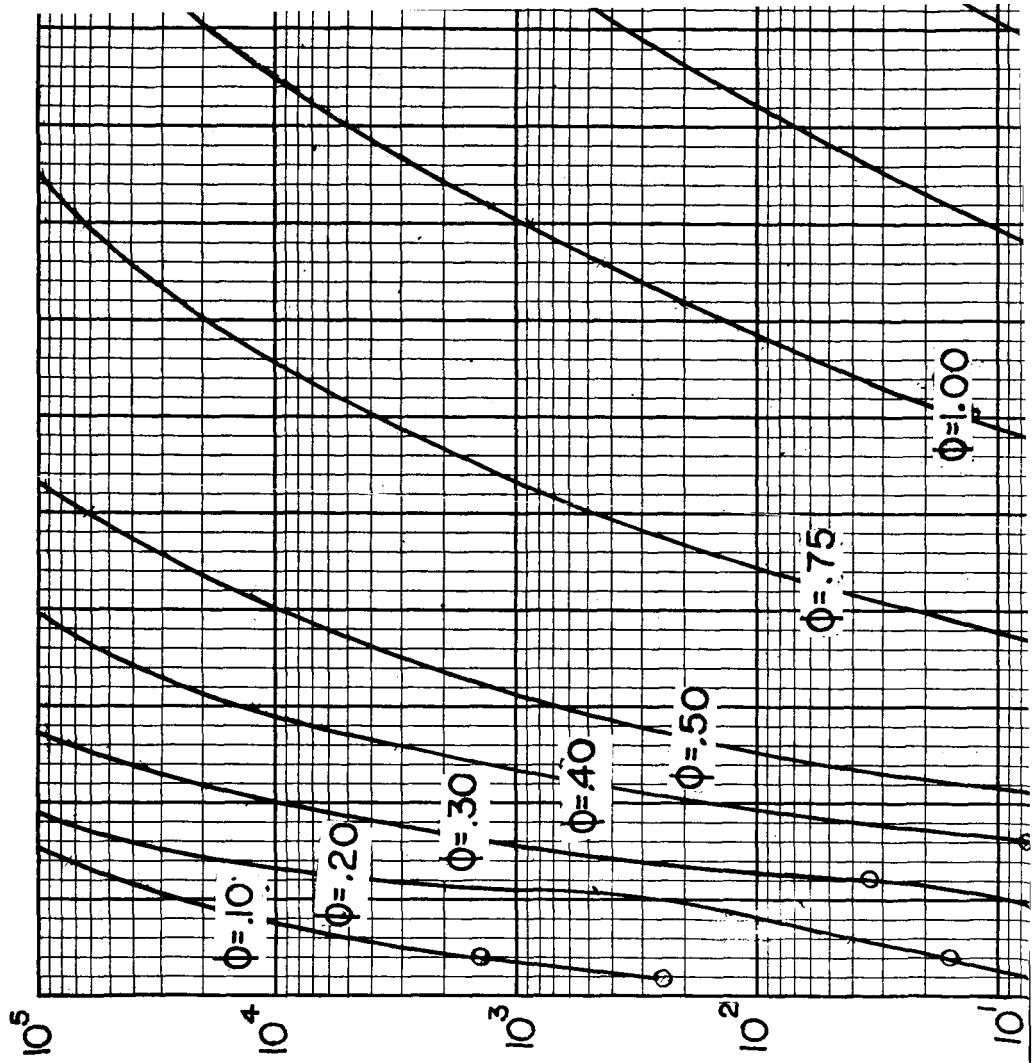
3



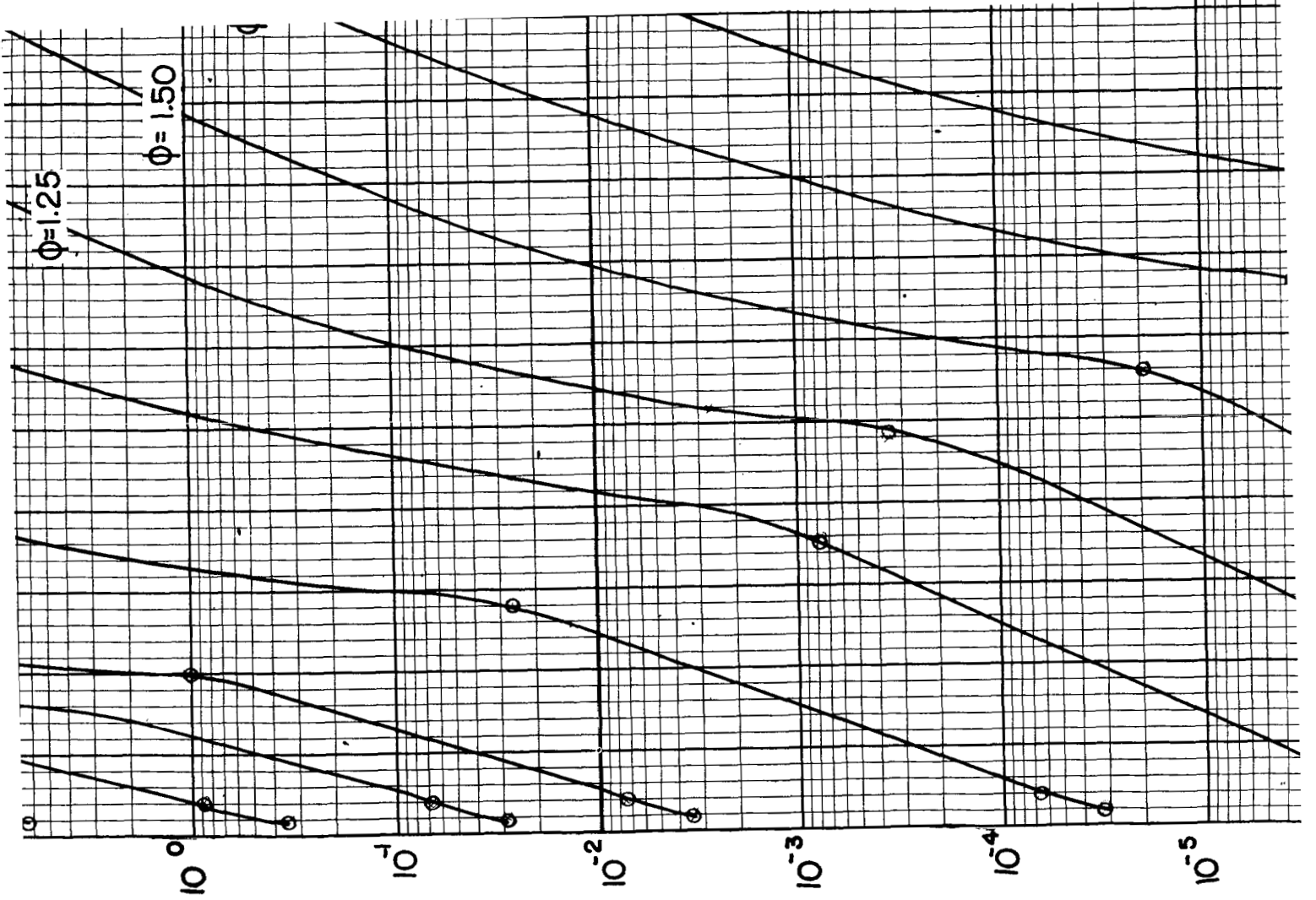
4



LTAGE [VOLTS]



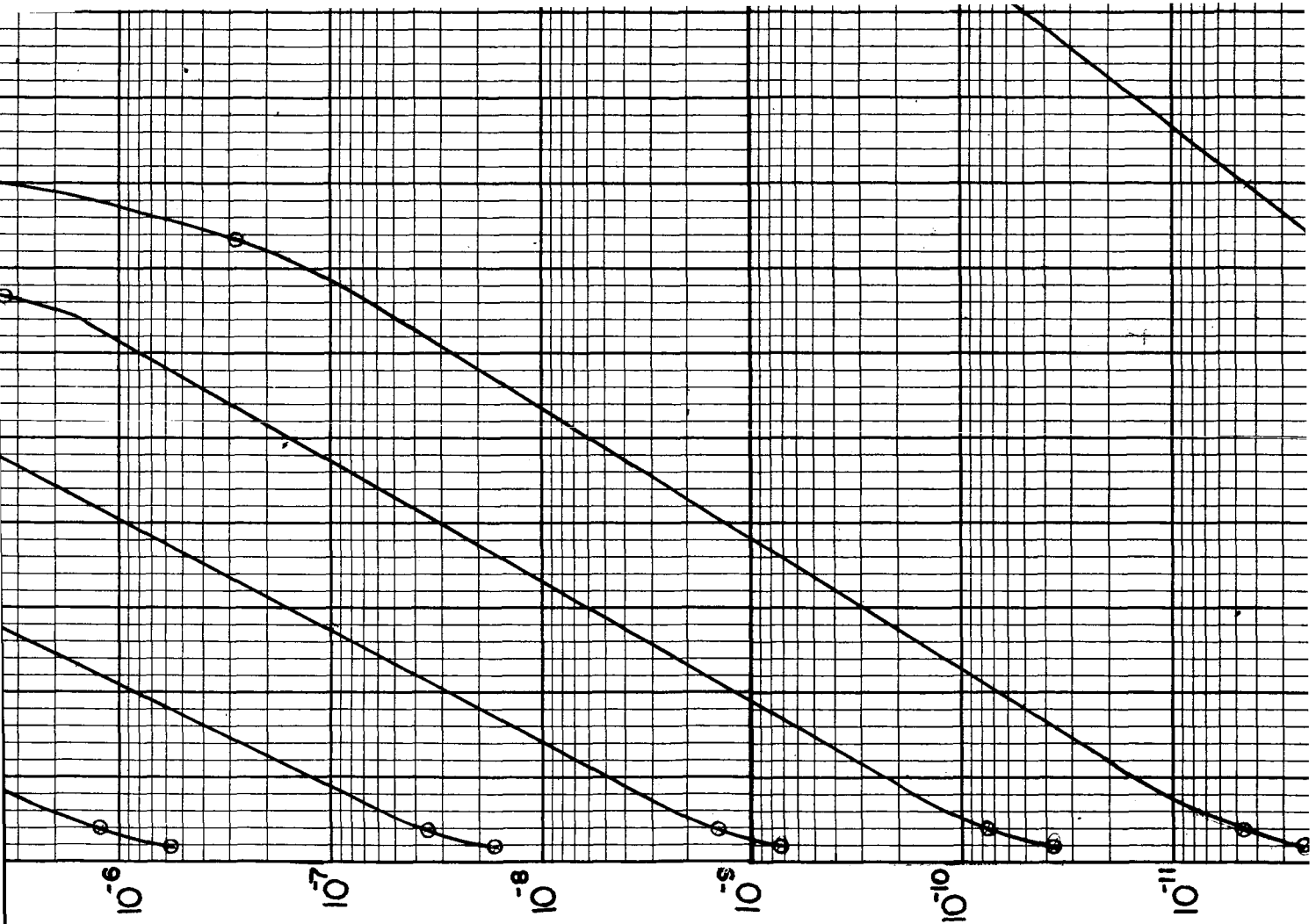
5



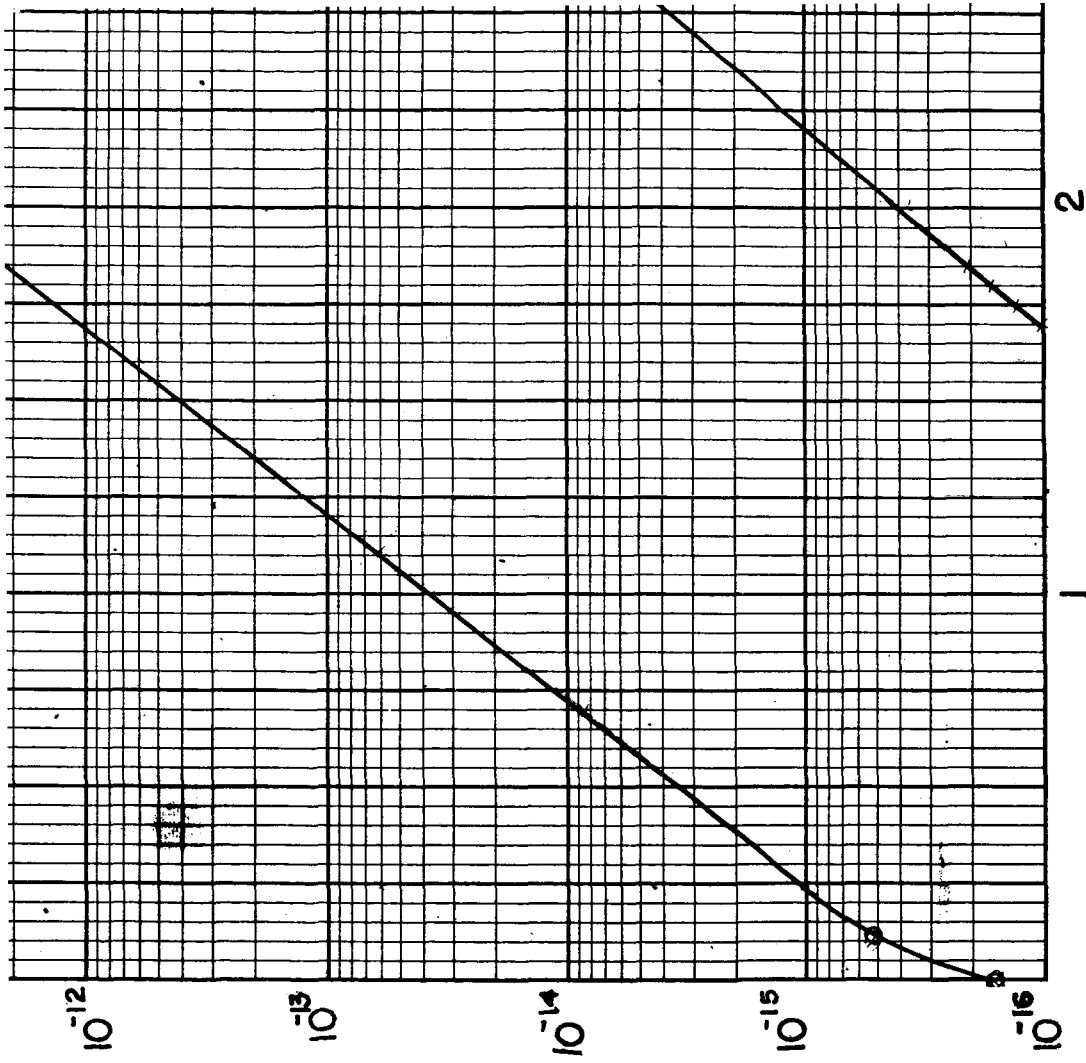
[AM/CM²]

DENSITY

9



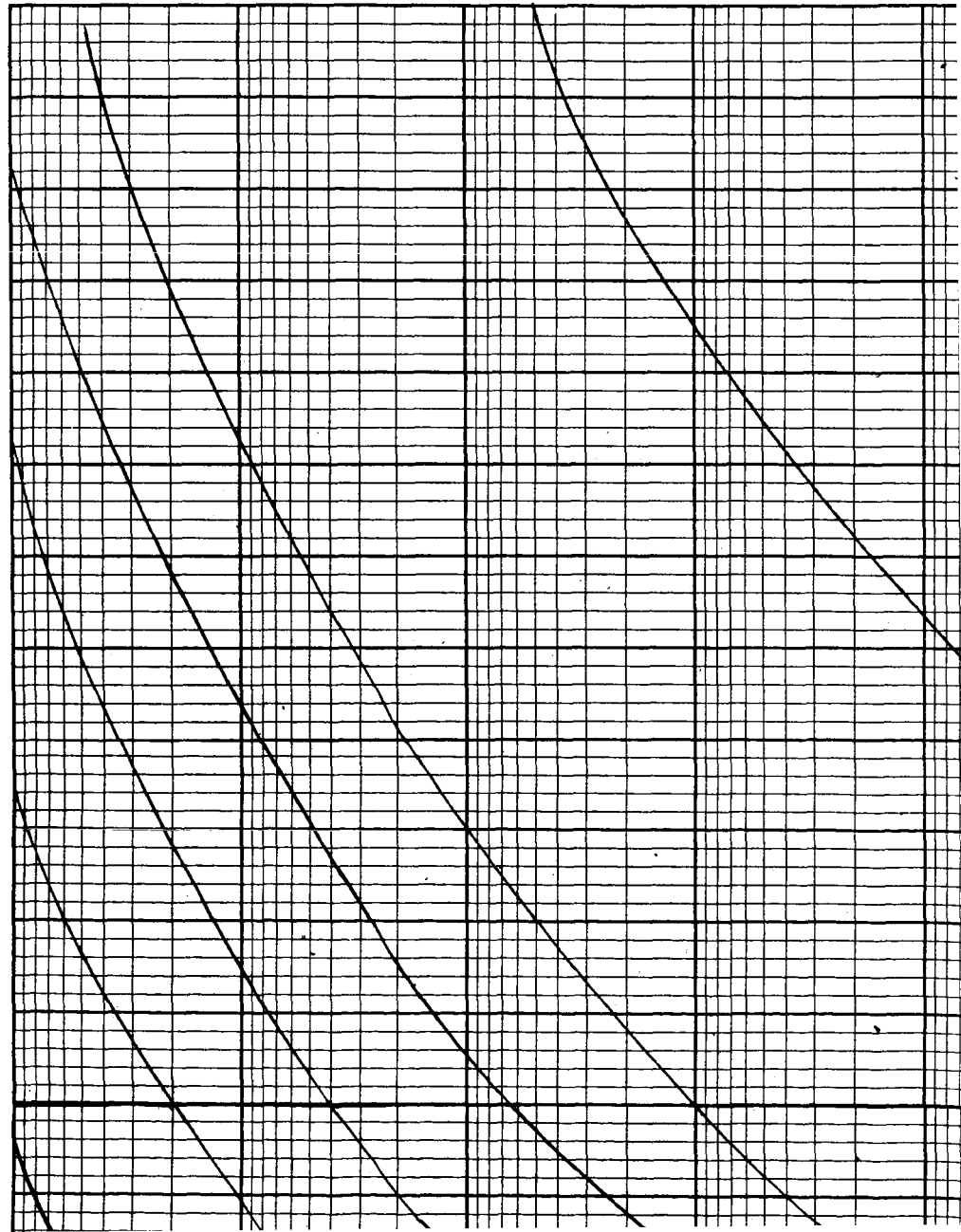
7 CURRENT DE



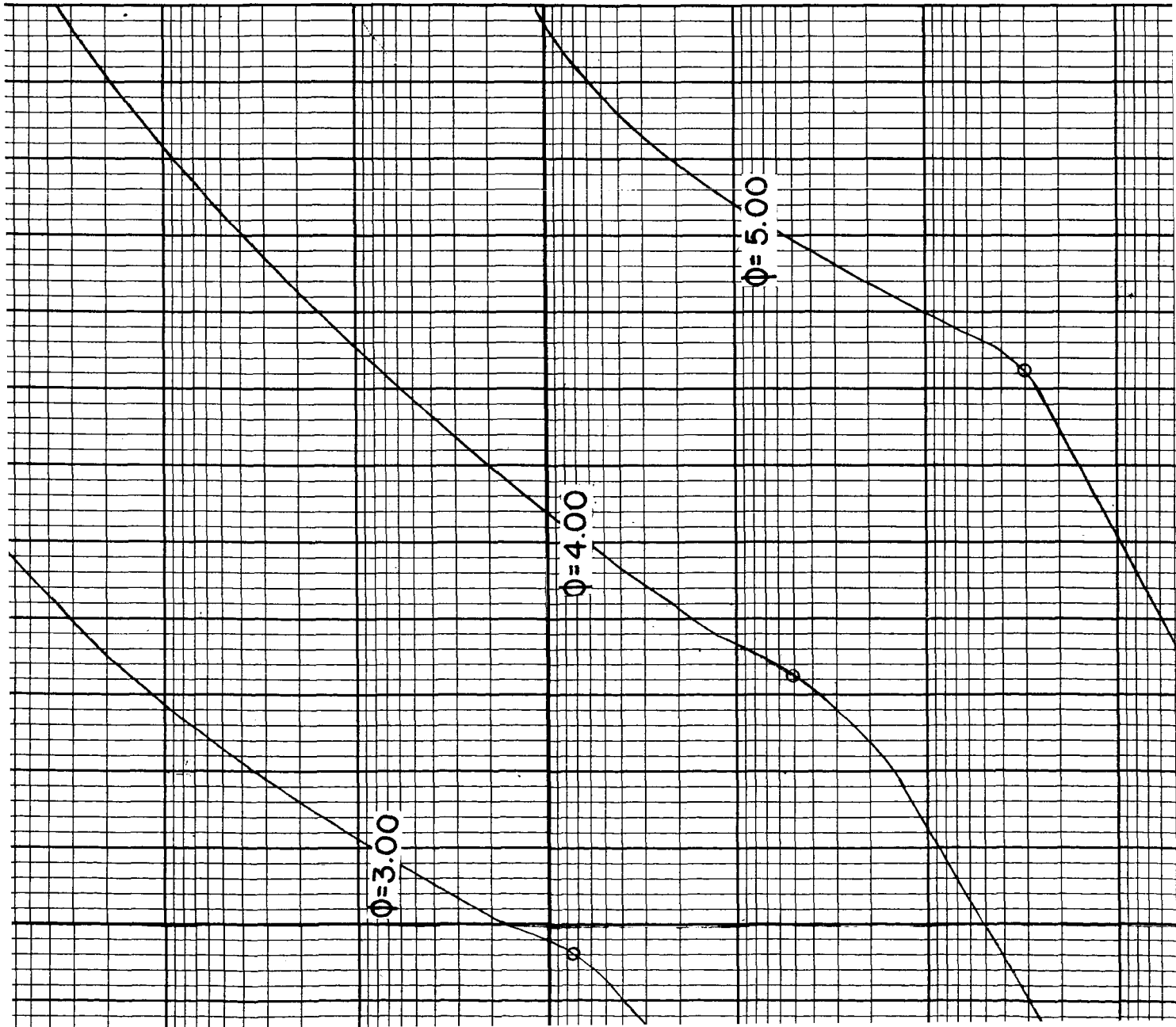
8

VC

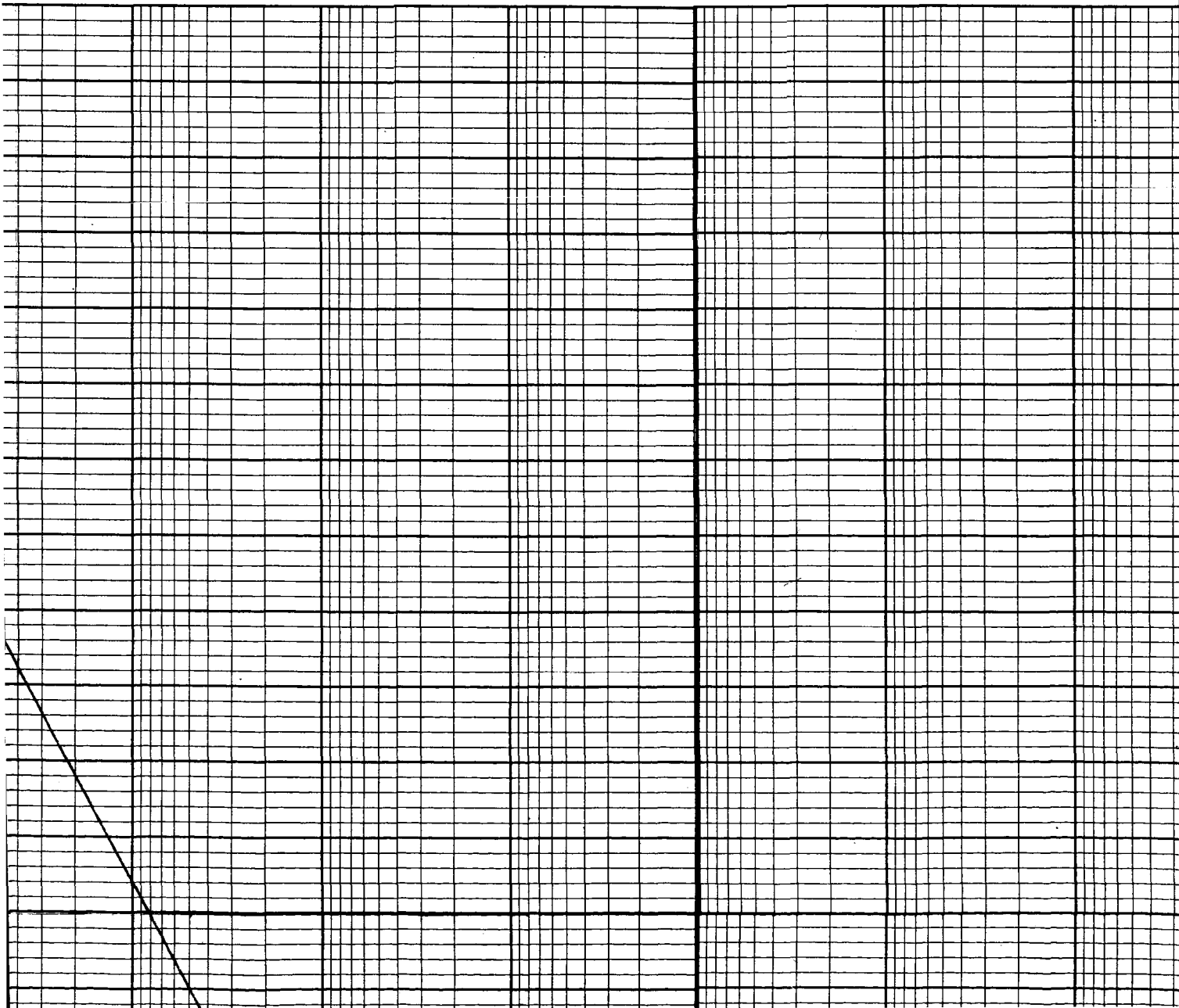
THICKNESS = 30 Å



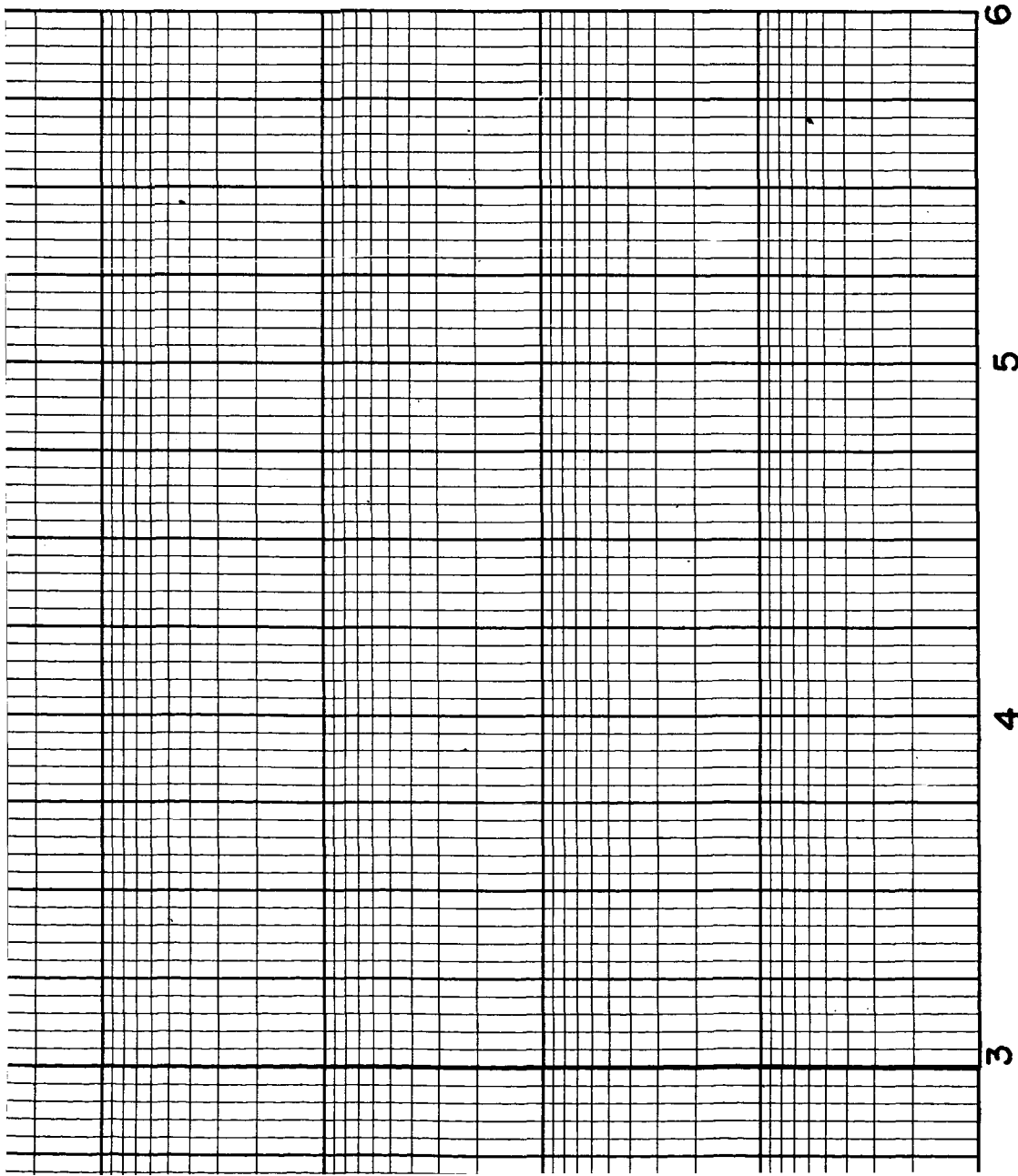
2



3

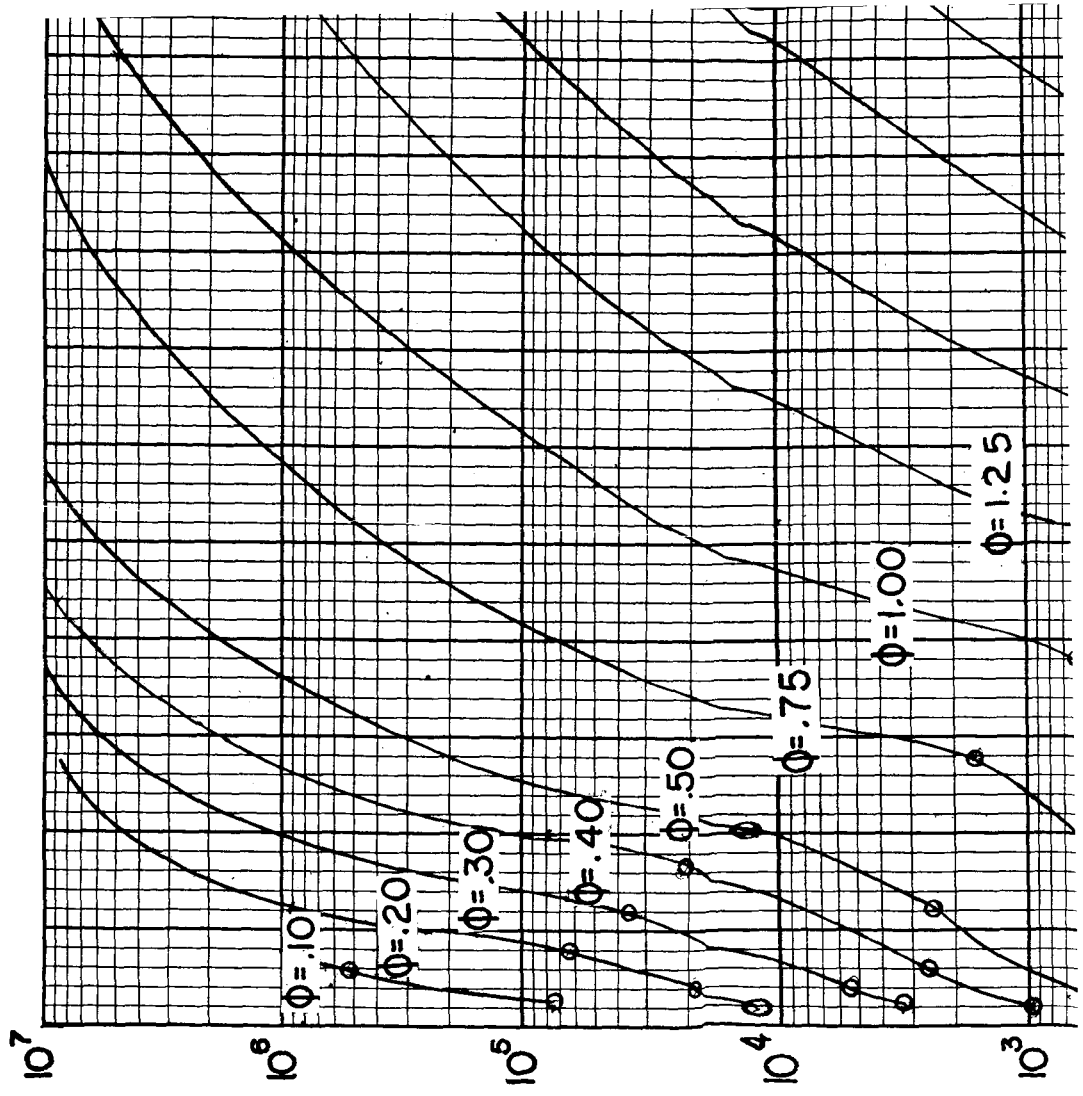


4

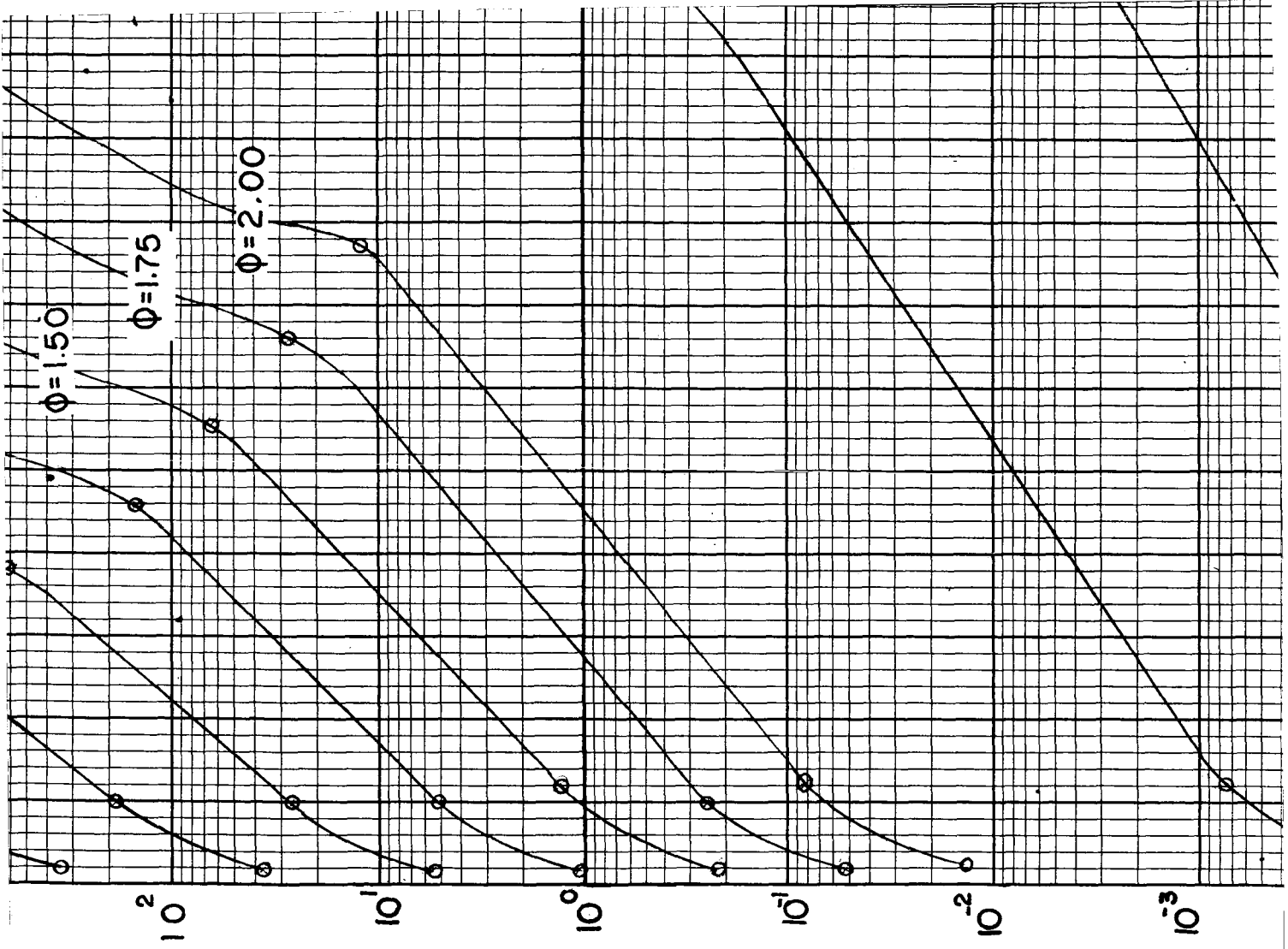


_TAGE [VOLTS]

2



5



9

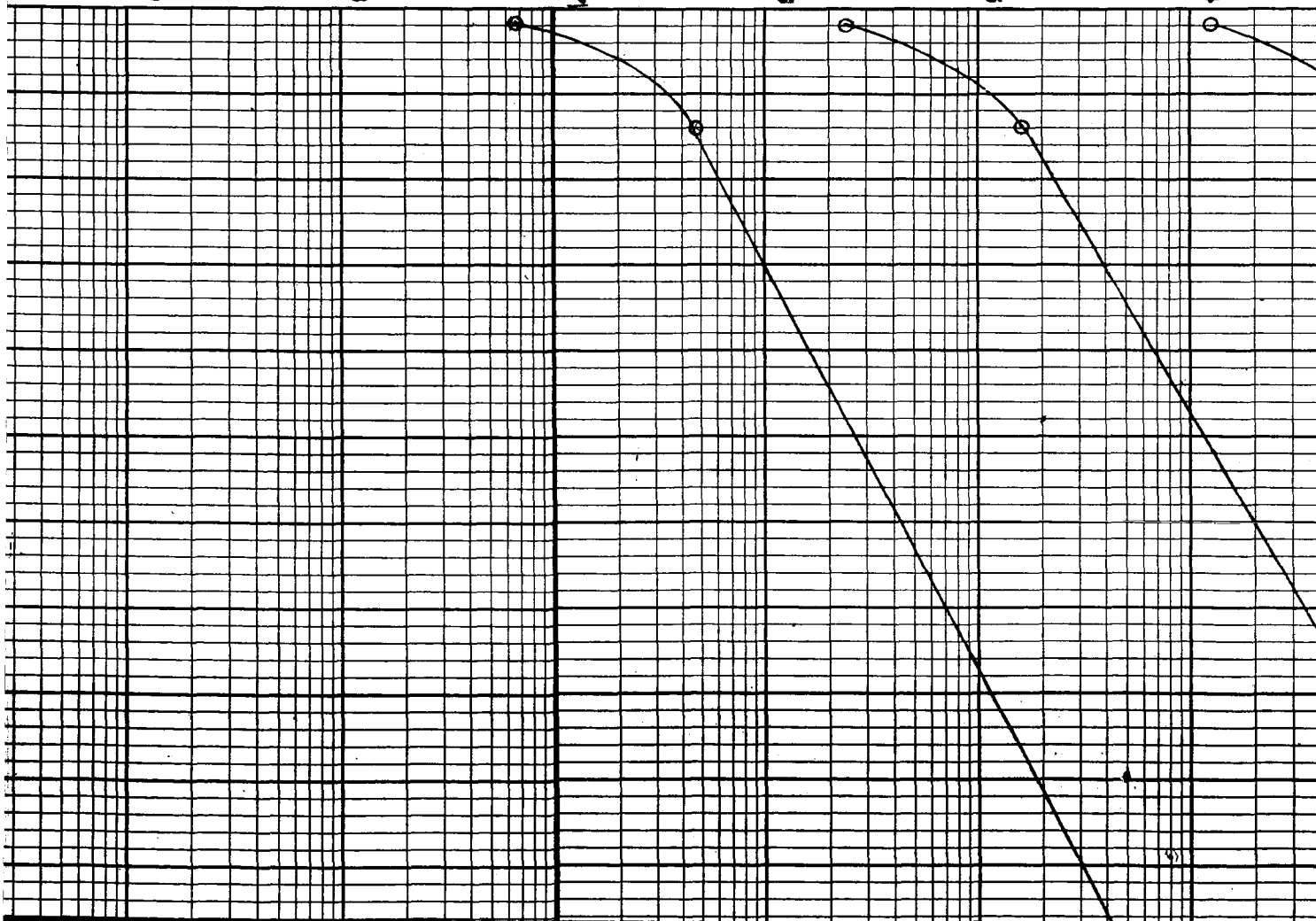
[AMP / CM²]

Y

CURRENT DENSITY

↓

10^{-9} 10^{-8} 10^{-7} 10^{-6} 10^{-5} 10^{-4}



10^{-10}

10^{-11}

10^{-12}

10^{-13}

10^{-14}

∞

2

1

VO